Master Thesis

Montanuniversität Leoben
Department Mineral Resources and Petroleum Engineering
Chair of Drilling and Completion Engineering

Subject:

Concept and Framework to Asses the Energy Losses Along the Drillstring

Submitted by:

Daniel Lackner

Advisor:

Univ.-Prof. Dipl.-Ing. Dr.mont. Gerhard Thonhauser

Leoben, December 2015

Abstract

For the time being the O&G industry relies on simple procedures and models to get an idea if the way it operates is to some extend reasonable respectively efficient or not. The application of an energy balance that could help to evaluate the efficiency of the total drilling system is for now constrained as it is not account for all the energy consuming physical processes going on downhole along the entire drillstring. Missing knowledge about wellbore geometries, string and borehole interaction and drilling dynamics along the whole string limits the informative value of current models. A possible approach is a breakdown of the system and the processes occurring along the drillstring and an itemization of the single processes helps to have a proper discussion. Based on the lack of appropriate models describing each process sufficiently it is further suggested to analyze the system with the help of additional data gained through measurements along the whole drillstring becoming doable with new telemetry systems. Reasonable predictions where such downhole measurement subs may be positioned along predefined vertical-, tangential- and horizontal well paths are stated based on the capabilities and resolution of different sensors deployed as well as a minimalistic torque and drag and hydraulic model conducted for the corresponding well paths. As a final result the setup of the drillstring and measurement subs are presented for each of the three suggested well profiles. The layout of the drillstring is chosen in a way to achieve the maximum resolution possible under given constrains. An optimum resolution is achieved through a uniform allocation of multiple subs along different sections of the wellbore that is based upon the sensor with the worst resolution at the point of interest.

Kurzfassung

Bis jetzt hat sich die O&G Industrie auf relativ simple Modelle verlassen, um einen Eindruck zu bekommen, ob Ihre Art und Weise, wie Sie arbeitet kostengünstig und effizient ist. Die Anwendung einer Energiebalance zur Evaluierung und Kontrolle des gesamten Systems ist bis dato begrenzt, da nicht alle auftretenden, Energie konsumierenden Prozesse entlang des Bohrstranges erfasst, beziehungsweise ausreichend beschrieben werden können. Fehlendes Wissen über die Bohrlochgeometrie, das Zusammenspiel zwischen Bohrstrang und Bohrloch, sowie die dynamischen Effekte während des Bohrvorgangs, beschränken die Aussagekraft von derzeitigen Modellen. Im Laufe einer Aufschlüsselung der einzelnen Prozesse, welche entlang des Bohrstranges auftreten, werden diese spezifiziert und kurz erläutert. Aufgrund des Fehlens von angemessenen Modellen, die jeden dieser Prozesse ausreichend beschreiben, wird vorgeschlagen, das System genauer zu analysieren. Eine genauere Analyse soll mit Hilfe von zusätzlichen Daten ermöglicht werden, die mit Hilfe von zusätzlichen Messungen entlang des gesamten Bohrstranges gewonnen werden. Vielfache Messungen sollen möglich werden durch die Einführung und Verwendung von neuen Telemetrie Systemen. Nachvollziehbare Vorhersagen, wo Messgeräte, entlang vordefinierter vertikaler-, tangentialer- und horizontaler- Pläne eines Bohrloches verbaut werden können, beruhen darauf, wie genau die Sensoren Änderungen im Bohrloch und Bohrstrang wie Druck, Temperatur, Verformung, etc. erfassen können. Um einen ersten Eindruck zu bekommen, auf welcher Länge Veränderungen zu erwarten sind, helfen simplifizierte Modelle der Reibungskräfte sowie des hydraulischen Systems, bezogen auf die entsprechenden Pläne. Mit Hilfe dieser Modelle, wird für alle vorgegebenen Pläne, die minimale Anzahl an Messgeräten eruiert, die erforderlich sind, um eine maximale Auflösung zu erhalten.

EIDESSTATTLICHE ERKLÄRUNG

Ich erkläre an Eides statt, dass ich die vorliegende Diplomarbeit selbständig und ohne fremde Hilfe verfasst, andere als die angegebenen Quellen und Hilfsmittel nicht benutzt und die den benutzten Quellen wörtlich und inhaltlich entnommenen Stellen als solche erkenntlich gemacht habe.

AFFIDAVIT

I hereby declare that the content of this work is my own composition and has not been submitted previously for any higher degree. All extracts have been distinguished using quoted references and all information sources have been acknowledged.

Date, Signature

Acknowledgments

I would like to express my gratitude to the people who have helped throughout this Master Thesis project.

I wish to thank Dipl.-Ing. Andreas Nascimento, Departametno de Mecânica (DME/ PRH48), from *Faculdade de Engenharia – campus de Guaratinguetá, Universidade Estadual Paulista* (UNESP), for his help, ideas of improvement and support on this project.

Last but not least I would like to express my gratitude to my family and my friends for their undivided support.

Table of Content

List of Figures

List of Tables

1 Introduction

Over the last decade “Drilling Models and Simulations” (DMS) are used to get an idea of the drilling process. They are used to increase drilling efficiency, productivity and performance (Dykstra et al., 2001). Drilling in the most efficient way, assumes that the energy at the bit is the energy brought into the system on the surface less the energy that dissipates along the trajectory due to string and wellbore interactions that cannot be averted up to a certain level. The models used reflect an “ideal drilling process” where it is not accounted for drilling problems or severe losses due to divergences in the wellbore trajectory. As Sugiura states it: *“Modeling and simulating every aspect of the drilling process and drilling system is still considered too complex to be realized.” (Sugiura et al., 2015)*

Unfortunately, being diligent, neither the wellbore nor the dynamically behavior of the drillstring can be seen as ideal. Although the industry has seen an extensive development of DMS over the last years, missing knowledge about possible divergences of wellbore geometries and drillstring dynamics along the whole string, limits their informative value. In his paper Sugiura defines the problem as follows: *“The challenges of modeling and simulation include uncertainties in model inputs as some inputs are difficult, if not impossible to measure. This creates model assumptions and limitations, which should be clearly communicated with the users of the models and simulators.” (Sugiura et al., 2015)*

Through the emergence of downhole measurement over the last decade, additional data helped the industry to reduce uncertainties and get a better understanding to a certain extent of the processes going on downhole. These new gained knowledge helps further to verify, validate and certify drilling models and simulations.

“Models need to be verified, validated, certified, and benchmarked.”(Sugiura et al., 2015)

Nevertheless, theses measurements commonly just take place near the bit and along the *Bottom Hole Assembly* (BHA) for the moment, but not along the major remaining part of the string as visualized in Figure 1. Therefore there is no measured data for the whole section in-between the BHA and the surface.

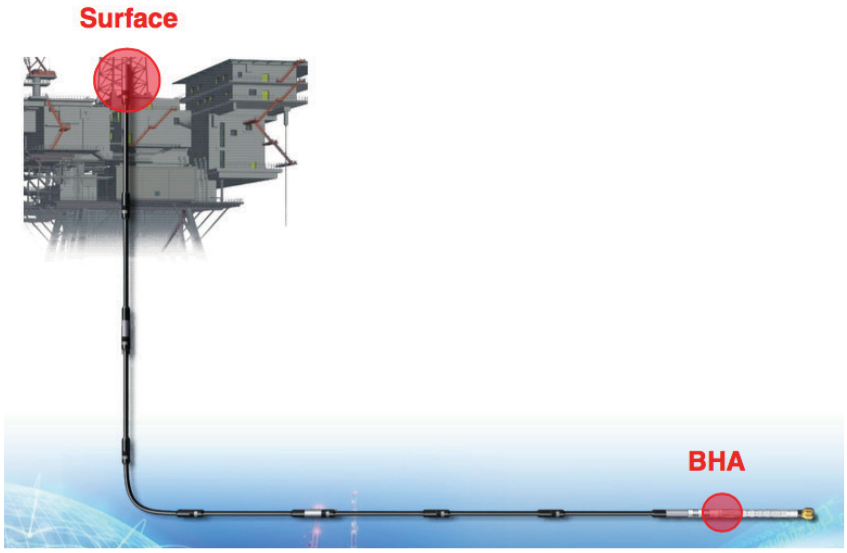

Figure 1: Visualization of Todays most common Points of Measurement in the Drillstring

The consequences due to the lack of measurement along the drillstring are:

- No data in-between BHA and surface.
- Conditions along the string need to be inferred or modeled.
- No possibility to accurately monitor and model the entire drillstring.

New high-speed, wired-pipe telemetry systems were introduced in the industry over the last years. Besides the advantage, that this technology enables instantaneous upward and downward data transmission between the surface and the downhole measurement sub, it also enables multiple sensor measurements like Johnson & Hernandez have realized too: *"…this technology also enables measurements to be acquired and transmitted to surface from many points along the string while drilling." (Johnson & Hernandez, 2009)*

In this thesis, I will address, where and how many additional measurements should be placed along three pre-defined well profiles to get theoretically a good picture of the energy losses along the entire drillstring.

- For the beginning the idea is to identify the governing theoretical models that describe the system and list and describe some processes that contribute to one or more of the governing models.
- Identify the essential physical parameters that describe the system and could verify complex solutions of the governing models.

- Specify which downhole sensors can measure these physical parameters and how accurate.
- Based on the results of a minimalistic T&D and hydraulic model of three pre-defined well paths identify the sensor with the worst resolution along different parts of the well profiles.
- Name a minimum number of downhole subs for each well to get a maximum resolution for each well profile, based on the results from the findings defined in the previous bullet point.

Further it has to be stated, that this thesis is seen as a starting point for a subsequent project, involving multiple people with a different technical background and expertise to address different problems. Therefore an overview of the essential drilling topics is provided to give an idea what is needed to drill, how the wellbore and drillstring is set up in general and how their dimensioning plays an essential role in context with the drillstring and wellbore interaction.

2 Essential Drilling Topics

This chapter provides an overview of the essential aspects that have to be addressed when drilling a well. An introduction is seen as helpful, insofar it is expected that a subsequent project will involve multiple people without a drilling background. The basic concept of the drilling process, the setup of the drillstring and the wellbore and their interaction will be discussed in a first step. In the second part an insight in essential rock mechanics is provided to understand how much energy is required to break the rock and generate a borehole. In a last part it is explained how the efficiency of the drilling system is evaluated nowadays.

2.1 Overview of Drilling Components

A short introduction into the basic drilling process itself will help as a refresher for the theoretical approaches in the following chapters to assess the energy consumption throughout the drilling system. The general goal is to drill from a point A at the surface to a point B at a certain depth and normally a lateral displacement x, as safe and fast as possible. There are essential components both for the equipment needed on the surface and downhole described more in detail below.

2.1.1 Planning the Well Trajectory

Planning a well means first of all to design a well profile to drill a wellbore and reach a target or a number of targets. The targets are either located directly below the surface drilling facilities representing a vertical well or with some horizontal displacement from the top of the hole indicating the need of a directional well. In the oil industry path and trajectory are used both, although per definition a well path is a planned sequence of wellbore course coordinates due to a design method not taking time into account, whereas the trajectory is the actual constructed well path with respect to time (Samuel & Liu, 2009, p. 14). Some common used well path types and profiles in the industry, as well as the basics to get an idea how to read a directional well plan, will be discussed subsequently. This is essential as the trajectory design influences other designs such as the drill string design, casing design, torque and drag estimation etc. For further information on the mathematical

models standing behind the well path design see “Advanced Drilling Engineering: Principles and Designs” Chapter 3 and higher. (Samuel & Liu, 2009)

2.1.1.1 Directional Drilling Basic Definitions

The well path looked at from the side in Figure 2 (a) is a tangential well path. Together with the plain view (Figure 2 (b)) all the key parameters describing a directional well stated below can be explained and understood more easily.

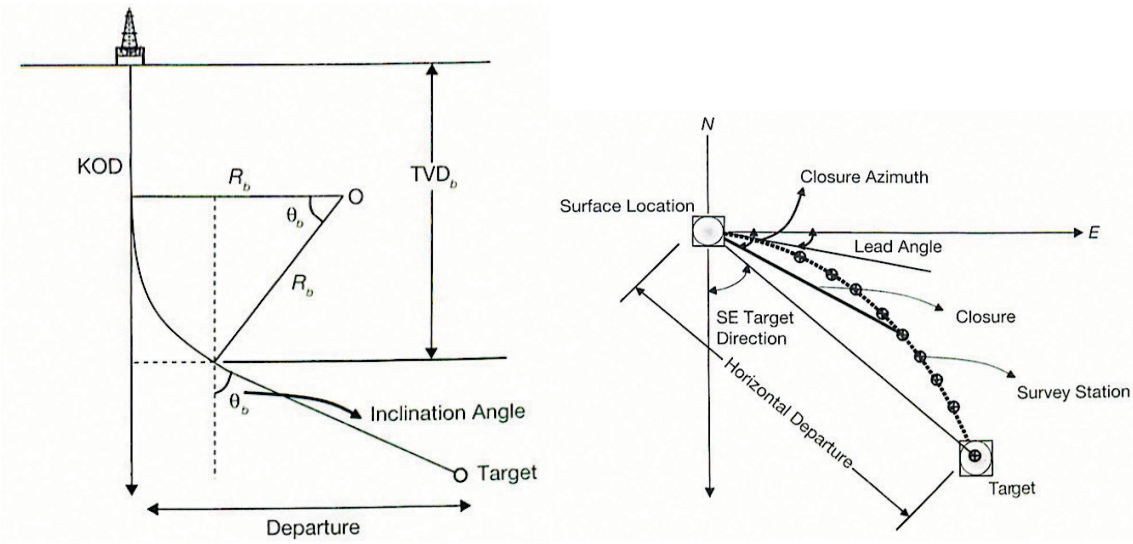

(a) (b)

Figure 2: Sketch of a Well Profile including (a) a side view of the well path and (b) a plane view of the well path. (Samuel & Liu, 2009, p. 52)

Inclination Angle

It is the angle between a tangential line through any point on the wellbore and the vertical line through this point.

Azimuth Angle

It is the angle between a tangential through any point in the well and the north direction on a horizontal plane. Azimuth is measured relative to the north clockwise from 0° to 360°.

Measured Depth

The measured depth, MD, is the actual length of the trajectory.

True Vertical Depth

The true vertical depth, TVD, is the vertical distance between a point on the wellbore and the reference starting point of the wellbore on the surface.

Kick of Point

The kick of point, KOP, or kick of depth, KOD, is the point at a certain depth on a wellbore at which the change in inclination or azimuth begins.

Lead Angle

The lead angle is a correction angle, as the bit due to the clockwise rotation of the string may tend to walk to the right or left in the horizontal plane. The magnitude of the correction is generally based on experience from previously drilled offset wells.

Survey Station

A survey station or point is a point along the wellbore where inclination and azimuth are measurement.

Departure

Departure is the horizontal distance between two survey points whereas the total departure is the total horizontal distance between the target and the wellbore surface starting point.

Course Length

This is the length between two survey points along the wellbore.

Closure

The closure is the horizontal distance between the well and the well origin. Reaching the target the closure is equal to the total departure.

2.1.1.2 Trajectory Planning

The planning of a well is normally split into two phases. In the first phase the connection of the target to a surface location gives the well path. In the second phase it is accounted for external influences that may change the final trajectory. Concerning this thesis a fictional target is assumed and based on this target the trajectory is planned.

Basically in a first step the two-dimensional trajectory is planned in the z – y plane (Figure 2 (a)) where the z – axis represents the depth and the y – axis the departure controlled through the inclination angle. Next the x – axis has to be taken into

consideration indicating the departure of the trajectory from the vertical plane controlled through the azimuth angle introducing the three-dimensional layout of the well. The "minimum curvature method" used for the minimalistic model is nowadays the accepted industry standard where the trajectory consists out of a set of circular arcs where each arc connects two survey points. All the formula and theory behind the minimum curvature method can be found in the book: "Fundamentals of Drilling Engineering; Chapter 8.1.6: Directional Well Profiles". (Mitchell et al., 2011, p. 458 ff.)

2.1.1.3 Different Well Profiles

Besides just straight vertical wells there is a number of directional well profiles commonly used in the industry like the tangential-, s-shaped- and horizontal- well described shortly below.

Tangential Well Profile

The well profile as shown in Figure 3 is made up of a vertical section, a buildup section and a tangential section. This type of profile is also called Build and Hold trajectory or L – Profile. For this well type the KOP is normally in a relatively shallow depth followed by the build section with a steady and smooth deflection from the vertical until a maximum inclination and azimuth is achieved. From then on the desired inclination and azimuth is hold until the target is reached.

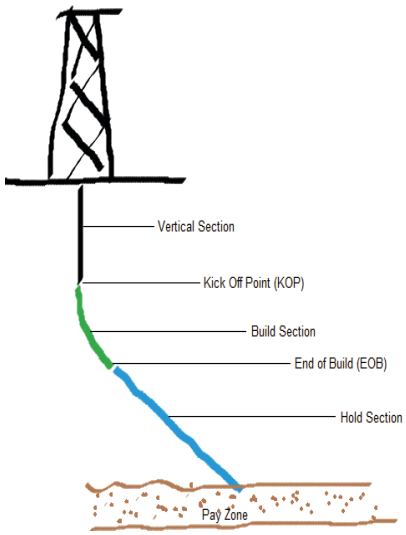

Figure 3: Sketch of a Tangential Well Profile (Choudhary, 2011a)

S – Shape

Figure 4 represents an S – Shape profile of a wellbore. Up to the end of the tangential section the well is drilled in the same way as the tangential well described before. As a certain depth and horizontal departure is reached angle is continuously and smoothly dropped until the well is near vertical. It is tried to hold it vertically until the target depth is reached. This profile type results in higher torque and drag for the same horizontal departure compared to the tangential profile.

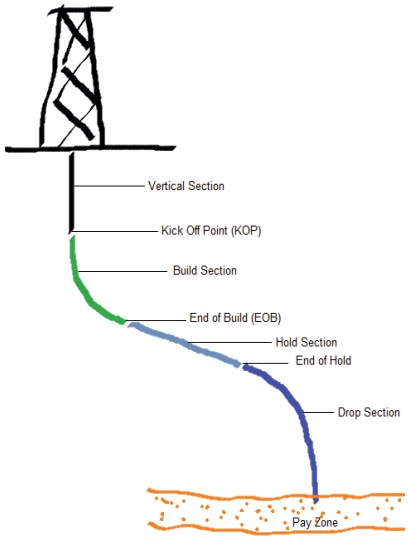

Figure 4: Sketch of a S-Shape Well Profile (Choudhary, 2011a)

Horizontal Well Profile

Horizontal wells can be made of any of the profiles presented above. The one in Figure 5 has a horizontal section attached to a so-called J-Profile. The characteristic of a J-Profile is that it has a deep KOP and high inclination after a smooth and steady build section. The horizontal part is normally drilled at 90° within the reservoir and therefore the TVD usually stays almost the same depending on dip variations in the reservoir. Productivity is increased as the formation surface exposed to the wellbore is increased. The increase of surface area exposed to the formation is especially useful in unconventional reservoirs with a low permeability and therefore this type of well is especially common in shale and tight reservoirs.

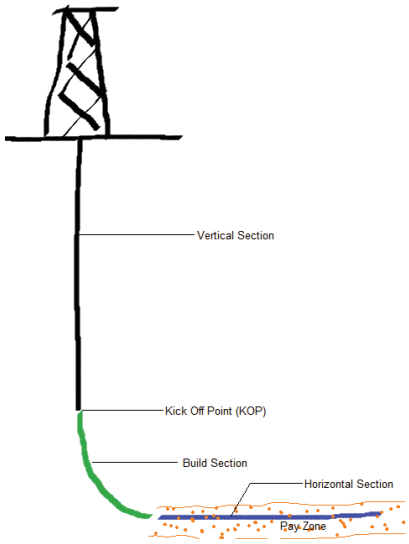

Figure 5: Sketch of a Horizontal Well Profile (Choudhary, 2011a)

2.1.1.4 Dogleg Severity (DLS)

The dogleg severity is defined by Choudhary as follows: *"Dogleg severity is a measure of the amount of change in the inclination, and/or azimuth of a borehole, usually expressed in degrees per 100 feet of course length. In the metric system, it is usually expressed in degrees per 30 meters or degrees per 10 meters of course length." (Choudhary, 2011b)*

In a directional well the dogleg severity (DLS) has always to be taken into consideration, as the borehole will change continuously in inclination and/or azimuth. Several survey stations along the wellbore are needed to obtain the dogleg angle, which is the angle included between two tangents at two different measurement points of a wellbore. As the tangents at these points aren't in the same plane or meet at any point the dogleg angle is mathematically called space or bending angle including both the change in inclination and azimuth. The DLS is the measure of the amount of change in the inclination, and/or azimuth over a certain course length. The visualization of the bending angle and its mathematical derivation can be found in the book: "Advanced Drilling Engineering; Chapter 3: Well Path Trajectory" (Samuel & Liu, 2009, p. 73 ff.).

2.1.2 Surface Components

In Figure 6 everything above ground level, here represented by the transition from yellow soil to atmosphere, is part of the surface equipment. The basic structure is

kept in red with the substructure and the vertical “tower” (derrick/mast) attached to it. The substructure is there to support the derrick or mast and other rig components as well as to provide storage space below the main rig floor. Whereas the derrick respectively the mast serves as the load – bearing structure holding and positioning the drillstring over a wellbore.

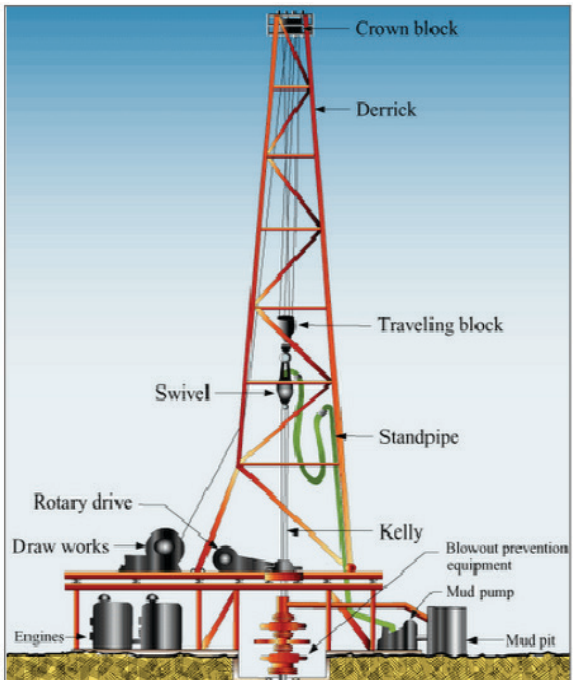

Figure 6: Schematic of a Basic Onshore Drilling Rig (M.Sc. Eng. Andreas Nascimento, 2012, p. 29)

2.1.2.1 Rig Power System

The power system of the rig nowadays normally consists out of a prime mover that generates the power and a system that transmits the power to the end – use equipment. On modern rigs the prime movers are diesel engines that drive an alternating – current (AC) generator generating electricity. With the help of silicon – controlled rectifier (SCF) the power is transmitted to direct current (DC) motors driving end – use equipment. (Mitchell et al., 2011, p. 17) For further information on the rig power system, concerning the prime mover, the AC – generator and the silicon-controlled rectifier, see “Development of an Energy Consumption Model Based on Standard Drilling Parameters” chapter 2.1 and 2.5. (Gabriel Gomes Müller, 2015)

2.1.2.2 Hoisting System

The vertical movement of the pipe in and out of the well is provided by the primary hoisting system including drawworks and the block – and – tackle arrangement. Whereas the drawworks is a big drum with a specially grooved surface to reel in cable on the drum to lift the drillstring and spool out cable to lower the drillstring. The rig – power system, provides the power needed for lifting heavy loads up to 500 – tons. The block and tackle arrangement includes the crown block, traveling block and the drilling line, which is the link between the drawworks and the loads that need to be moved. For more information concerning the needed power at the drawworks and its transmission to the block and tackle arrangement see "Applied Drilling Engineering" chapter 1.4. (Bourgoyne, 1986)

2.1.2.3 Rotary System

Rotation to the drillpipe and further to the bit is provided by the rotary system consisting in general out of a swivel, rotary hose and a rotary driving mechanism that may either be a top drive on modern rigs or a rotary table including a kelly and a kelly bushing on older rigs. More information about the power consumption and the functionality of a rotary table can be found in "Drilling Engineering, A Complete Well Approach" chapter 16 "Rig Sizing and Selecting". (Adams & Charrier, 1985, p. 581 ff.)

2.1.2.4 Circulating System

The task of a circulating system is to maintain a circular flow of the drilling fluid in and out of the well. Drilling fluid is the prime instrument that helps to keep control over the wellbore and also lubricates and cools the drillstring. Further it is used as a transport medium to clean out the generated cuttings as the bit penetrates further into the formation. As stated by Bourgoyne: "*Drilling fluid is most commonly a suspension of clay and other materials in water is called drilling mud*. T*he drilling mud travels (1) from the steel tanks to the mud pump, (2) from the pump* through *the high-pressure surface connections to the drillstring, (3)* through *the drillstring to the bit, (4)* through *the nozzles of the bit and up the annular space between the drillstring and hole to the surface, and (5)* through *the contaminant-removal equipment back to the suction tank*" (Bourgoyne, 1986, p. 12). The power needed at the pump to circulate the fluid at a given flow rate and a more precise description of

the single components of the circulating system can be found in his book “Applied Drilling Engineering; Chapter 1: Rotary Drilling Process”.

2.1.3 Downhole Components

Downhole it is distinguished between the drillstring and the wellbore excavated within the drilling process both designed with respect to a planned well path. To understand the whole concept of energy losses and how they interrelate with the structure of the wellbore and different drillstring elements following an overview of the wellbore body and its segmentation itself is presented as well as single elements of the drillstring; their functionality and dimensional ranges.

2.1.3.1 Hole Geometry

Talking about borehole geometry the planning is essential not just from the economic perspective but also from the standpoint of an engineer as due to an improper size selection there is the chance that the hole has to be abandoned due to drilling or completion problems. The wellbore, the drilled hole or borehole itself, is normally separated into a “Cased Hole” (CH) and “Open Hole” (OH) section, whereas the OH section represents the freshly drilled part of the hole with the rock exposed to drilling operations.

Cased Hole

Before drilling a new section the casing is run into the hole and cemented into place to eliminate well integrity issues sealing off the formation. Casing is defined as a tubular pipe with an OD range of 4.5 to 20 inch. Although shorter casings are available the most common used casing lengths are in the range of 34 to 48 feet to reduce the number of connections as casing is made up in single joints. The dimensional selection is controlled by the casing inner and outer diameter, coupling diameters, bit sizes and the forces it will be exposed to. The minimum inner diameter is controlled by a specified drift diameter, which is smaller than the inner diameter and controls the bit selection for next OH section to be drilled, as it is the minimum mandrel diameter that must pass unrestricted through the pipe.

Depending on the planned trajectory and downhole conditions a casing program may have more or less casing sections planned. An average casing program common in the O&G industry with the aligned OH sizes is presented in Table 1.

Table 1: Typical Casing and Open Hole Size Program

Open Hole Size in [inch]		Casing Size in [inch]	
Surface Section:	17 1/2	Surface Casing:	13 3/8
Intermediate Section #1:	12 1/4	Intermediate Casing #1:	9 5/8
Intermediate Section #2:	8 1/2	Intermediate Liner #2:	7
Production Section:	6 1/8	Production Casing:	5

A surface casing is essential and normally set at a depth sealing of all the groundwater layers so further drilling and fluid from layers yet to drill won't contaminate them. Therefore it is continuously cemented up to the surface and forms the foundation for the "Blowout Preventer" (BOP) on top of it being an essential safety barrier in the drilling process if necessary.

Open Hole:

The OH has a smaller diameter as the previous section as the new bit has to fit through the inside diameter of the previously cased section. The geometry of the hole has a significant influence on the forces acting on the string resulting in torque and drag. These forces are in general calculated for reasons of simplicity for a wellbore represented by a straight or curved cylinder with a plain inner surface from the last casing shoe through to the next casing setting point. The inner diameter of this cylinder is defined by the diameter of the bit used to drill this section.

Figure 7 is a reflection of a wellbore in the form of the cross section of a wellbore discussing all its elements discussed above. It is differentiated clearly between the CH and OH indication the too the different diameters.

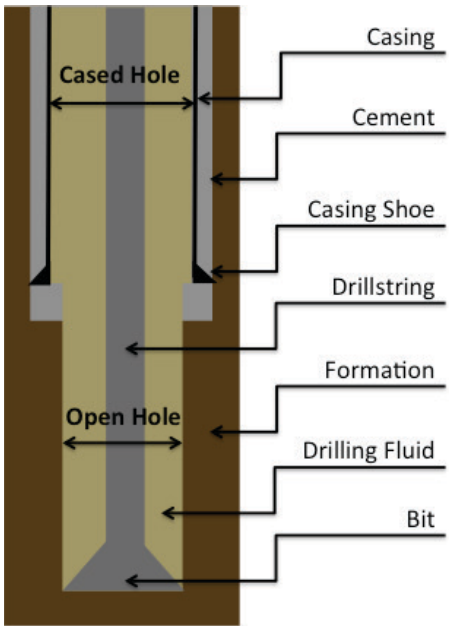

Figure 7: Sketch of a Cased and Open Hole Section

2.1.3.2 Drillstring

The drillstring can be split into three major groups the Bit, Bottom Hole Assembly (BHA) and Drillpipe. Altogether assembled they form the drillstring as represented in Figure 8 with the main section made out of drillpipe and a relative short BHA with the bit attached to the end of it.

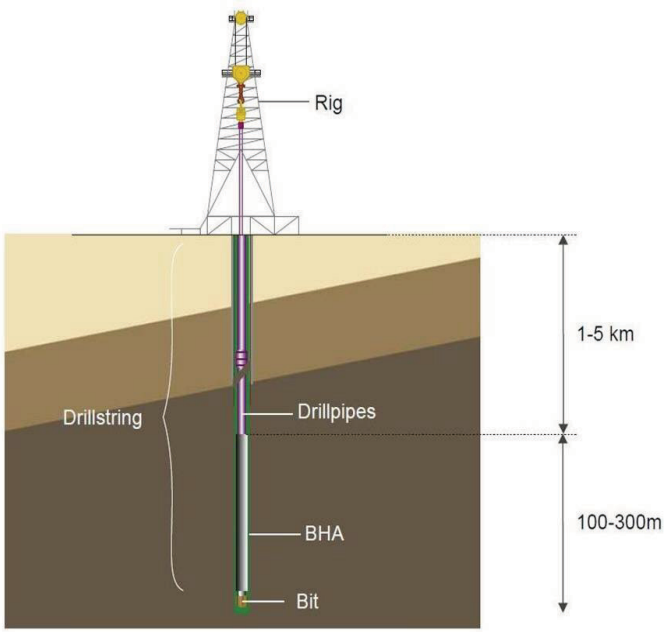

Figure 8: Schematic of a Basic Drillstring (The University of Aberdeen, n.d.)

Before an overview of the single elements of each section will be discussed more in detail, the general geometrical shape of the drillstring will be explained and its mechanical behavior as certain key dimensions will be changed.

Drillstring Basic Geometrical Layout

Basically the string excluding the bit can be seen as several round pipes (hollow cylinders) that are screwed together. Along the string the pipes may have different types of connections further they may differ in length, outer and inner diameter depending on their functionality. Certainly it is not as simple as that as single elements have transitions from one outer diameter to another (e.g.: Drillpipe to Tool Joint (Connection)). An example of a cross sectional area for any round tool is presented in Figure 9.

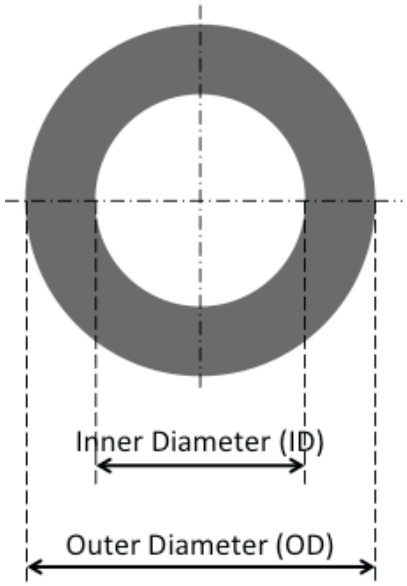

Figure 9: Cross Sectional Area of a Pipe

The purpose of the string is to transmit the power as efficient as possible from the surface to the bit penetrating the formation. Dependent on the trajectory as well as a set WOB different segments of the string will be under tension or compression and experience bending forces too.

That is where the dimensioning comes into play, as it is tried to avoid a bending of the string due to compression, whereas a certain bending of the string along trajectories with a high DLS is unavoidable and to a certain degree needed.

Stiffness of a Hollow Cylinder

The product of the Area Momentum of Inertia (I) and Young's Modulus (E) is an indicator of the stiffness of the pipe where Young's Modulus is a material property and the Area Momentum of Inertia.

$$Stiffness = E * I \quad (1)$$

Having a closer look at equation (1) it can be concluded that with an increasing area momentum of inertia its stiffness increases playing a key role in the drillstring design. The area momentum of inertia is given by Equation (2) where the capital D is the outer diameter of the pipe and small d the inner diameter. This equation indicates that the stiffness increases as the wall thickness of the pipe increases.

$$I = \frac{\pi}{64} * (D^4 - d^4) \quad (2)$$

Therefore concerning the setup of the string ticker pipes (stiffer pipes) are normally found in zones with high compressional forces to avoid severe bending of the pipe in this section.

2.1.3.3 Drillpipe

The longest section of the drillstring is normally the drillpipe having a fraction of 90 – 95%. It is a seamless pipe with threaded connections called tool joints. Each length of pipe is known as joint or single and is specified by the API into three ranges (Table 2) whereas range 2 is the most common. Nevertheless, the real length of each single joint must be measured on the rig site, as they are not of uniform length due to the manufacturing process.

Table 2: API Single Drillpipe Length Range Classification

API Range	Joint Length [ft]
1	18 - 22
2	27 - 30
3	38 - 45

Figure 10 gives an overview of a drillpipe and its components. Mainly it is made of three different parts: a tool joint pin, a tool joint box and the pipe body itself. The pipe body commonly is made out of one piece of steel and the tool joints are

adapted to the ends by friction welding. The pipe size is defined by the outside diameter (OD) in inches. There are nine commonly used pipe sizes used in the field ranging from 2 3/8" to 6 5/8". The nominal weight in lb./ft is an indicator of the wall thickness but excludes the tool joints.

Due to the friction welding of the tool joints to the pipe body the material properties alter at the weld and commonly result in a loss of strength. To counteract this problem an upset on the last 3 to 5 inches on both sides of the pipe is generated which increases the wall thickness. It is distinguished between three different types of upset configurations displayed in Figure 11.

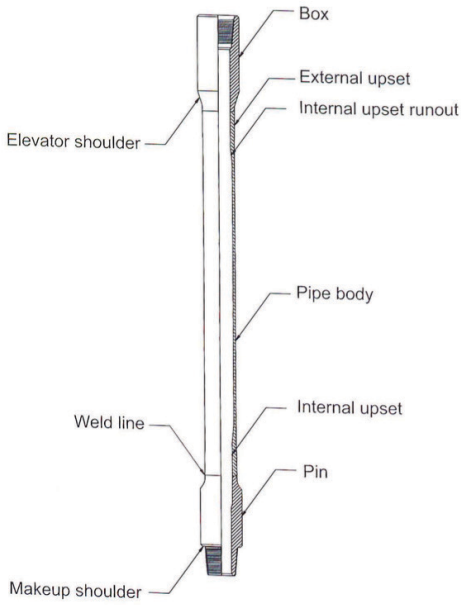

Figure 10: Schematic of a Drillpipe Joint (Aadnøy et al., 2009, p. 86)

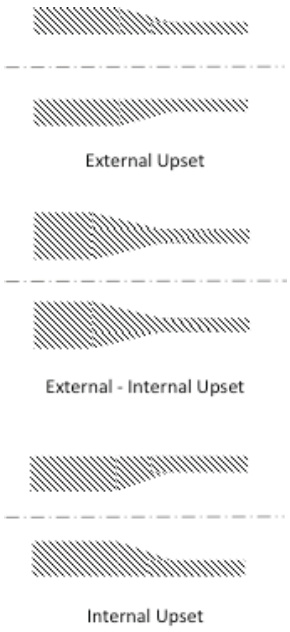

Figure 11: Sketch of the Pipe Upset Configurations

Welded to the upset of the drillpipe are the tool joints with threated rotary-shouldered connections (Figure 12). Tightening the pin and box against a shoulder makes up connections. The wall thickness and the outer diameter of the tool joint are in general thicker compared to the pipe to accommodate the treads of the connections. Additionally some joints have a hardfacing to increase the lifetime of the joint, as it tends to wear rapidly in a dogleg and abrasive formation. The size of the tool joint depends on the pipe and forces it has to withstand. The tool joint dimensions commonly used for a 4½" drillpipe are shown in Table 3.

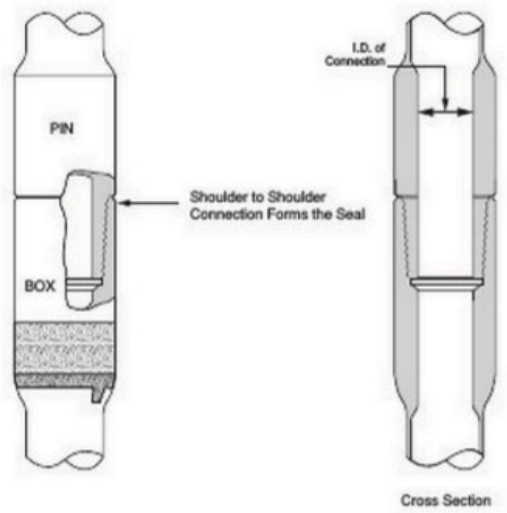

Figure 12: Sketch of a Tool Joint with the Threaded Rotary Shoulder Connection (Jack, 2015)

Table 3: Typical Tool Joint Dimensions for a 4 1/4 Drillpipe

Drillpipe	Tool Joint	
OD [in]	OD [in]	ID [in]
4 1/2	5 1/2	2 1/4
4 1/2	5 3/4	3
4 1/2	6	3 1/4
4 1/2	6 1/8	3 3/4

To define the loads a drillpipe can withstand a classification system was introduced by the API (American Petroleum Institute) introducing four grades of drillpipe. Each grade implies most important a minimum yield and tensile strength listed in Table 4. Additionally API implies minimum torsional yield strength, burst strength and collapse strength for a joint.

Table 4: API Drillpipe Grades including Strength Limits

API - Grade	Min. Yield Strength [psi]	Max. Yield Strength [psi]	Min. Tensile Strength [psi]
E-75	75,000	105,000	100,000
X-95	95,000	125,000	105,000
G-105	105,000	135,000	115,000
S-135	135,000	165,000	145,000

2.1.3.4 Bit

At the front end of the drillstring conducting the cutting action the bit takes the entire load. Different actions like scraping, chipping, gouging or grinding are approaches how the rock is destroyed depending on the type of bit used. It is

differentiated between roller-cone and fixed-cutter bits whereas roller cones have one or more cones rotating about the axis of the cone as the bit is rotated downhole. Fixed cutter bits have fixed cutter blades that are part of the body and don't move. Due to technological innovations over the last decade fixed-cutter bits became more efficient and their durability extended. Therefore fixed-cutter bits, especially the Polycrystalline Diamond Compact (PDC) bits, will be the general type of bit, which is referred to in this thesis.

Fixed-Cutter Bits

Polycrystalline diamond compact (PDC) bits and natural diamond bits are the two main groups of the fixed cutter bits. The PDC bit is said to fail the rock by shearing and natural diamond bits by grinding. A side view of the cutting action by sharing of a single PDC cutter is given in Figure 13. The arrow pointing away from the cutter indicates the direction of movement. The blank is the drag-cutting element made out of a polycrystalline, man-made diamond layer. With help of a brazing alloy (indicated by the dashed layer) the blank is fixed to the tungsten carbide stud.

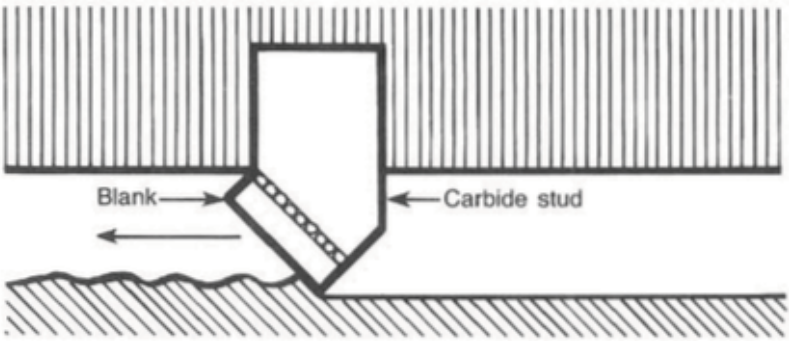

Figure 13: Cutting Animation of a Single PDC Cutter (Adams & Charrier, 1985, p. 201)

As the cutter fails the rock by shearing, less effort is needed to fail the rock compared to the cutting principles of roller cone and diamond bits (cracking respectively grinding of the rock). Less effort translates into less weight required what is especially useful for deviation control. A typical PDC commonly used in the industry is displayed in Figure 14 with two arrows one highlighting one nozzle out of six being the exit of the drilling fluid cleaning away the freshly generated cuttings and cooling the bit. The second arrow points out a single polycrystalline diamond cutter. Further it can be seen that this bit has seven blades with the cutters aligned

along their edges. In-between the blades so-called flow paths allow for the fluid to slip through for proper cleaning.

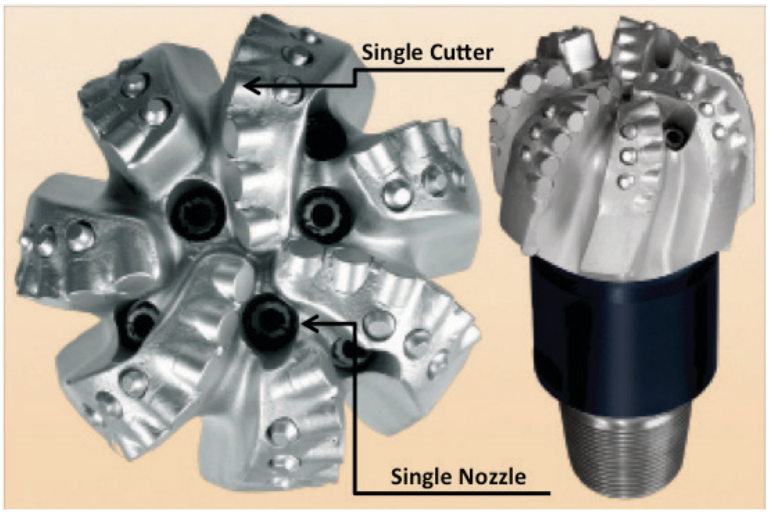

Figure 14: Top and Side View of a PDC Bit by Halliburton (Hsieh, 2010)

As a total description of the individual design parameters and newest advances in the bit sector would be a thesis by itself everything about single bit design parameters can be looked up in the book “Fundamental of Drilling Engineering; Chapter 6” (Mitchell et al., 2011).

2.1.3.5 Bottom Hole Assembly (BHA)

The BHA is a part of the string above the bit meant to provide load to the front end of the string by simultaneously increasing the stiffness of this part. Further more complex tools are part of the BHA concerning directional control and measurements. A BHA can be composed quite simple consisting only of drill collars (DC) and drillpipe (DP). Becoming more complex, multiple sizes of DC’s and DP’s may be part of the BHA and for some directional control stabilizers may be introduced. In general it can be said that over the last years as directional wells became more popular in any design the complexity of the wells increased and with them the complexity of the BHA. Meaning that more tools are used downhole trying to reduce the drilling complications. Common components and their role within the BHA will be mentioned for a better understanding how they have an impact on the system but as above to interpret different BHA designs and all the single parts of a BHA in detail would be a thesis by itself. Therefore for a deeper insight have a look into Chapter 8.2.2 of the “Fundamental of Drilling Engineering” (Mitchell et al., 2011, p. 479 ff.)

Drill Collar

A Drill Collar (DC) is a thick walled drillpipe used in the BHA providing additional stiffness reducing the buckling tendency of the BHA being under compression as WOB is applied.

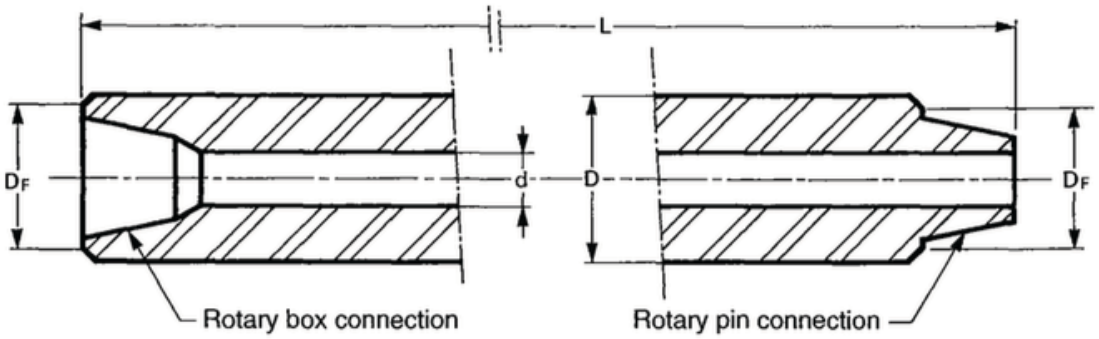

Figure 15: Drill Collar Side – Cut (Gabolde & Nguyen, 2006)

Dimensions of a typical thick walled DC are shown in Figure 15 visualizing that DC's are usually made out of one solid bar of steel with the connections cut into the pipe, male (pin) on the one end and box (female) at the other end, making inner or outer upsets redundant. The large diameter of DCs leads to a reduced clearance between the DC and the borehole wall resulting in larger contact area with the wellbore and therefore a higher risk of severe drillstring/wellbore interactions like differential sticking.

Heavy Weight Drillpipe

A sketch of a "Heavy Weight Drillpipe" (HWDP) is shown in Figure 16. The pipe is available with conventional drillpipe outer diameters although due to an increased wall thickness of about 1" for different sizes the weight is 2 – 3 times higher. Most of the heavy weight DP's have an integral center upset acting like a centralizer and a wear pad when run in compression. The tool joints are extra long to allow room for recutting connections and to reduce the wear of the pipe itself. Further the tool joints are normally like the center upset armed with a hardfacing to ensure a longer life. The pipes are used in the string above the collars in the transition zone from the stiffer collar and more limber drillpipe. In some small diameter holes HWDP is deployed instead of the thicker DCs.

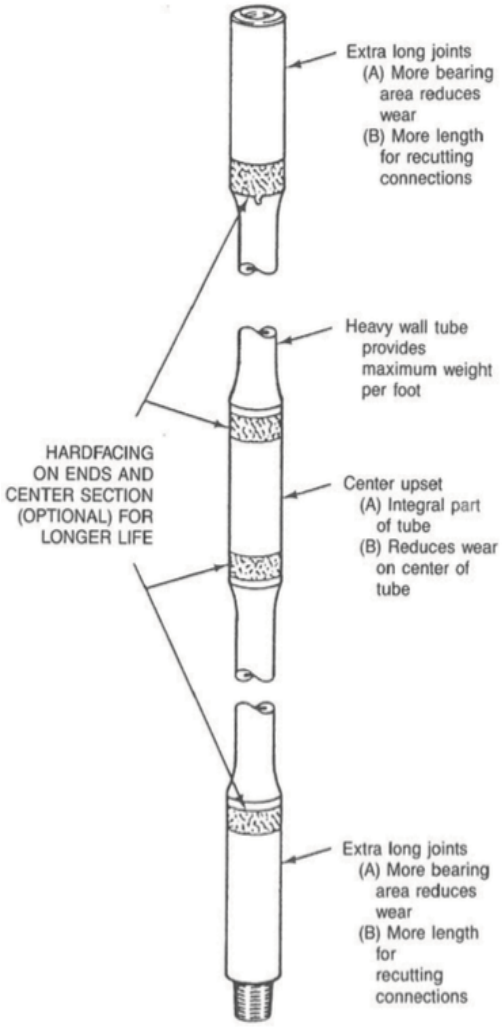

Figure 16: Sketch of a Heavy Weight Drillpipe (Adams & Charrier, 1985, p. 496)

The letters in Figure 17 are assigned to design parameters as A is the nominal pipe size, B the inside diameter, C the outside diameter of the central upset, D the outside diameter of the end upset and E the outside diameter of the tool joint for a range 2 pipe with a length of approximately 9,300 mm and tool joint minimal lengths for the box and pin.

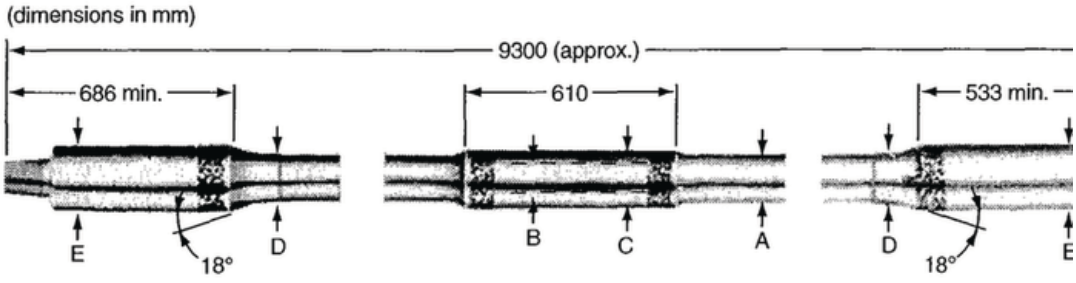

Figure 17: Heavy Weight Drillpipe Dimensions (Gabolde & Nguyen, 2006, p. B47)

The transition zone is the zone above the DCs, where often fatigue occurs, as most of the bending stresses are placed on the first few joints above the DCs. Normally using 5 to 7 HWDP joints above the DCs provides a more graduate change of stiffness and will reduce the fatigue damage.

Stabilizers

Stabilizers are an indispensible part of the BHA providing a centralization of the BHA and offering some directional control of the string through the contact forces at the contact points at the borehole wall. Different types of stabilizers are available fulfilling the same goal with different pros and cons. In general the basic form of stabilizer is based on the one of a normal drillpipe with the exception that it has a thicker middle section with so-called blades providing a flow path. This section acts like a bearing centralizing the string. Depending on the position of one or more stabilizers a certain directional control and additional stiffness of the string may be achieved. More information about the different types and pros and cons of different stabilizers like the Integral Blade Stabilizer, Welded Blade Stabilizer, Non – Rotating Stabilizer presented in Figure 18 can be found in the blog “Directional Drilling Technology” (Choudhary, 2011c).

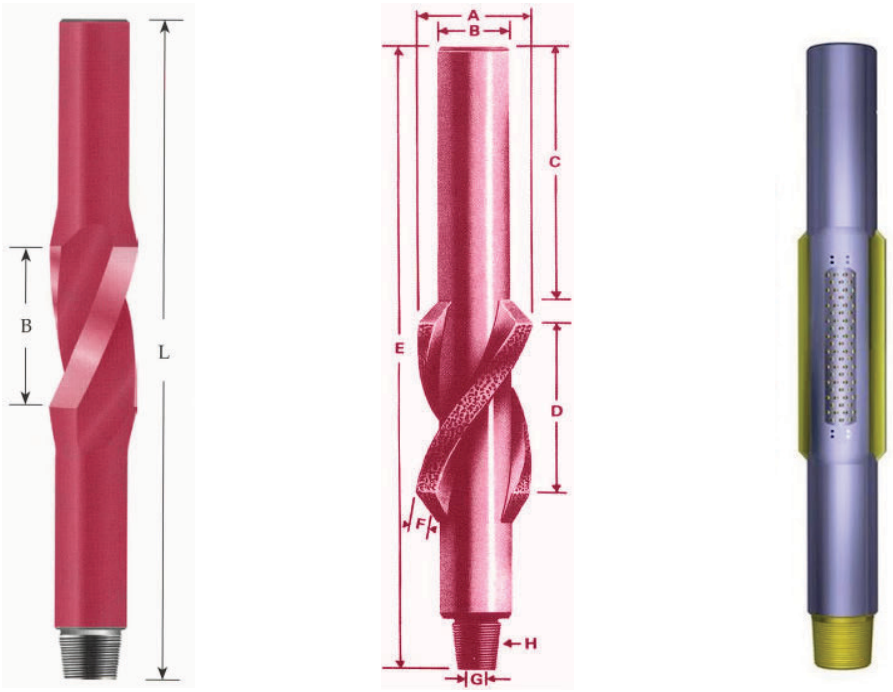

(a) (b) (c)

Figure 18: Sketch of Different Stabilizer Types; (a) an Integral Blade Stabilizer (b) a Welded Blade Stabilizer and (c) a Non – Rotating Stabilizer. (Choudhary, 2011c)

Directional Control Basics

With the right placement of stabilizers in the BHA it is possible to have a certain control over the inclination angle but the control of the azimuth is traditionally poor. There is always a side force at the bit that indicates if the BHA tends to build or drop or make it hold the inclination angle. This side force depends on the side forces along the BHA. Stabilizers help to introduce side forces artificially at pre-defined positions, acting like a bearing. Depending on the number of stabilizers deployed and their position the bending of the BHA alters as well as the side force at the bit.

Below in Figure 19 it is shown how near bit forces influence the directional control of the BHA as well as the bit tilt, which is the angle between the bit axis and hole axis as the bit tends to drill parallel to it. The presented assembly is a so-called build assembly with a full gauge near bit stabilizer acting as a lever pushing the bit to the upper side of the hole.

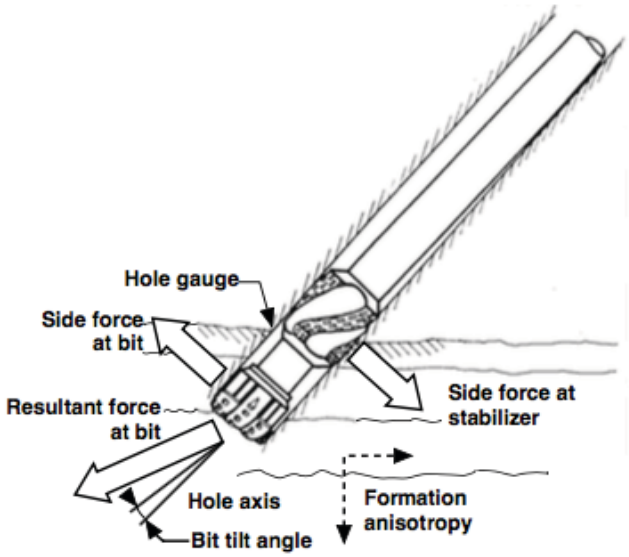

Figure 19: Sketch of the near Bit Forces Influencing Directional Control (INTEQ, 1995, p. 5–52)

Three directional control principles give an overview where to position stabilizers and how many along the BHA to get a certain directional control.

- Fulcrum Principle (built angle)
- Stabilization Principle (hold angle)
- Pendulum Principle (drop angle)

The background of these principles can be found in several textbooks. The Baker Hughes "Drilling Engineering Workbook" provides a good overview in chapter 6: "Directional Control with Rotary Assemblies". (INTEQ, 1995, p. 5–52)

Concerning a mathematical description of the side force at the bit and stabilizers with the help of the mechanical equilibrium can be found in the textbook "Fundamentals of Drilling Engineering" with the derivation of the model in chapter 8.2.2 "Mechanics of BHAs", (Mitchell et al., 2011, p. 479 ff.), or in the textbook "Applied Drilling Engineering" chapter 8.7 "Principles of BHA Design" (Bourgoyne, 1986, p. 426 ff.).

Drilling Downhole Motor

Downhole mud motors are nowadays commonly a part of the BHA directly above the bit to transmit additional torque and rotation to the bit. As directional control

equipment is part of the BHA a downhole motor may be essential to provide rotation of the bit while the string is sliding (nonrotating).

It is differentiated between two motor types a turbine motor and a positive displacement motor (PDM). Both the turbine motor and the PDM are hydraulically driven through the mud circulation system. To the longer-term use of PDMs an overview of their functionality and power consummation will be annotated quickly. For a deeper insight in PDMs and turbine motors see “Applied Drilling Engineering; Chapter 8.6.4” (Bourgoyne, 1986, p. 407 ff.).

Positive Displacement Motor (PDM)

The power assembly of a PDM that provides torque and rotation to the bit consists out of helical rod and stator (see Figure 20). The stator is made out of an elastomer and has always one lobe more than the rotor represented by the longer turning rod in the middle. Both together form enclosed helical cavities highlighted in black. Fluid pressed through these cavities leads to a rotation of the rotor, which is connected through a connection rod to the drive shaft and further to the bit. It is important that the stator provides an effective hydraulic seal around the rotor while at the same time letting it rotate freely.

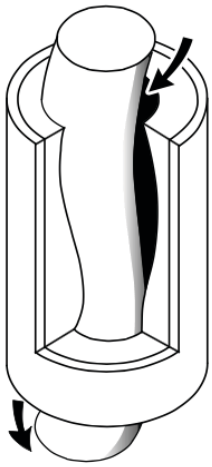

Figure 20: Sketch of Rotor and Stator forming a Helical Cavity in a PDM (INTEQ, 1995, p. 5–22)

As mentioned above the stator is constructed in a way that it has always one lobe more than the rotor. Consequently the lobe ratio influences the torque and

rotational output of the power section that may be transmitted to the bit as shown in Figure 21. The ratios are read in a way like 1:2 for one lobe of the rotor and 2 for the stator.

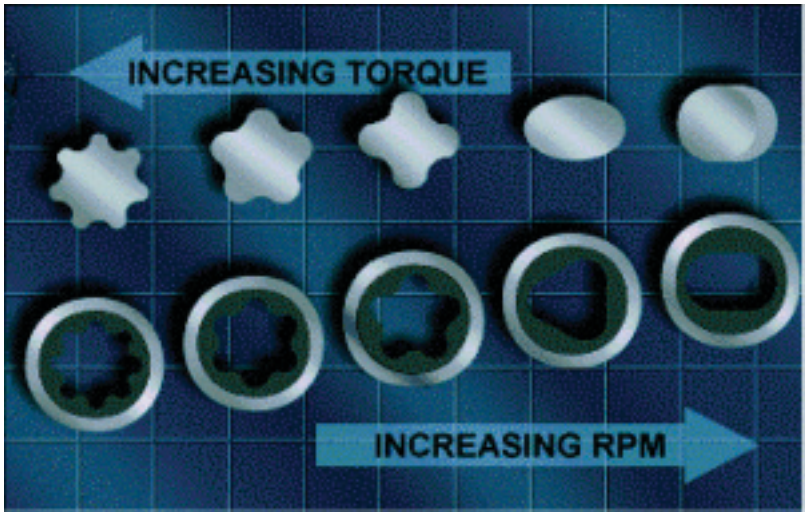

Figure 21: Visualization of Different Lobe Ratios for a PDM and their Influence on Torque and RPM (Society of Petroleum Engineers (U.S.), 2015)

The theoretical background as well as a mathematical description of the power exhibited by a PDM expressed in torque is given in the Appendix A.1.

Navigation Drilling Systems

To avoid the need of continuous repositioning of the stabilizers along the BHA to accomplish the given well path further directional control methods and tools were introduced to have a better and continuous directional control over the section to be drilled. These downhole navigation systems are based on the same principles as discussed above with the use of stabilizers. A side force is introduced artificially through a bend in the string or other gear pressing the string continuously in one direction. This side force gives the bit the tendency to drill a curved path in the desired direction.

It is distinguished between two different types of modern directional control equipment, the steerable system with Steerable Motor (SM) and the Rotary Steerable System (RSS). The SM system is designed in a way to achieve curvature by sliding, meaning that just the bit is rotated and not the string whereas the rotary steerable system (RSS) allows rotation of the whole string and maintaining at the same time directional control. The general idea is to tilt the axis of the bit with

respect to the axis of the borehole creating a side force at the bit generating curvature.

Steerable Motor System

SM's are downhole motors with a bent housing. The whole system can be operated in two ways either sliding or rotating. In the sliding mode the drillstring is not rotated to guide the bit in the direction of the target. In the rotational mode no guidance of the trajectory is provided. Both scenarios sliding and rotating are visualized below in Figure 22 showing that in sliding mode (left side) a smooth curved borehole is drilled out whereas rotating (right side) the drillstring results in a straight but eccentric wellbore. Furthermore it is to reckon that operating in sliding mode the friction will be way higher and the Rate of Penetration (ROP) normally lower.

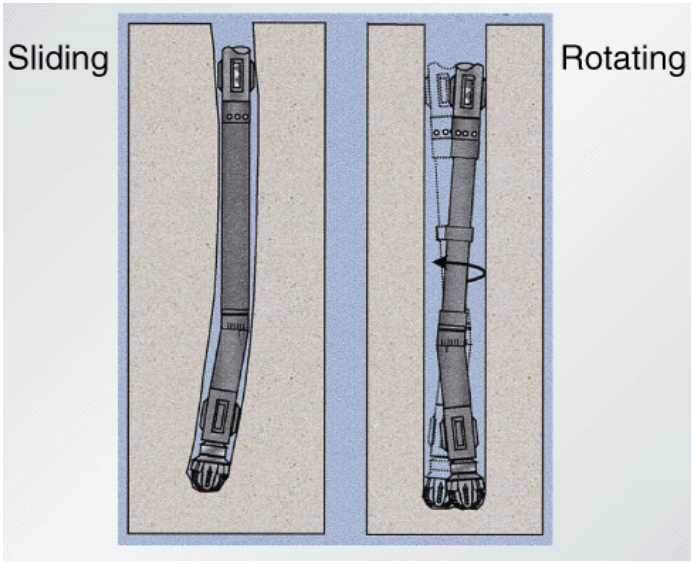

Figure 22: Steerable Motor Activities (Anon, 1998)

Coming to the bent housing the upper end is concentric with the normal drillstring body and the lower end of the housing is inclined in relation to the upper end. Bent subs with a motor attached are not that effective and not as common. Speaking about holes with inclinations >20° a motor with bend housing becomes necessary. The angel of the bend housing is normally adjustable setting the tilt angle somewhere between zero and a given maximum.

Rotary Steerable Systems (RSS)

These systems allow for a continuous rotation of the drillstring while steering. In general RSS systems have a better ROP compared to the standard SM systems. Further it results in better hole cleaning, less torque and drag and less eccentricity of the borehole as the string favorably rotates. Their increase in mechanical and electrical complexity result in a higher price and limits their use to extended reach wells. The two common RSS systems used in the industry are either the push-the-bit or point-the-bit system.

Push-the-bit RSS systems can achieve curvature of the wellbore by applying a side force with the help of stationary respectively non-rotating pad or stabilizer pressing against a segment of the borehole wall. This side force deflects the bit into the wanted direction.

Point-the-bit RSS systems control the direction in which the bit points by orienting a tilted shaft with the help of an internal hydraulic system. Attached to the end of this tilted shaft, which is repositioned continuously, the bit is points in desired direction in an ideal case with its tool face.

2.1.3.6 Interim Discussion: Drillstring and Wellbore Geometrical Relationships

The discussion above outlines that the wellbore is separated into an OH and CH section and introduces several different elements that all screwed up together form the drillstring. Looking at the overall picture this leads to the question how the drillstring and borehole geometries fit together and influence the overall drilling process itself. Therefore first some basic definitions have to be discussed concerning geometrical terms that arise as both drillstring and wellbore are put together.

Clearance & Annulus

With clearance the length of the gap between the round wellbore wall and the outer diameter of the normally round tool sitting in the wellbore is meant assuming that the tool is perfectly centralized. The clearance varies depending on the outer diameter of the tool and therefore severely influences the drillstring behavior, the string and wellbore interaction and the drilling hydraulics. As an example the clearances of two different tools are visualized below in Figure 23 pointing out the larger clearance of the DP with a smaller OD compared to the DC.

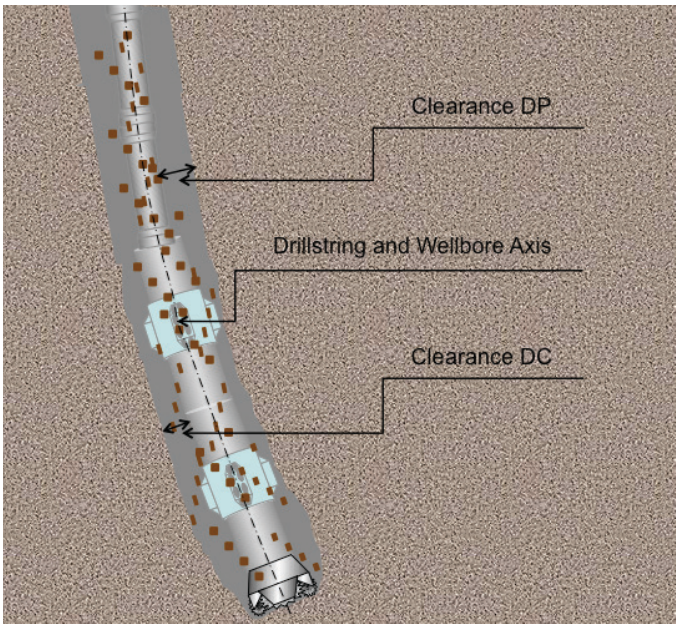

Figure 23: Centralized Drillstring Segment pointing out Different Clearances

The annulus is the cross section of any void in the wellbore between a tool (piping, tubing, etc.) and the formation being drilled in an OH. The cross sectional area of the annulus is given mathematically by Equation (3) whereas the capital D is the wellbore diameter, d the diameter of the drillpipe and A the cross sectional area of the annulus.

$$A = \frac{\pi}{4} * (D^2 - d^2) \quad (3)$$

The Effect of Different Annuli on Hydraulics

The annulus is used to circulate fluid in the well to clean out the cuttings generated by the drilling process. Therefore the cross sectional area (A in m^3) of the annulus plays a key role as it directly influences the velocity of the drilling fluid (v_m in m/s) at the point under investigation. Assuming that it is pumped at a constant rate (Q in m^3/s) through the annulus the continuity equation reads as follows.

$$Q = A * v_m \quad (4)$$

Rearranging Equation (4) shows it evidently that as the cross sectional area increases the fluid velocity decreases. Generally it is tried to keep the velocity in the annulus above a certain threshold value for both the vertical (±120 ft/s) and horizontal sections (± 240 ft/s) to achieve proper cleaning. Improper cleaning may result in an accumulation of cuttings (cutting beds).

Low fluid velocities can be expected in sections having large annular cross sectional areas and thin drillpipe sitting in it as encountered frequently while drilling the surface section. Concerning deeper sections (as the wellbore drilled becomes smaller) fluid velocities are less of a concern especially having drill collars with a larger diameter reducing the annular cross section.

Contribution to the Pressure Drop

Talking about the hydraulic design the pressure drop in the system is evaluated that has to be overcome with the help of surface pumping units to achieve the desirable fluid velocities. Knowing that the fluid velocity allows a conclusion about the pressure loss it can be said that high fluid velocities result in a larger pressure drop along a pipe of same diameter due to higher shear forces. Further the pressure drop is dependent on the type of fluid flow, which mainly can be described with the help of the fluid velocity and its viscosity. As a description of the different rheological types of fluid defining viscosity, yield point, etc. would be a thesis by itself this thesis won't cover that here. A detailed description about the different rheological models can be found in the book "Applied Drilling Engineering; Chapter 4.8: Rheological Models" (Bourgoyne, 1986). A mathematical background that shows how the cross sectional area influences the pressure drop can be found in the Appendix A.3.1.

Mechanical Effect of Different Annuli

A smaller annulus either due to an increase in the diameter of the tool or a decrease of the wellbore diameter can lead to an increase in the contact area of the tool and the wellbore. This can lead to drilling problems like differential sticking. The principles of differential pressure sticking can be found in the book "Applied Drilling Engineering" chapter 2.5.11 "Oil Muds for Freeing Stuck Pipe" as it will not be discussed in this thesis on its own.

From the other point of view a reduced clearance can also be beneficial when for example thinking about problems associated with the bending of the pipe under compression referred to as buckling discussed later.

Eccentricity

Eccentricity is the deviation of the tool in the wellbore from its centralization as shown below in Figure 24. This especially happens having an inclined borehole as the pipe rests on the lower side of the wellbore due to gravitational forces.

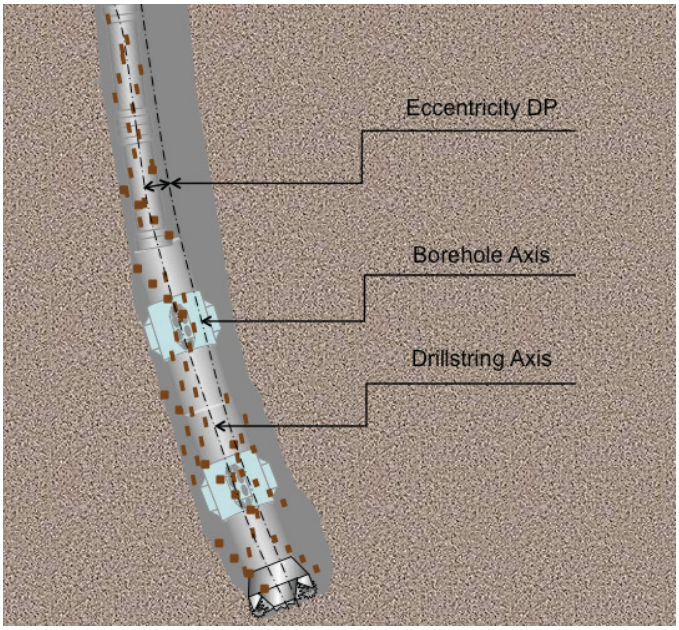

Figure 24: Sketch of a Wellbore and an Eccentric Drillpipe

Contribution to the Pressure Drop

Eccentricity plays a significant role concerning well cleaning problems as with a pipe lying on the lower side of the borehole enlarges the gap between the upper sided of the borehole and the drillpipe. A larger gap results in a reduced fluid velocity and therefore a reduced pressure drop. A lower velocity results further in inefficient cleaning abilities of the wellbore leading to drilling problems associated with e.g. accumulated cutting beds. A description of the frictional pressure drop in an eccentric annulus can be found in the Chapter 4.1 “Advanced Wellbore Hydraulics” of the book “Advanced Drilling and Well Technology” (Aadnøy et al., 2009, p. 214)

Mechanical Effect of Eccentricity

Eccentricity has a significant influence on the estimation of T&D taking into consideration that for example cutting beds may add an extra barrier to the axial movement.

Concerning the torque it will change depending on the actual position of the pipe, as it is less as the pipe tries to roll up the borehole wall as it is rotated and higher when

it rotates on the lowest side of the borehole wall. This phenomenon will be illustrated mathematically in the context with the T&D calculations discussed in the Appendix A.2.

2.2 Essential Rock Mechanics

Having introduced the different equipment needed downhole and different scenarios how it interacts with the wellbore this chapter will cover the principal aim of drilling. All what drilling is about is to penetrate the rock to generate a hole with the help of a long string that is simultaneously pushing and rotating the bit at its other end deeper into the formation. Doing that a significant amount of energy is needed which is tried to but into action as efficient as possible. To get an idea how much energy is needed to destroy different rocks the basic concept has to be understood how the rock fails as it is penetrated with a PDC bit and how much energy it consumes. Therefore here the commonly used rock failure mechanism in the oil and gas industry is introduced in context with failure due to shearing.

2.2.1 Rock Strength

Elementarily an axial load and torque at the bit lead to an energy transfer from the bit to the rock. At a sufficient level this energy transfer leads to the failure of the rock and this failure limit is commonly referred to as the “strength” of the rock. The strength is determined through laboratory tests depending if we simulate confining pressure (surrounding pressure) we speak of a tri – axial test otherwise of a uniaxial test. Below in Figure 25 a sketch shows the typical results for a uniaxial stress test wherein a slowly increasing axial force (F_z) is applied on a cylindrical rock sample without a confining pressure that leads to an axial stress (σ_z) and the advancing deformation (ε_z, strain of the sample along the x - axis), which is measured. Whereas the elastic region is a region of non-permanent deformation and the sample will regain his original state after a stress release. In the ductile region starting with the yield point a permanent deformation of the sample is introduced but it still can withstand loads whereas in the brittle region this feature rapidly becomes less with increasing stress till the rock breaks. The Uniaxial Compressive Strength (UCS) is the peak stress the sample can take. The sketch in Figure 26 represents basically the same except that now it is accounted for a constant confining pressure that leads to

a radial stress (σ_r). By applying different magnitudes of pressure as the sample is immersed in a closed oil bath that can be pressurized, the difference between the load applied and the confining pressure are plotted versus the strain. The strength of the rock sample in this case is the Confined Compressive Strength (CCS). (Fjar et al., 2008, p. 56)

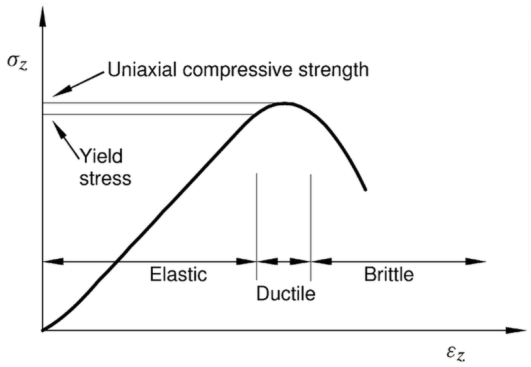

Figure 25: Sketch of a Typical Result from a Uniaxial Compression Test; (Fjar et al., 2008, p. 56)

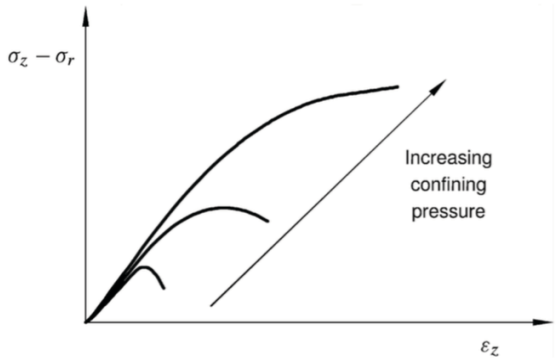

Figure 26: Triaxial Stress Test Sketch pointing out Confining Pressure Influence (Fjar et al., 2008, p. 57)

The confining pressure as seen in Figure 26 has a severe influence as it is increased the samples ability to support load is not lost despite its stiffness is reduced.

2.2.2 Failure of Rock

Although there can't be a generalization as there are different views when failure occurs it is assumed that a uniform definition of failure exists. With this assumption it is distinguished between tensile failures, shear failure and collapse of the pores.

Due to the assumption that a uniform definition of failure exists and the comparison of the two tests in the previous section it can be said:

- At a certain level of stress rock fails whereas below this level it stays intact.
- The total stress state has to be taken into consideration concerning this level and not just only the stress in one direction.

2.2.2.1 Shear Failure

Due to the tests the failure most often seen is the shear failure discussed here more in detail. As the shear stress along a plane reaches the upper limit the specimen can withstand shear failure occurs. It starts to gape resulting in a fault zone along the failure plane. The two sides of the plane will move relative to each other as indicated

in Figure 27 by the two parallel arrows in a frictional process. As the friction force acting against the relative movement is dependent on the applied axial force it is assumed that the critical shear stress (τ_{max}) can be put in relation with the normal effective stress (σ') acting over the shear plane stated below in Equation (5). (Fjar et al., 2008, p. 60)

$$\left|\tau_{\max}\right| = f\left(\sigma'\right) \qquad (5)$$

The effective stress (σ'), is the stress just carried by the matrix of the sample and not the stress as loaded on pore fluid for example in an undrained system (system where the fluid can't escape and therefore gets loaded). (Fjar et al., 2008, p. 33)

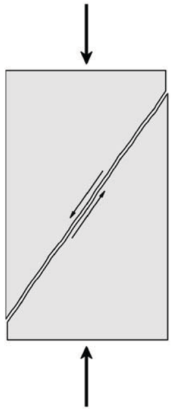

Figure 27: Sketch of Shear Failure along a Shear Plane (Fjar et al., 2008, p. 60)

The line in Figure 28 with the shear stress on the y – axis and the normal effective stress on the x – axis represents the hypothesis described above. It separates a safe region (below the line) where the rock is exposed to stress but will not fail from the region above the line where failure will occur. Furthermore an illustration of a Mohr's cycles connecting the indicated three principal stresses is shown representing a safe situation as no τ and σ' combination acts on a plane in the rock that is above the failure line.

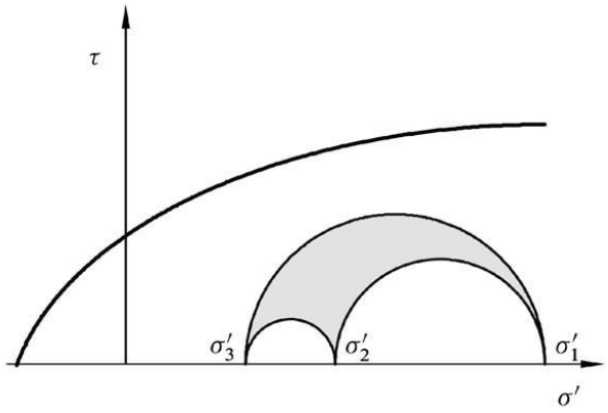

Figure 28: Sketch Representing a Failure Line and the Mohr's Cycles (Fjar et al., 2008, p. 61)

2.2.2.2 The Mohr – Coulomb Failure Criterion

Various solutions for Equation (5) can be found in literature. One of the most frequently used solutions as failure criterion for the oil and gas industry is the Mohr – Coulomb failure criterion. It assumes that the function f(σ') is a linear function of σ'.

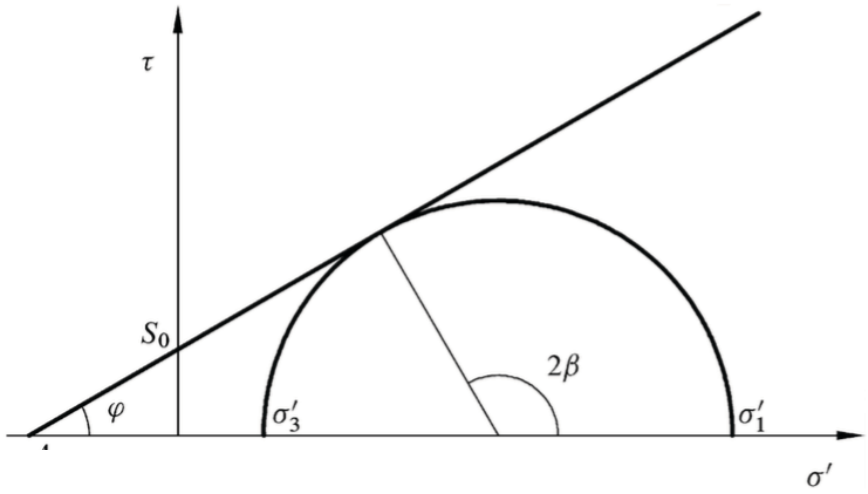

Figure 29: Representation of Mohr – Coulomb Failure Criterion (Fjar et al., 2008, p. 62)

The line in Figure 29 can be described by Equation (6) whereas S_0 is the cohesion or inherent shear strength of the material and μ the coefficient of internal friction that is related to the angle of internal friction (ϕ) by tan(ϕ) = μ.

$$|\tau| = S_0 + \mu * \sigma' \qquad (6)$$

The angel 2β representing the point where the Mohr Circle touches the failure line. Hence β as it is the angle where the failure criterion is fulfilled, gives the orientation of the failure plane.

2.3 Concepts to Evaluate the Drilling Efficiency

Having an idea now how much energy is needed to destroy a certain rock a reference value is provided to compare if the real drilling process is efficient or not. Although this reference parameter exists as discussed before it was, and still is common to use first as simple procedure, that gives an idea about the best drilling setting for the current setup. In this so-called "Drill off Test" the Rate of Penetration (ROP or R) is monitored as the Weight on Bit (WOB or W) changes continuously. Doing that the system is said to drill in the most efficient way when ROP is the highest. This test gives kind of a clue about the efficiency for a given set of drillstring and applied forces although it doesn't point out setups that could enhance drilling and therefore the efficiency. Considering that point the parameter "Mechanical Specific Energy" (MSE) was introduced in 1965 by Teale and implemented more frequently in the Industry in the last decade. Used as a trending tool objective changes in the system setup and drilling process can be verified and lead to an enhanced efficiency of the overall system itself.

2.3.1 Drill off Test

Data gathered for the cross plot like in Figure 30 to evaluate the fastest and therefore in this sense meaning the most efficient way to drill with a certain setup are typically gained from a drill off test. The test is normally executed several times with a different fixed rotation rate of the drillstring starting by applying a high WOB and locking the brake to prevent the string from advancing while it is continued to circulate and rotate. The bit drills ahead and due to the elongation of the string the WOB starts do decrease with time. With the help of Hook's law of elasticity implementing the change of WOB over time the ROP can be derived. Whereas equation (50) represents Hook's law broken down into its single contributing parameters, where E is the longitudinal Elastic Modulus of the material (Steel ≈ 200,000 MPa), Δσ the change in the stress on the cross sectional area broken down into ΔF the change in force acting axially here represented by ΔWOB in Newton and

A the cross sectional area of the drillpipe in m^2, ε the strain split into the ΔL the change in length and L the original length both in meter.

$$E = \frac{\Delta\sigma}{\Delta\varepsilon} = \frac{\Delta F/A}{\Delta L/L} = \Delta F * \frac{L}{\Delta L * A} = \Delta WOB * \frac{L}{\Delta L * A} \quad (7)$$

Rearranging equation (50) so that ΔL is expressed with the help of the other parameters and dividing it by the time drilled that yielded this difference in length and change in WOB results in an averaged ROP over this time period.

$$ROP = \frac{\Delta L}{t} = \frac{\Delta WOB}{t} * \frac{L}{E * A} \quad (8)$$

Equation (51) yields the averaged ROP over a given time interval normally computed with the help of data gathered in a drill off test delivering a curve as shown below in Figure 30.

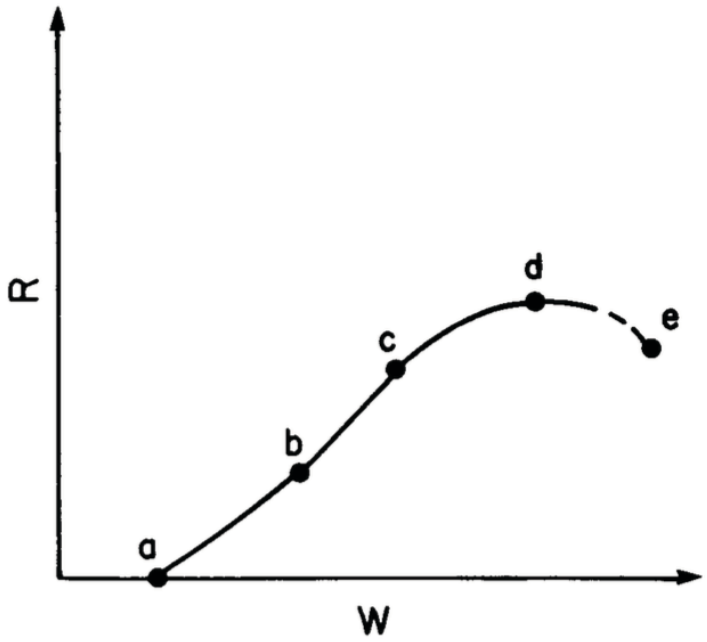

Figure 30: Sketch of a Typical Curve Obtained from a Drill Off Test (Bourgoyne, 1986, p. 226)

For a better understanding of the curve, resulting from a drill off test, here is given a short explanation by dividing it into three regions:

I. a – b: Due to insufficient WOB the performance is not given as the cutters of the bit do not intrude deep enough into the rock to operate on their peak efficiency.

II. b – c: With increasing WOB the Depth of Cut (DOC) becomes sufficient and the bit starts to operate with its peak efficiency (ability to transfer energy from the bit to the rock) between 30 – 40% due to its intrinsic design (Dupriest & Koederitz, 2005, p. 2). Therefore ROP increases linear with increasing WOB for a given formation up to the deflecting point even though the bit efficiency is not changing.

III. c – e: Reaching point c the "Founder Point" the third section starts including point d representing the highest ROP that can be achieved with the current setup. From the founder point ahead the energy transfer from the bit to the rock becomes inefficient again and the curve deflects.

Due to this analyze it can be said that the part where we drill the fastest and most efficient is in region II close to the founder point. Another essential realization is that due to environmental changes (like a change in drilling fluid from aqueous to non aqueous) applied to the drilling system in region II the ROP won't increase. Just by increasing the energy at the bit applying a higher WOB or RPM the ROP can be increased.

2.3.1.1 Drilloff Test Setting the Benchmark

The drill of test is a tool used to find out the maximum ROP that could be achieved with the current system in the given formation but it doesn't give information about changes to be made to become more efficient. To increase the overall linear portion of the drill off curve (region II) a redesign of the system is necessary that may extend the constraining limits and the point at which founder occurs. (Dupriest & Koederitz, 2005, p. 2)

2.3.2 Introduction of Mechanical Specific Energy (MSE)

In 1965 the parameter MSE was introduced by Teale to provide a better understanding how much energy is needed to excavate a certain volume of rock in the context with drilling. He stated that: *"It is axiomatic that, to excavate a given volume of rock, a certain theoretically attainable minimum quantity of energy will be required. Its amount will depend entirely on the nature of the rock. Real mechanical process might or might not approach this theoretical minimum: the difference*

between actual and theoretical requirements would be a measure of work dissipated." (Teale, 1965, p. 59)

This work dissipated may be due to mechanical losses breaking the drilled rock further into smaller fragments, friction losses between tools and rock or other mechanical losses.

By measuring the axial and rotational work on the surface or downhole and linking it to the volume drilled, Teale introduced a mathematical model that illustrates the energy needed to excavate this certain volume of rock.

Specific Axial Energy:

As work is defined as the force acting on a body, times the displacement due to the force, the axial work can be defined as the WOB times the ROP. Dividing the work done by the volume drilled where A is the cross section of the bit the specific axial energy to excavate this volume is obtained through Equation (9).

$$SE_a = \frac{Work}{Volume} = \frac{WOB * ROP}{A * ROP} = \frac{WOB}{A} \quad (9)$$

Specific Rotational Energy:

The applied force here is the torque (T) measured at the surface or downhole that rotates the drillstring times the displacement due to rotation. The specific energy term then is again obtained by dividing this work done by the volume drilled.

$$SE_R = \frac{Work}{Volume} = \frac{2\pi * RPM * T}{A * ROP} \quad (10)$$

Mechanical Specific Energy:

Adding these two terms together the total energy needed to excavate a certain volume of rock is obtained in Pascal.

$$MSE = SE_a + SE_R = \frac{WOB}{A} + \frac{2\pi * RPM * T}{A * ROP} \quad (11)$$

2.3.2.1 Efficiency Based on MSE and a Reference Parameter

MSE alone is not worth much what applies the need of a reference parameter. Testing MSE in the laboratory Teale found out that, the minimum energy needed to drill through a certain rock is in the order of the unconfined compressive strength of

this rock. The relation between MSE and UCS is not precise as there is no obvious physical similarity though as compressive strength and specific energy is both a function of the rock strength there must be some kind of relationship between them. Since this relationship is dimensionally identical and of the same order, it seems convenient to use it for the time being till a better reference value is found.

Having UCS defined as the reference parameter representing the minimum theoretical energy needed to excavate a given volume of a certain rock the efficiency of the actual drilling process can be evaluated by Equation (12).

$$Efficiency = \frac{MSE_{Min}}{MSE_{Actual}} * 100\% = \frac{UCS}{MSE_{Actual}} * 100\% \quad (12)$$

Mechanical Specific Energy as a Trending Tool

MSE, if at all, may indicate that it is drilled efficient or inefficient with the current system according to too much measured energy needed to drill a current formation. It does not tell what setting or equipment is operated inefficient respectively which bit rock interactions lead to a waste of energy loss but with its help nowadays trend patterns can serve as a trending tool to foretell near bit inefficiencies and verify changes in the drilling system. Therefore the paper by (Dupriest & Koederitz, 2005) provides a deeper insight into different trend patterns associated with inefficiencies in the drilling process.

2.3.2.2 Interim Discussion: The Generalization of MSE

Using MSE in the field requires first filtering out the energy losses along the drillstring from the surface down to the front end of the string the bit. Normally this is done by subtracting the energy needed for rotating the bit off bottom from the MSE measured as drilling continues. Doing this UCS should with all small inaccuracies roughly equal MSE as presented below in equation (13) in an efficient working system.

$$UCS \approx MSE = \frac{F}{A} + \frac{2\pi * RPM * T}{A * ROP} \quad (13)$$

Having a system that precedes inefficiently the energy input and therefore the MSE as visualized in Equation (14) will be expectedly way higher compared to the UCS expected for the formation currently drilled.

$$Inefficiency \rightarrow MSE >> UCS \quad (14)$$

Considering the fact that significant more energy is needed at the bit to drill a certain volume of rock drilling inefficiently the measured MSE for such a system may be split up (Figure 31) into the expected energy needed equal the UCS and the extra energy needed spend in to dissipated energy.

Figure 31: Splitting up MSE

The dissipated energy is tried to breakdown into main terms influencing energy consumption at the bit whereas it can be said that the needed cutting force at the bit is related to the UCS in an ideal state. Therefore for the beginning it is assumed that the extra energy is spent into torque, drag, hydraulics and vibrations (Figure 32).

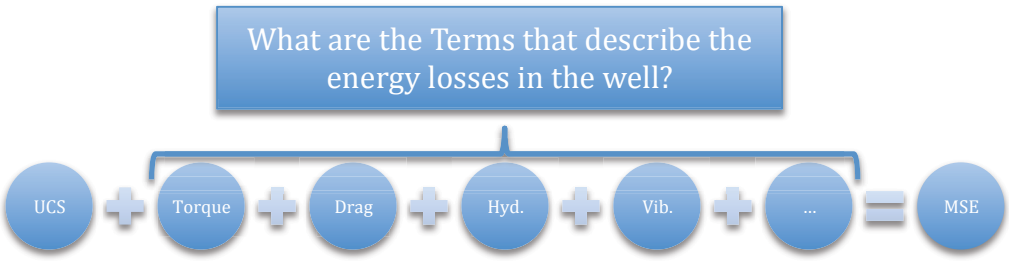

Figure 32: MSE and the Missing Terms

MSE seems to be a reasonable try to assess the energy loss at the bit, unfortunately there are no mathematical terms yet included into the general form of the MSE Equation (11) assigning energy losses to the different processes responsible for a waste of energy if drilling inefficiently.

3 The Governing Models Describing the System

T&D, hydraulics and drilling dynamics are identified as the three superior models describing the behavior of the system. Behind each model stands a general theoretical principle that defines the unavoidable type of process responsible dissipating energy downhole.

Following the models will be discussed shortly and the governing differential equations quoted that are standing behind these models. Additionally, several single processes contributing to the superior models will be identified to get an idea what has to be counted for, when and where.

3.1 The Models in their General Form

In general a T&D model represents a system of equations that is used to calculate forces and moments in the pipe, as well as the forces generated due to the interaction between the pipe and the wellbore. The task of a hydraulic model is to display the pressure at various points in the well, what becomes rather complex when either the drilling mud or the drillstring is moving. Vibrations and shocks can't be seen as static processes, like it is normally done for T&D and hydraulics, they are continuously present but of different magnitude along the drillstring.

3.1.1 Torque & Drag

As the drillstring is in contact with the wellbore, it will, depending on its position in the wellbore, the axial load and drilling dynamics, experience contact forces of different magnitude. These contact forces result in frictional forces, acting against the direction of movement of the string, and bending forces. Drilling engineers try to model the state of the drillstring, at every point in the wellbore, through so-called torque and drag models.

The two following equations are the governing differential equilibrium equations describing the forces acting along the drillstring. Further the equilibrium equations revealing the different loads acting on the drillstring are presented with respect to a curvilinear coordinate system. For a better understanding it has to be stated that this system is a moving coordinate system where $\vec{u}(s)$ defines the position of the

drillstring and the triad of $[\vec{t}(s), \vec{n}(s), \vec{b}(s)]$ form the axis of the moving coordinate system. The additional two derivatives needed to define the coordinate system are, $\kappa\ (s)$ defining the curvature, and $\tau\ (s)$ that is the torsion of the curve. In detail the coordinate system is derived in Aadnøy book. (Aadnøy et al., 2009, p. 162)

3.1.1.1 The Force and Momentum Balance in a Drillstring

Force Balance in a Drillstring: Equation (15) describes the change in pipe force $\vec{F}$ due to an applied-load vector $\vec{w}$ (the resultant of all external forces), which is a force per unit length of the drillstring.

$$\frac{d\vec{F}}{ds} + \vec{w} = \vec{0} \qquad (15)$$

Moment Balance in a Drillstring: Equation (16) describes the change in moment $\vec{M}$ that comes from an applied-moment vector $\vec{m}$ per unit length and a pipe force $\vec{F}$.

$$\frac{d\vec{M}}{ds} + \vec{t} \times \vec{F} + \vec{m} = \vec{0} \qquad (16)$$

<u>The Loads on a Drillstring</u>

The loads acting on the drillstring are defined by the load vector $\vec{w}$ and the applied-moment vector $\vec{m}$. The load vector $\vec{w}$ is composed out of following terms:

$$\vec{w} = \vec{w}_{bp} + \vec{w}_{st} + \Delta\vec{w}_{ef} + \vec{w}_c + \vec{w}_d \qquad (17)$$

where:

$\vec{w}_{bp}$ = the buoyant weight of the pipe,

$\vec{w}_{st}$ = the stream-thrust forces,

$\Delta\vec{w}_{ef}$ = the load on the string due to complex flow patterns in the annulus,

$\vec{w}_c$ = the resultant normal contact force acting on the string as the drillstring contacts the wellbore, and,

$\vec{w}_d$ = the frictional load that is associated with the contact force.

The last two terms are the mechanical force terms.

Friction is taken into account through the relative simple Coulomb friction model described by Aadnøy in his book as follows: "*If two surfaces in contact with a normal force F_N are sliding relative to each other, the frictional force points in the direction opposite to the motion and has the magnitude of the product of the contact force and dynamic coefficient for friction μ_f.*"

$$\vec{w}_d = \pm \mu_f w_c \vec{t} \quad (18)$$

The applied-moment vector $\vec{m}$ is further associated with the friction force and given by the following equation:

$$\vec{m} = \pm \mu_f w_c \vec{t} \times r_0(-\cos\theta\, \vec{n} - \sin\theta\, \vec{b}) \quad (19)$$

indicating that, as the drillstring is rotated, the friction force is no longer orientated axially whereas it now acts against the direction of rotation. Here r_0 is the lever between the center of rotation and the tangential friction force.

Mechanical Response of the Drillstring

The force and the momentum experienced by the drillstring are given by the force vector $\vec{F}$ and the momentum vector $\vec{M}$. The force vector is composed out of following forces:

$$\vec{F} = F_a \vec{t} + F_n \vec{n} + F_b \vec{b} \quad (20)$$

where $F_a$is the axial force and F_n and F_b the two shear forces in the normal and binormal direction. The moment experienced by a pipe is composed of the following terms:

$$\vec{M} = EI\kappa \vec{b} + M_t \vec{t} \quad (21)$$

where EI gives an idea of the bending stiffness of the pipe, κ is the curvature and M_t the axial torque.

General Equilibrium Equations

By substituting the above defined load equations (17) - (19) into the equilibrium equations (15) and (16) yields the general equilibrium equations, assuming a general-curvature trajectory. (Aadnøy et al., 2009)

$$\frac{d}{ds}F_e - \kappa F_n + w_{bp}\left(\vec{t}\cdot\vec{\imath}_z\right) + \vec{w}_d \cdot \vec{t} = 0 \quad (22)$$

$$\frac{d}{ds}F_n + F_e\kappa - F_b\tau + w_{bp}(\vec{n}\cdot\vec{\imath}_z) - w_c\cos\theta + \vec{w}_d \cdot \vec{n} = 0 \quad (23)$$

$$\frac{d}{ds}F_b + F_n\tau + w_{bp}\left(\vec{b}\cdot\vec{\imath}_z\right) - w_c\sin\theta + \vec{w}_d \cdot \vec{b} = 0 \quad (24)$$

$$\frac{d}{ds}M_t + \vec{m}\cdot\vec{t} = \vec{0} \quad (25)$$

$$-ET\kappa\tau + M_t\kappa - F_b + \vec{m}\cdot\vec{n} = \vec{0} \quad (26)$$

$$ET\frac{d\kappa}{ds} + F_n + \vec{m}\cdot\vec{b} = \vec{0} \quad (27)$$

3.1.1.2 Simplifications and Limits of T&D Models

Soft String Model

Standardly in the industry it is account for T&D through the so-called “soft string” models. These models assume:

- Continuous contact between the pipe and the wellbore along a specified drilling trajectory (effects of couplings, tool joints, wellbore irregularities and tortuosity are ignored).
- Inertial effects due to pipe sliding and rotation are ignored.
- Effects due to the drilling-fluid flow are not taken into account.
- Friction is modeled with the help of the Coulomb friction model.
- It is not accounted for bending moments.
- The force acting on the drillstring acts tangential to the trajectory.

These assumptions lead to a significant simplification, as just a single force and a single torque need to be determined to solve the equilibrium problem. Without the simplifications all the forces, moments, and displacements along the drillstring are unknown. Therefore the locations of the contact forces between the drillstring and the wellbore are also unknown.

Additionally, the loads defined by the terms $\vec{w}_{st}$ and $\Delta\vec{w}_{ef}$ that contribute the load vector $\vec{w}$, are normally left out due to their advanced nature of computation.

Stiff String Model

Besides the soft string models more complex models came up accounting for bending and clearance. These more complex models are the so-called stiff string models and should be closer to reality compared to the soft string model.

Due to the available survey data today the accuracy of the soft string model seems to be efficient as the stiff string model relies on accurate knowledge of the downhole hole- and string- geometry, radial clearance and tortuosity effects. This means that stiff string models just will offer an advantage in accuracy as more accurate input parameters are computed from real-time multi sensor measurements. (Philipp Doppringer, 2014)

3.1.2 Hydraulics

The complexity of the system makes it difficult to determine the pressure loss at every point of the system. Nevertheless according to Mitchell et al., it is important to know: *"(1) flowing bottom hole pressure or ECD during drilling; (2) the bottom hole pressure or ECD during tripping operations; (3) the optimum pump pressure, flow rate, and bit nozzle size during drilling operations; (4) the cuttings-carrying capacity of the mud; and (5) the surface and downhole pressure that will occur in the drillstring during well-control operations for various mud flow rates."* (Mitchell et al., 2011, p. 194)

The movement of the fluids is described through physical laws represented by the continuity-, momentum- and energy- equation. These governing equations are presented in the form of partial differential equations below.

3.1.2.1 Mass Balance Equation

The general form of the mass balance- or continuity- equation is given in form of equation (28), stating that mass is neither produced nor destroyed.

$$\frac{\partial \rho}{\partial t} + \frac{\partial \rho v_i}{\partial x_i} = 0 \qquad (28)$$

Equation (39) is the mass balance equation in Cartesian coordinates for a Newtonian fluid.

$$\frac{\partial \rho}{\partial t} + \left(v_x \frac{\partial \rho}{\partial x} + v_y \frac{\partial \rho}{\partial y} + v_z \frac{\partial \rho}{\partial z} \right) + \rho \left(\frac{\partial v_x}{\partial x} + \frac{\partial v_y}{\partial y} + \frac{\partial v_z}{\partial z} \right) = 0 \qquad (29)$$

The equation in general states that in a steady state process, the amount of a mass that enters a system is equal to the amount of mass that leaves the system. The first term $\frac{\partial \rho}{\partial t}$ gives the change of the density over time, the second and third term give the rate at which mass is flowing in and out of a control volume.

Simplifications Concerning the Mass Balance Equation

For drilling purposes this model is normally simplified due to the complexity of the system and the unknowingness how fluid parameters change along the system. Several of these assumptions to simplify the governing mass balance equation are stated below:

- Single-phase flow.
- A drilling engineer commonly just considers steady-state flow conditions (all time derivatives become zero).
- A constant flow area is assumed.
- Drilling fluid is assumed to be incompressible (no change in density).
- The flow rate of an incompressible fluid is the same at all points in the well.
- Flow is along the wellbore and varies perpendicular to it (no flow in the other directions).

Therefore the mass balance equation takes the relative simple form:

$$Q = \rho v A \qquad (30)$$

where:

Q = the mass flow rate, kg/s, and

A = the flow area, m^2.

3.1.2.2 Momentum Balance Equation

Following the partial differential equation of the momentum balance equation is presented for an incompressible Newtonian fluid in tensor notation:

$$\rho \frac{\partial v_i}{\partial t} + \rho v_j \frac{\partial v_i}{\partial x} - \mu \frac{\partial^2 v_i}{\partial x_j \partial x_j} = -\frac{\partial p}{\partial x_i} + \rho g_i \quad (31)$$

where the first two terms represent the inertia forces acting on the fluid as the term $\rho \frac{\partial v_i}{\partial t}$ represents the velocity change over time and $\rho v_j \frac{\partial v_i}{\partial x}$ the convectional forces within the fluid. The next two terms represent divergences of stress where the first term $\mu \frac{\partial^2 v_i}{\partial x_j \partial x_j}$ equals the diffusion and $\frac{\partial p}{\partial x_i}$ equals the force due to an internal source. The last term ρg_i represents the body force acting on the fluid.

Simplifications Concerning the Momentum Balance Equation

For the momentum balance applies the same. To reduce the complexity of the equation normally the same simplifications as for the mass balance equation are taken into account. Equation (31) presented above is already simplified in a way that it is just valid for incompressible Newtonian fluids.

3.1.2.3 Energy Balance Equation

Aside the pressure losses driving the drilling fluid down the pipe, through the bit and up the annulus the fluid also experiences a change of its internal energy along its round trip. When we speak of a single phase drilling fluid the energy conservation equation is an extension of the first law of thermodynamics. The energy balance equation for a single-phase fluid for an incremental control volume in integral form follows:

$$\int_{\Delta z} \rho \dot{\varepsilon} A dz = -\int_{\Delta z} p \frac{dv}{dz} A dz + \phi + Q + R \quad (32)$$

where

$\dot{\varepsilon}$ = rate of change of internal energy = $\frac{\partial \varepsilon}{\partial t} + v \frac{\partial \varepsilon}{\partial z}$, W/kg,

ϕ = viscous dissipation, W,

Q = heat transferred into the volume, W,

R = rate of volume energy added, W.

The first term in equation (32) represents the rate of change of internal energy of the control volume. The second term represents the rate of work done due to external forces, which is of significance when compressible flow is involved. The third term ϕ gives the work done to overcome friction (viscous forces). Q represents the total heat influx into the control volume and R any additional sources of heat. (Aadnøy et al., 2009, p. 806)

Equation (32) can be rewritten in a way so that pressure and temperature are the independent variables:

$$\int_{\Delta z} \rho C_p \frac{\partial T}{\partial t} A dz + \int_{\Delta z} \rho v C_p \frac{\partial T}{\partial z} A dz - \int_{\Delta z} v \beta T \frac{dp}{dz} A dz = \phi + Q + R \qquad (33)$$

where

C_p = heat capacity at constant pressure, J/kg*K,

β = isobaric coefficient of thermal expansion, 1/K, and

T = the absolute temperature in K. (Aadnøy et al., 2009, p. 806)

Simplifications Concerning the Energy Balance Equation

For drilling operations the same general simplifications are taken into account for energy balance equation as for the mass balance and momentum balance equation.

Further it can be stated that the term R representing any additional source of heat is neglected in most wellbore flow situations.

3.1.3 Drilling Dynamics

The dynamical behavior of the drillstring can be split into two dominant processes the so-called “Shocks” and “Vibrations”. A shock is given through the unexpected input of energy due to the impact of downhole components with the borehole. The vibrations are the periodic response as a result of the shock. Vibrations and shocks lead depending of the type of vibration to an axial or radial displacement of the affected tool. This movement is measured in Gs where one G equals the gravity that is defined by the acceleration (9.81 m/s^2, or 32.3 ft/s^2). A theoretical background for

the different vibration types and their impact on the system is presented in the Appendix C.1.

The main underlying governing differential equation for the axial and torsional vibration is the undamped classical wave equation (equation(34)), which is a second-order partial-differential equation for the undamped axial motion of a linear elastic bar. (Aadnøy et al., 2009, p. 118)

$$\frac{\partial^2 \xi(x,t)}{\partial x^2} = \frac{1}{c^2}\frac{\partial^2 \xi(x,t)}{\partial t^2} \quad (34)$$

With regard to the drillstring it is differentiated between axial, torsional and lateral vibrations. Therefore, following the equations of motion, for a drillstring, are stated below for each vibration type.

3.1.3.1 Continuous Axial Vibration Model:

The first equation, equation (35) is the equation of motion for the axial vibrations:

$$\rho\frac{\partial^2 \xi}{\partial t^2} - E\frac{\partial^2 \xi}{\partial x^2} + c_a\frac{\partial \xi}{\partial t} + \rho g_z = g_a\left(x, t, \xi, \frac{\partial \xi}{\partial x}, \frac{\partial \xi}{\partial t}\right) \quad (35)$$

where

ξ = the axial motion,

c_a = the dampening factor,

E = Young's modulus,

ρ = the density of the material,

g_z = the acceleration by gravity and

g_a = the eternal axial force per unit mass applied on the drillstring.

Concerning the equation the first term $\rho\frac{\partial^2 \xi}{\partial t^2}$ = inertial force, $E\frac{\partial^2 \xi}{\partial x^2}$ = the rate of strain change, $c_a\frac{\partial \xi}{\partial t}$ = the force due to viscous dampening and ρg_z force due to the deadweight of the element. (Aadnøy et al., 2009, p. 118 f.)

3.1.3.2 Continuous Torsional Vibration Model:

The governing differential equation for the torsional vibration of the drillstring, equation (36) is very similar to the axial equation of motion. A proper substitution of

the variables and the consideration that there is no initial strain from gravity yields following equation:

$$\rho J \frac{\partial^2 \phi}{\partial t^2} - JG \frac{\partial^2 \phi}{\partial x^2} + c_\theta \frac{\partial \phi}{\partial t} = g_T(x, \phi, t) \quad (36)$$

where

J = the polar momentum of inertia of the cross section of the drillstring,

ϕ = the angular displacement of the section,

G = shear modulus of the material of the drillstring

c_θ = the dampening factor and

g_T = the torsional applied load.

In the torsional equation of motion $\rho J \frac{\partial^2 \phi}{\partial t^2}$ = the inertial force, $JG \frac{\partial^2 \phi}{\partial x^2}$ = the torsional rate of strain change and $c_\theta \frac{\partial \phi}{\partial t}$ = the force from viscous dampening.

3.1.3.3 Continuous Lateral Vibration Model:

The continuous lateral vibration model is described with the help of the Euler-Bernoulli beam theory and an adoption of the small-slopes assumption. Further several hypotheses are made. First of all the beam is considered to be elastic where the stresses and strains are related through Hooke's law. The second hypothesis is that plane sections that are normal to the beam axis remain plain and normal to the beam axis after deformation. Additionally the effect of an axial force has to be taken into account. (Aadnøy et al., 2009, p. 126) All these assumptions lead to the following differential equation:

$$\rho \frac{\partial^2 u}{\partial t^2} + \frac{\partial^2}{\partial x^2}\left(EI_z \frac{\partial^2 u}{\partial x^2}\right) - P \frac{\partial^2 u}{\partial x^2} = g(x, t) \quad (37)$$

Where

u = the lateral displacement,

ρ = the density of the material,

E = Young's Modulus,

I_z = the moment of inertia of the cross section and

g = the external loading.

Simplifications and Limitations Concerning the Vibration Models

As it was identified that the wave equation can be used to some extend for analytical solutions it is almost impossible to model the different vibration modes realistically due to their immense complexity. However, models could be used to study the different vibration modes and their interplay with additional downhole equipment designed to absorb some of the vibrational energy.

Aadnøy et al. summarize the factors leading to the complexity of the system in one sentence: "*Drillstring vibrations are extremely complex because of the random nature of a multitude of factors such as bit/formation interaction, drillstring/wellbore interaction and hydraulics.*

Furthermore, the governing vibration models above just give an idea of the vibration itself, but don't say anything about the relationship of the vibration and the causing circumstances.

3.2 The Processes Contributing to the Superior Models

To get an idea how many different processes take place simultaneously during drilling and contribute to the different models some of the essential processes are listed here in this chapter.

3.2.1 Unavoidable Energy Consuming Processes

Unavoidable energy consuming processes represent intentional processes and also parasitic processes that are always present during the drilling processes and can't be eliminated.

Torque & Drag

During drilling the drillstring is lowered and rotated at the same time resulting in T&D forces acting on the string changing the axial- and rotational- load on the string. Both torque and drag are resultant forces due to friction. The calculations and the theory behind a soft string T&D model and the estimation of bit torque are presented in the Appendix A.2.

Cutting

Cutting is the action describing the destruction of the rock through the bit. The idea is that the bit is in contact with the formation with its tool face and the gauge protection both armed with numerous cutting elements transmitting energy from the bit to the rock. Every single cutter should feel a certain cutting force, which is the force needed to destroy the rock. In fact this process is the intentional process of drilling and results in T&D accompanied by an excessive heat generation changing the temperature of the drilling fluid, equipment and environment.

Directional Control

Changes of the loads on the drillstring due to directional control play a significant role at the bit and along the BHA.

A side force or a reorientation of the tool face pointing in the desired direction to drill is introduced at the bit for directional control resulting in extra T&D.

Curvature of the wellbore will be achieved nowadays normally with the help of directional control equipment placed along the BHA. These tools for the directional control introduce additional contact forces at different contact points leading to a change of the T&D readings.

Skin Friction

Ignored in the discussions till now was that the drilling fluid in the annulus counteracts the axial and rotational movement of the string caused by the so-called skin friction which is the friction of the fluid against the “skin” (surface) of the object that the fluid is moving along. This additional friction acting on the string results in additional torque and drag. The question is how big the influence of the skin friction is and if it does play a role in the T&D readings.

Hydraulic Lift

The pressure needed at the bit to clean properly can negatively affect the axial load put into the system to drill ahead. The hydraulic lift is the counter force also called the “Pump Off Effect” acting against the WOB due to the hydraulic backpressure beneath the bit.

3.2.2 Unintentional Energy Consuming Processes

By now in the preceding chapters just energy losses were presented that are expected to occur in context with “ideal” drilling operations not counting for drilling problems or irregularities. Meaning events that may occur and disappear on occasion associated with drilling problems were left out so far as in a first account it was assumed to assess the downhole energy consumption of a well working system. Now having covered all the events occurring in an efficient system it is tried to itemize some main processes associated with drilling problems that lead to a waste of energy.

Torque and Drag

Two main groups are identified that may severely contribute to the T&D readings if they arise during drilling operations. The first group leading to additional forces on the drillstring is related to “Wellbore Geometry Irregularities”. Secondly extensive bending of the pipe due to overloading of the drillstring may lead to “Buckling” introducing high contact forces at additional contact points. In the worst-case problems with wellbore geometry irregularities and buckling may end in a stuck pipe.

Wellbore Geometry Irregularities

With wellbore geometry irregularities the change of the geometrical shape of the wellbore compared to an ideal shape is meant. In other words the deviation from the concept of an ideally shaped wellbore represented by a straight or curved cylinder with a plain inner surface. In general there is no restriction how the shape of the wellbore can look like but over time several basic elements associated with drilling problems helped to get a better understanding how the wellbore geometry over a given length may look like under certain circumstances. Some of such elementary irregularities like key seats, micro doglegs, ledges or mobile formations are shortly discussed and visualized via comics in the Appendix C.1.2: “Wellbore Geometry Irregularities”.

Bending

By applying load to the bit to achieve penetration a part of the BHA will be under compression. If the compression of the string exceeds certain limits the BHA may bend. Severe bending may lead to contact points changing the T&D reading. In the soft string models used for the simulations above it is not accounted for the bending of the string. More complex so-called “stiff string models” account for bending and additional contacts points. A closer insight into stiff string models and a case study can be found in the thesis “Drillstring Mechanical Modeling and Real-time Monitoring” (Philipp Doppringer, 2014).

Buckling

It has to be differentiated between two types of buckling, the sinusoidal and helical buckling. Whereas the sinusoidal buckling is the first stage and as the axial load continuous to increase the sinusoidal buckling goes over into helical buckling, which is worse concerning the damage it can cause. Both can lead to drill string failures due to the extensive bending and in the worst case due to the simultaneously increasing contact forces to a stuck pipe situation. As a mathematical expression showing the relationship between the axial force and the mode of buckling appear to be to complex it is common to describe the critical limit of axial force when buckling occurs. This critical force is depending on the dimensions of the borehole and the drillstring and was also taken into account for the minimalistic models presented. Additional frictional forces that result from buckling if it occurs have usually not been taken into account.

Cutting Beds

If the hydraulics works not properly especially in inclined sections where the drillstring due to gravitational forces tends to lie on the lower side of the wellbore cuttings may accumulate and so-called cutting beds may develop. These cutting beds can affect the pipes movement and influence the T&D readings. In the worst case it even may lead to stuck pipe.

Severe Vibrations

The vibrations introduced before in chapter 3.1: “The Models in their General ; Drilling Dynamics” lead in there most severe form to serious drilling problems like bit bounce, whirl or stick/slip. Whereas “Bit Bounce” is mainly related to axial-, “Whirl” to lateral- and “Stick/Slip” to torsional- vibrations. A short theoretical background and introduction into these more problematic processes can be found in the Appendix C.1: “Drilling Dynamics”.

3.3 Interim Discussion: The Limits of the Models

For each of the governing differential equilibrium equations presented at the beginning of this exist different solutions to describe the respective process. However the number of different processes of varying magnitude led to a complexity of the system that it is almost impossible to model the different elements satisfyingly.

Aadnøy puts it this way: *“The complexity of numerical models makes them less suited for parametric studies or analyzing the system behavior.”* (Aadnøy et al., 2009, p. 842) That is because the accuracy of a model is dependent on the error of each input parameter. Unknowns or assumed input parameters and the above-discussed simplifications, falsify the result of the different models. Unfortunately as the complexity of the system increases so does the number of input parameters.

This is countered for the moment up to a certain level along the BHA and near the bit as through downhole measurements unknowns can be reduced and a matching of the different models can be conducted. Regrettably a more detailed description of the behavior of the string and hydraulic system along the entire wellbore is not present, as many continuously changing unknowns between the BHA and the surface cannot be identified.

Measurements along the entire will be a step forward to increase or verify the accuracy of the different models. Multiple measurements reduce the distance between two points that need to be described. A shortened interval simultaneously reduces the complexity of the section to be modeled, as special parts of the drillstring can be analyzed separately.

4 Assessing the Energy Loss Over the Whole System

Having identified the governing models describing the energy losses in a drilling system and several processes that contribute to these models, the question arises how to quantify them. As there are no models describing each process sufficiently it is suggested to analyze the system with the help of measurements.

In a first step, the losses along the drillstring for three predefined well profiles are quantified through relative minimalistic standard models. Referring to the first step, it is evaluated in a second step, which sensors can measure which process today and how accurate. The results from the first and second step play a further role analyzing possible positions for multiple downhole measurement subs.

4.1 Minimalistic Models to Benchmark the Energy Loss

Based on the idea of another project to be carried out at the Montanuniversität Leoben including several wells to be drilled for scientific reasons the models are based upon one eventuality of the requirements given by this project.

For all three well plans it is assumed that the target is located at a depth of 1,000 meter and the well will be completed with a 5-inch casing. The three well profiles analyzed are a vertical-, a tangential- and a horizontal- well. The models will take into consideration Torque and Drag (T&D) according to the “soft string” theory as well as basic analysis of the hydraulics of the system.

The models standing behind these processes are commonly used in the industry and don’t account for abnormalities, neither their effect of their simultaneous occurrences along the string.

Torque & Drag

The T&D forces along the trajectory are based upon solutions of the force and moment balance equations that don’t account for bending moments and shear forces. These models are so-called *soft-string* models due to the simplification of the drillstring equilibrium problem. The calculations and the theory behind the models for T&D analysis and the estimation of bit torque are presented in the Appendix A.2.

Hydraulics

The solutions of the governing equilibrium equations take several simplifications into consideration. An important simplification is that all the models account for an incompressible, single-phase steady state flow. The solutions of the governing equilibrium equations used to calculate the pressure loss of they system for a steady state, single-phase, incompressible flow are presented in the Appendix A.3.

4.1.1 Assumptions for the Minimalistic Model

Several assumptions concerning the lithology (represented by a Metamorphic Greywacke Zone) and other drilling parameters that are essential to proceed with further simulations are listed in Table 5. It has to be stated that such a model is a snapshot in time of the forces needed to drill the last section for the 5-inch casing with the supposed boundary conditions, presented in Table 6. These boundary conditions stay the same for the vertical-, tangential- and horizontal- well plan.

Table 5: Minimalistic Model Assumptions – Lithology

Metamorph Greywacke Zone		
Blasseneck Porphyroid		
UCS:	150	Mpa
Pore EMW incl. Safety:	1123	kg/m^3
Frac EMW incl. Safety:	1582	kg/m^3

Table 6: Minimalistic Model – Boundary Conditions

Drilling Parameters		
Target Depth:	1000	m
Production Casing OD:	5	inch
CH - Friction Coefficient:	0.15	-
OH - Friction Coefficient:	0.30	-

Taking into account that the last section, the production section should be completed with a 5 inch casing, the dimensions for the bit and casing program were chosen as listed in Table 7 for the three well profiles.

Table 7: Minimalistic Model – Casing and Bit Program

	Surface Section	Production Section	
OH Diameter:	7 7/8	6 1/8	inch
Casing OD:	7 5/8	5	inch
Casing ID:	7	-	inch

For reasons of simplicity it is further assumed that single BHA elements like a mud motor, bend housing, stabilizers, MWD tools, LWD tools, etc. are not pointed out on their own. Since every BHA element must fulfill the dimensional standards and the expected loads along the BHA, DC's represents these elements in this thesis. Table 8

represents the dimensions for the drillpipe and drill collar selected for the three models.

Table 8: Minimalistic Model – Drillstring Dimensions

	Drillpipe	Drill Collar	
Length:	10	10	m
OD:	4	4 1/8	inch
ID:	3 1/3	2	inch
Tool Joint OD:	5 1/2	-	inch
Weight incl. TJ:	24	52	kg/m

Concerning the drilling fluid it is assumed that the fluid used in this model follows the behavior of a Bingham model. The rheological key data for the fluid used in all three models is given in Table 9.

Table 9: Rheological Key Data

Hydraulic Setting		
Plastic Viscosity:	4	cP
Yield Point:	15	$lb/100ft^3$
EMW:	1200	kg/m^3

4.1.2 Results – Vertical Well Model

The first well to be modeled is the vertical well whereas a visualization of the well profile refereed to in this first approach is visualized in Figure 38 in the Appendix B.1. For this well plan the corresponding key points of the well path are listed in Table 10 and Table 11.

Table 10: Vertical Well – Well Path Key Data

Well Path:		
Max. TVD:	1020	m
Total MD:	1020	m
Max. Inclination Angle:	0	°/30m
Max. Inclination:	0	°
KOP:	-	m
Max. Easting:	0	m
Casing Length:	300	m
Open Hole Length:	720	m
Horizontal Length:	-	m

Table 11: Vertical Well - Drillstring Setup

Drillstring Setup:		
Single Pipe Length:	10	m
Drillpipe:	96	#
Dril Collar:	9	#

The T&D model assumes ideal conditions and doesn't count for additional side forces due to directional control or drilling problems. Resulting from the predefined well

path and the drillstring setup the resulting T&D seen by a single drillstring element as well as the cumulative friction and torque are listed in Table 12. With the friction modeled along the drillstring the tensional respectively compressional force acting on a pipe is listed in Table 13.

Table 12: Vertical Well – T&D Key Data

Torque & Drag		
Max. ΔFriction per Pipe:	0	N
Min. ΔFriction per Pipe:	0	N
Cumulative Friction:	0	N
Max. ΔTorque per Pipe:	0	Nm
Min. ΔTorque per Pipe:	0	Nm
Estimated Bit Torque:	3511	Nm
Cumulative Torque:	3511	Nm

Table 13: Vertical Well – Energy Dispersion in Tension/Compression

Tension/Compression		
WOB:	14715	N
Max. ΔTension per Pipe:	4297	N
Min. ΔTension per Pipe:	2031	N
Max. Ten. while Drilling:	212828	N
Max. ΔComp. per Pipe:	-4297	N
Max. Comp. as Drlling:	-14715	N

An ideal behavior of the string and borehole interaction is also assumed to be valid for the hydraulic model not accounting for eccentricity or other restricting occurrences. The pressure losses through the pipe and the annulus for the hydraulic setting fitting the model are broken down to losses along a single pipe element. These losses as well as the total losses in the system at a flow rate of 250 gpm are listed in Table 14.

Table 14: Vertical Well – Dynamical Pressure Losses

Hydraulics				
Flow Rate:	946	l/min	250	gpm
Max. Inner Δp per Pipe:	1.22	bar	17.69	psi
Min. Inner Δp per Pipe:	0.11	bar	1.55	psi
Max. Annular Δp per Pipe:	0.10	bar	1.39	psi
Min. Annular Δp per Pipe:	0.06	bar	0.86	psi
Trough Pipe Pressure Loss:	21	bar	303	psi
Pressure Loss Across Bit:	36	bar	525	psi
Annular Pressure Loss:	8	bar	120	psi
Total Pressure Loss:	65	bar	948	psi

4.1.3 Results – Tangential Well Model

The key data for the tangential well path are presented in Table 15 and Table 16. A 2 – dimensional visualization of the well plan can be found in the Appendix B.2. Given an OH of 900 m and a CH of 300 m length results in a total length of 1,200 m. The KOP is set at a depth of 300 m building steady with a DLS of 3 °/100 m. The hold

angle of 45° gives a tangential length of 450 m. This planned well path includes 114 DP's and 9 DC's.

Table 15: Tangential Well – Well Path Key Data

Well Path:		
Max. TVD:	1023	m
Total MD:	1200	m
Max. Inclination Angle:	3	°/30m
Max. Inclination:	45	°
KOP:	300	m
Max. Easting:	505	m
Casing Length:	300	m
Open Hole Length:	900	m

Table 16: Tangential Well – Drillstring Setup

Drillstring Setup:		
Single Pipe Length:	10	m
Drillpipe:	114	#
Dril Collar:	9	#

The T&D model for the tangential well also assumes ideal conditions and doesn't count for additional side forces due to directional control or drilling problems. The frictional forces resulting from the predefined tangential well path are given below in Table 17. As for the previous model the maximum and minimum tensional and compressional as well as frictional forces expected along the drillstring due to its dead weight in the drilling fluid are listed in Table 18.

Table 17: Tangential Well – T&D Key Data

Torque & Drag		
Max. ΔFriction per Pipe:	912	N
Min. ΔFriction per Pipe:	8	N
Cumulative Friction:	35207	N
Max. ΔTorque per Pipe:	48	Nm
Min. ΔTorque per Pipe:	1	Nm
Estimated Bit Torque:	3493	Nm
Cumulative Torque:	5809	Nm

Table 18: Tangential Well – Energy Dispersion in Tension/Compression

Tension/Compression		
WOB:	29430	N
Max. ΔTension per Pipe:	3039	N
Min. ΔTension per Pipe:	1436	N
Max. Ten. while Drilling:	155836	N
Max. ΔComp. per Pipe:	-3039	N
Max. Comp. as Drlling:	-29430	N

The values listed in Table 17 and Table 18 given an idea of the T&D along the entire tangential well plan. Taking a closer look just at the tangential section the friction forces, the deadweight and the resulting axial load seen at the DC's and DP change and are listed in Table 19.

Table 19: Tangential Section T&D Readings

	Tangential T&D				
DC:	Friction per Pipe:	912	N	205	lbf
	Axial Dead Weight per Pipe:	3039	N	683	lbf
	Axial Load per Pipe:	2127	N	478	lbf
	Torque per Pipe:	48	Nm	35	ft lbf
DP:	DP Friction per Pipe:	431	N	97	lbf
	Axial Dead Weight per Pipe:	1436	N	323	lbf
	Axial Load per Pipe:	1005	N	226	lbf
	DP Torque per Pipe:	30	Nm	22	ft lbf

An ideal behavior of the string and borehole interaction is also assumed to be valid for the hydraulic model of the tangential well plan. Meaning that it is not accounted for eccentricity or other restricting occurrences. The dynamic pressure losses through the pipe and the annulus for the hydraulic setting fitting the model are broken down to losses along a single pipe element as well as the total losses in the system and are listed in Table 20.

Table 20: Tangential Well – Dynamical Pressure Losses

Hydraulics				
Flow Rate:	946	l/min	250	gpm
Max. Inner Δp per Pipe:	1.22	bar	17.69	psi
Min. Inner Δp per Pipe:	0.11	bar	1.55	psi
Max. Annular Δp per Pipe:	0.10	bar	1.39	psi
Min. Annular Δp per Pipe:	0.06	bar	0.86	psi
Trough Pipe Pressure Loss:	23	bar	331	psi
Pressure Loss Across Bit:	16	bar	228	psi
Annular Pressure Loss:	10	bar	143	psi
Total Pressure Loss:	48	bar	702	psi

4.1.4 Results – Horizontal Well Model

The planned well path for the horizontal well (corresponding graphical visualization of the well path can be found in the Appendix 0) has the corresponding key values listed in Table 21. With a planned horizontal section of 1,000 m and a build angle of 3 °/30m the KOP is set at a depth of 450 m. The total length of the well adds up to 2,310 m with a casing set at 1,000 m of measured depth and an OH of 1,310 m. This results in a first planned setup of the drillstring consisting out of 195 DP's and 9 DC's for the horizontal well as given in Table 22.

Table 21: Horizontal Well Path – Key Values

Well Path:		
Max. TVD:	993	m
Total MD:	2310	m
Max. Inclination Angle:	3	°/30m
Max. Inclination:	90	°
KOP:	450	m
Max. Easting:	1604	m
Casing Length:	1000	m
Open Hole Length:	1310	m
Horizontal Length:	990	m

Table 22: Horizontal Well – Drillstring Setup

Drillstring Setup:		
Single Pipe Length:	10	m
Drillpipe:	225	#
Dril Collar:	9	#

Together with the key data from the well path and the general assumptions a soft string T&D model was conducted with the key results for the horizontal well listed in Table 23 and Table 24. Also here T&D model for the horizontal well assumes ideal conditions and doesn't count for additional side forces due to directional control or drilling problems.

Table 23: Horizontal Well – T&D Key Data

Torque & Drag		
Max. ΔFriction per Pipe:	1289	N
Min. ΔFriction per Pipe:	8	N
Cumulative Friction:	94447	N
Max. ΔTorque per Pipe:	68	Nm
Min. ΔTorque per Pipe:	1	Nm
Estimated Bit Torque:	3493	Nm
Cumulative Torque:	9888	Nm

Table 24: Horizontal Well – Energy Dispersion in Tension/Compression

Tension/Compression		
WOB:	29430	N
Max. ΔTension per Pipe:	2031	N
Min. ΔTension per Pipe:	0	N
Max. Ten. while Drilling:	71699	N
Max. ΔComp. per Pipe:	-2031	N
Max. Comp. as Drlling:	-102786	N

The values listed in Table 23 and Table 24 given an idea of the T&D along the entire horizontal well plan. Taking a closer look just at the horizontal section the friction forces seen at the DC's and DP are differently and listed in Table 25.

Table 25: Horizontal Section – T&D Readings

Horizontal T&D				
DC Friction per Pipe:	1289	N	290	lbf
DC Torque per Pipe:	68	Nm	50	ft lbf
DP Friction per Pipe:	609	N	137	lbf
DP Torque per Pipe:	43	Nm	31	ft lbf

Pumping the drilling fluid with the assumed rheological parameters for the Bingham drilling fluid as presented in Table 9 yields the dynamic pressure losses listed below in Table 26. An ideal behavior of the string and borehole interaction is also assumed

for the horizontal well plan. Meaning that it is not accounted for eccentricity or other restricting occurrences.

Table 26: Horizontal Well – Dynamical Pressure Losses

Hydraulics				
Flow Rate:	1514	l/min	400	gpm
Max. Inner Δp per Pipe:	2.78	bar	40.27	psi
Min. Inner Δp per Pipe:	0.24	bar	3.52	psi
Max. Annular Δp per Pipe:	0.06	bar	0.88	psi
Min. Annular Δp per Pipe:	0.03	bar	0.48	psi
Trough Pipe Pressure Loss:	79	bar	1145	psi
Pressure Loss Across Bit:	40	bar	583	psi
Annular Pressure Loss:	11	bar	153	psi
Total Pressure Loss:	130	bar	1881	psi

4.1.4.1 Interim Discussion: The Blindness of the Simple Model

The basic models presented above give a first overview of the main energy consuming process at a certain stage during drilling operations in an ideal case. To get an idea over the whole drilling process the model must be executed iteratively representing the actual drilling at different points along the planned well path. Further it is not differentiated if single processes or circumstances have a greater or less impact on e.g. T&D occurring at certain points along the drillstring. In this case a comparison of the modeled data (if present at that point) to measured data an extraordinary wastage of energy is not directly assignable to certain circumstances influencing the system downhole. Rather a general wastage of energy may be noticed and the reasons responsible for the reduction in efficiency guessed. Nevertheless these models provide a first idea about how the system should operate in an ideal case. Additionally justifying the approach of the models the point of investigation refers to the end of drilling. Knowing that, it is assumed that the string experiences a maximum of T&D and hydraulically pre-defined circumstances that must be accounted for.

4.2 What, How and How Accurate can the Energy Loss be Measured?

Actual drilling operations are guided by three main parameters, the Hook Load (HL), the Rotations of the Drillstring per Minute (RPM) and the Torque (T) needed to rotate the string. These parameters are most commonly measured at the surface and used to estimate the state of the drilling system. As these key parameters are

absolute values, they aren't revealing the single sources downhole. This points out that more precise quantification of these processes can just be achieved through additional information of the downhole condition. What better way could there be than the implementation of additional downhole measurements at numerous points? With the introduction of new high speed, high data bandwidth telemetry systems in the Oil and Gas (O&G) industry measurements along the string recording several physical parameter downhole become possible. These measurements may reveal processes and wastage of energy that can further be attributed to the different key parameters pointing out inefficiencies.

4.2.1 Telemetry System

For the sake of completeness, a short overview of the relatively new high speed and high bandwidth wired – pipe telemetry network is provided. For real time measurements this type of telemetry system is a big step up the ladder as the traditional mud – pulse telemetry can't handle the measured amount of data recorded all along the drillstring. A short introduction into both systems can be found in the Appendix D: "Introduction to Surface and Downhole Measurements". The wired – pipe technique discussed is based on the wired drillpipe technology used by NOV as it is the best reference material to be found although other industry competitors are also working on wired – pipe telemetry systems.

4.2.2 Introducing the Different Sensors to Measure the State of the System

Following it is identified, which sensors measure the different physical parameters controlling the governing differential equations. Additionally, it is revealed in which extend and resolution it is needed to measure to get meaningful as well as useful result. In general it can be said, that the accuracy required by the industry of the measurements varies from 2-3%.

To get a first indication, the resolution of different sensors deployed in a measurement sub from Schlumberger were translated into a reasonable minimum distances in-between two measurement point, so that their readings due to their resolution will not overlap. As the data sheet of the tool also provides an overview of the different sensor accuracies the influence of them is translated into a possible

length of faulty measurement. The whole analysis is done with respect to the drillpipe and the results from the minimalistic models conducted before.

4.2.2.1 Strain Gauges

Strain gauges measure the forces and moments acting on the string at the point of measurement. They reflect the stress by measuring the deformation or strain in unit of meter/meter seen by the gauge. The strain results in a change of electrical resistivity of the gauge, which can be measured. Stress is expressed in N/m^2 or in lbf/in^2 whereas in the O&G industry the acting load or force expressed in N or lbs is more of relevance to get an idea of the tensional, compressional-and torque loads action on the equipment. With the stain gauge it can be measured:

- Axial Load (through axial strain measurement)
- Torque (through shear/torsional strain measurement)
- Bending Moment (through bending strain measurement)

As T&D plays a significant role everywhere in drilling a good description of the theory behind strain as well as the measurement of it can be found in the thesis: "Challenges and Developments in Direct Measurement of Downhole Forces Affecting Drilling Efficiency; Chapter 3: Principles of Strain/Stress and Measurement Techniques" (Duncan James Junor, 2007).

Axial Load: Quality, Resolution and Meaningfulness of the Measurement

The strain gauges for the measurement of axial- (tension and compression) and radial- (Torque) stresses are all deployed in a so-called IWOB cell in the downhole measurement sub discussed. In the following Table 27 the resolution and the accuracies for the strain gauges measuring the axial loads are presented.

Table 27: MWD Strain Gauge Resolution and Accuracy for the Axial Sensor (Schlumberger, 2010)

IWOB Sensor	WOB
Measurement range	–65,000 to 190,000 lbf
Resolution	500 lbf
Absolute accuracy	see table below
Scale factor	500 lbf/count
IWOB Estimated Absolute Accuracy[†]	

Downhole Conditions	Error on WOB
30,000 lbf WOB	(total electronics error) ± 2.85%
5,000 ft.lbf torque	(cross talk) ± 1,410 lbf
± 50 psi differential pressure[‡]	± 885 lbf
±15° dogleg[§] (sliding, worst orientation possible)	± 3,330 lbf
Hydrostatic pressure	150 lbf/1,000 psi
Temperature	41 lbf/degF

[†] Accuracy depends on deviations of downhole conditions—such as applied WOB, running torque, sliding dogleg, hydrostatic pressure, and temperature—away from the corresponding values at the last downhole rezero point.

[‡] The effect of differential pressure (ΔP) will be eliminated by surface software based on standpipe pressure.

[§] The error due to dogleg exists when the MWD tool is in sliding mode. When the tool is in rotary mode, the error vanishes because of data filtering.

The measurement range given from -65,000 to 190,000 lbf or -378,100 to 845,160 N for the strain sensor is not a restricting factor with respect to the minimalistic models for the vertical, tangential and horizontal well plans conducted before. Where the maximum tension of about 221,000 N and the maximum compression of about -14,700 N are experienced by the pipe in the vertical well.

Resolution

The resolution of 500 lbf or 2,224 N provides a first idea of a meaningful spacing of the strain gauges. Assuming a pipe with a 4 inch OD and weight per length of 15.9 lb./ft (incl. TJ) the weight of one joint (length 30ft) hanging straight in the air is about 524 lb. Taking the buoyancy factor (±0.85 (ρ_{mud}=1,200 kg/m^3; ρ_{steel}=7,850 kg/m^3)) into account the weight of one joint in the drilling fluid equals about 445 lb. Therefore the resolution gives that another strain sensor makes sense after every second joint in a vertical section.

In the tangential section both the weight of the pipe and frictional forces which are a result of the deadweight contribute to the axial load that the single joint

experiences. Thinking of the less heavy drillpipe a frictional force of about 97 lbf or 431 N is expected per pipe in the tangential section meaning that a sensor could be placed after every sixth single joint.

In the horizontal section just the frictional force contributes to the axial load the pipe experiences. Taking the same pipe as above with an assumed friction factor of 0.3 for the OH the friction force equals about 133 lbf or 593 N. Rounded up this equals a minimum of 4 pipes or ± 40 meter between to strain gauges with a resolution of 500 lbf.

Electronics Error

With a given error of the electronics of 2.85% at a load of 30,000 lbf and assuming that that error stays constant for all loads it doesn't have a severe influence on the positioning of the sensor.

Cross Talk Error

It is assumed that there is a linear relationship between the errors due to cross talk due to torque where the reference error is stated to be 1,410 lbf at a torque of 5,000 ft lbf.

At the lower end of the string the error due to cross talk depends on the torque at the bit. Further up as the torque increases up to a maximum at the surface the error due to cross talk also increases. Thinking of the models before the torque at the bit is in the range of about 4,500 Nm or 3,300 ft lbf. A linear relationship of the cross talk error implies an error of about 940 lbf for near bit measurements. In a vertical well it is assumed that the torque stays constant up to the surface, as there is no additional source generating torque with a centered string that doesn't rub against the borehole wall. With the weight of a single joint in the drilling fluid of 445 lbf the error of measurement sub translated into length equals 3 single joints in one direction. In total this results in six joints as the error range of every measurement point include 3 joints up the string and 3 joints down the string.

Coming to a horizontal well as simulated before a torque increase due to friction of maximum 50 ft lbf after a single joint does not have a severe influence on the error magnitude. Though as the torque cumulatively increases up to a maximum at the

surface of about 9,900 Nm or 7,300 ft lbf the error due to cross talk changes too. Having a maximum friction of about 133 lbf in a horizontal section and an error at the bit of about 940 lbf implies an error translated into length of about 7 single joints. In total 14 as like above the error range of about 7 single joints go out in both directions. With a maximum torque of about 7,300 ft lbf at the point where the well starts to become vertical the error due to cross talk in the axial reading is about 1,520 lbf. That equals the weight of about 12 joints and covers therefore an error range of about 24 pipes in total.

Error due to Hydrostatic Pressure

The error for the axial strain gauge of about 150 lbf/1000 psi due to hydrostatic pressure is not of a big concern. In a well with a fluid density of about 1,200 kg/m^3 a pressure difference of 1,000 psi is given every 586 meter. This equals an error of about 260 lbf at 1,000 meter of depth assuming a linear relationship. In a horizontal well with a friction force of about 133 lbf the error equals two pipes. As the pressure in a horizontal section does not change this equals in total about 4 pipes of faulty measurement for every downhole sub in the horizontal section. In the vertical section with no friction occurring the error is not really of a concern as a single pipe with an axial weight force of 445 lbf has about three times more influence on the load measurement compared to the error.

Error due to Temperature

The error due to a change in temperature for this sensor is given by 41 lbf/°F or 73.8 lbf/°C. The change in temperature due to a geothermal gradient assuming 3 °C/100m is not too much of a problem. Although at 1,000 m this would mean a change in temperature of 30 °C resulting in an error of 2214 lbf this can be controlled through a frequently re – zeroing of the sensors. Meaning nothing else that the sensor is calibrated from time to time to the surrounding conditions. A stronger role that may lead to a wrong measurement is given through the temperature change by the heated fluid passing the sensors. Here in this thesis it won't be discussed in detail to which extend the fluid heats up or cools down on it's round trip in the wellbore. But to give a feeling how much influence the temperature might have it is assumed that

a drilling fluid with a temperature difference of about 10 °C compared to the surrounding temperature passes introducing an error of about 740 lbf in the axial measurement.

Torque: Quality, Resolution and Meaningfulness of the Measurement

The strain sensors measuring torque are orientated differently in the load cell but work in the same way.

Resolution

The resolution of 90 ft-lbf (122 Nm), ranges and errors are also listed in Table 28 for the torque sensor.

Along the vertical section it is assumed that the torque experienced at the bit stays the same along the drillstring up to the surface, as no additional friction forces should occur. This is just a theoretical approach and should not lead to the conclusion that no additional subs should be placed along the string as drilling a complete straight well is impossible and unpredictable friction forces will occur along the string. Therefore the torque sensor is not a criterion for the placement of a downhole sub in a vertical section although theoretically it would not measure any differences.

A drillpipe in the tangential section experiences a torque of 22 ft-lbf (30 Nm). Translated into the spacing needed between two subs to have different readings in the measurement equals 5 single joints.

In a horizontal section where the incremental increase in torque per drillpipe element equals 31 ft-lbf (42 Nm), a second measurements sub would make sense after every fourth pipe to record another reading in torque.

Table 28: MWD Strain Gauge Resolution and Accuracy for the Torsional Sensor (Schlumberger, 2010)

IWOB Sensor	**Torque**
Measurement range	–8,000 to 15,000 ft.lbf
Resolution	90 ft.lbf
Absolute accuracy	see table below
Scale factor	90 ft.lbf/count
IWOB Estimated Absolute Accuracy†	

Downhole Conditions	**Error on Torque**
30,000 lbf WOB	(cross talk) ± 2.85%
5,000 ft.lbf torque	(total electronics error) ± 25 ft.lbf
± 50 psi differential pressure‡	± 7 ft.lbf
±15° dogleg§ (sliding, worst orientation possible)	± 438 ft.lbf
Hydrostatic pressure	5 ft.lbf/1,000 psi
Temperature	4 ft.lbf/degF

† Accuracy depends on deviations of downhole conditions—such as applied WOB, running torque, sliding dogleg, hydrostatic pressure, and temperature—away from the corresponding values at the last downhole rezero point.

‡ The effect of differential pressure (ΔP) will be eliminated by surface software based on standpipe pressure.

§ The error due to dogleg exists when the MWD tool is in sliding mode. When the tool is in rotary mode, the error vanishes because of data filtering.

4.2.2.2 Lateral Shock Accelerometer

Lateral shocks can be measured with a single axis accelerometer whereas the number of shocks (measured in G's) is counted with a magnitude greater than a fixed shock threshold. Normally a time interval is set that counts the total shocks over this period. The shocks over this period are also represented by an average shock value and a peak shock, which is the largest shock magnitude, recorded in this period.

The measurement provide an indication for:

- Sudden lateral energy input into the system.
- Peak Shock (max. energy input for the given time period)
- Average Shock (average energy input for the given time period)

Shock: Quality, Resolution and Meaningfulness of the Measurement

Table 29 lists the frequency in counts per second (cps (1 cps = 1 Hz)) and the possible measurable impact of the shocks in G's as well as the resolution of both. Shock measurements are not constrained by axial displacement of the acceleration sensors. They can occur all along the string of different magnitude.

Table 29: MWD Shock Accelerometer Resolution (Schlumberger, 2010)

Measurement	Range	Resolution
Shock count	0 to 255 cps	1 cps
Shock peak	0 to 1,020 g_n	4 g_n

This shock accelerometer can measure shocks with a frequency range of 0 to 255 Hz and a resolution of 1 Hz. Although it can measure shocks with energy up to 1,020 G the cutoff of the frequency at 255 Hz is a restricting factor concerning a better understanding of the energy wastage due to shocks. This can be stated as true as due to the theory behind vibrations the energy of vibrations is higher the higher the frequency and the shorter the wavelength is. Therefore sensors that could capture frequencies greater than 400 Hz could provide a new picture of the energy going into shocks.

4.2.2.3 3 – Axis Accelerometer

The 3 – Axis Accelerometer puts out a wave pattern for each axis with a positive and negative response measured in G's, showing the magnitude and frequency of the vibration like in Figure 33. Normally for a better visualization the measured vibration is averaged over a time interval using the root mean square (RMS). The RMS scales the magnitude of the measurement and the end result provides an averaged measurement that accounts for the energy exhibited by the vibration of the predefined time period.

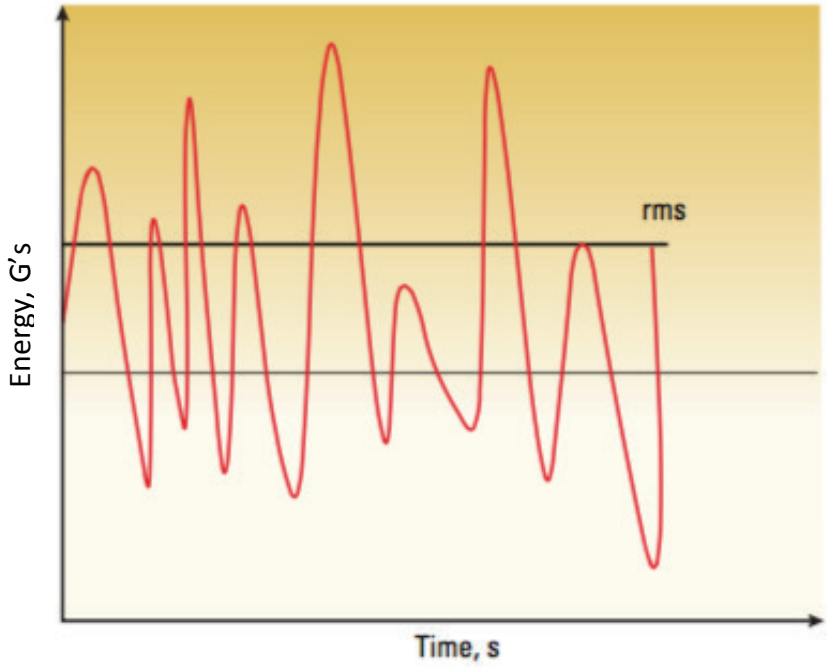

Figure 33: Accelerometer Wave Output and Processing; The read line is a visualization of a wave response whereas the area under the wave represents the shock energy; The black straight line represents the RMS value of the curve, which stays constant for the same time interval and encloses the same area underneath it as the area under the curve. (Schlumberger, 2010)

The measurement provides an indication of:

- Average amount of energy exhibited in x – direction (axial measurement)
- Average amount of energy exhibited in y – direction (lateral measurement)
- Average amount of energy exhibited in z – direction (lateral measurement)

Axial and Lateral Vibrations: Quality, Resolution and Meaningfulness of the Measurement

Vibrations are like shocks not constrained by axial displacement of the acceleration sensors. They can occur all along the string of different magnitude due to different external influences in relation with the string wellbore interaction. The restricting factor for vibration measurements lies in high frequency measurements and not in the range standards of measurement for the single axis accelerometer, which are listed in Table 30.

Table 30: MWD 3 – Axis Accelerometer Resolution Data Sheet (Schlumberger, 2010)

Measurement	Range	Resolution

X-axis axial rms vibration	0 to 30.02 g_n	0.125 g_n
Y-axis lateral rms vibration	0 to 60.08 g_n	0.25 g_n
Z-axis lateral rms vibration	0 to 60.08 g_n	0.25 g_n
Lateral rms vibration	0 to 60.08 g_n	0.25 g_n

From feedback from professionals from the field the cutoffs for the axial and lateral vibrations for the sensor presented as an example are in the range of 0.2 Hz and 150 Hz. Therefore higher frequencies are not recorded although the opinion of some professionals indicated that vibrations above 400 Hz are reflecting vibrations seen permanently along the drillstring and could provide a new picture of the downhole dynamics. Additionally the RMS value sent to the surface is the last 30 seconds, which also reduces the resolution.

4.2.2.4 Torsional Vibrations

Torsional vibrations are measured also with a strain gauge as used for torque measurements in the example tool. The output is also given as a RMS value over a certain time period with a higher resolution of 5 ft-lbf but reduced measurement range from 0 to 5,100 ft-lbf as presented in Table 31.

Table 31: Torsional Vibrations Strain Gauge Data Sheet (Schlumberger, 2010)

Measurement	Range	Resolution
Torsional rms vibration	0 to 5,100 ft.lbf	5 ft.lbf

As the sensor measures torsion due to torque and is not affected by the axial load it could be positioned everywhere along the string. With the increased resolution of the sensor compared to the normal torque sensor minimum spacing between two measurement points in a horizontal section where the incremental in increase of torque is the highest per element.

4.2.2.5 Magnetometer

With the help of the magnetometer the RPM of the tool (normally a drill collar) the magnetometer is attached to, can be measured. Differences in RPM at a certain point may be due to sudden influence of an external force at this point restricting

the rotation of the string. This force normally results in a higher torque, which may also help to identify possible stick/slip behavior introduced before in Chapter 3.1: "The Models in their General ; Drilling Dynamics".

RPM: Quality, Resolution and Meaningfulness of the Measurement

Theoretically the RPM could be measured at any point along the drillstring and a range between 0 and 255 RPM as listed in Table 32 shouldn't be a restricting factor either.

Table 32: MWD Magnetometer Resolution (Schlumberger, 2010)

Measurement	Range	Resolution
Collar rotation speed	0 to 255 rpm	1 rpm

Yet it wouldn't make much sense to place an RPM measurement on every pipe, as the RPM will not change dramatically. The longer the distance between two measurement points the greater might be the difference in RPM if there is any at all.

4.2.2.6 Pressure Gauge

As the name implies the pressure gauge is used to measure the surrounding pressure. Dependent on its placement on the pipe it can either measure the internal pressure or external pressure. If both pressures are needed two sensors should be deployed. The sensor is based on the principle that a measured pressure change is converted into a mechanical displacement respectively deformation. This deformation is further converted into an electrical signal that can be processed.

Pressure: Quality, Resolution and Meaningfulness of the Measurement

According to Table 33 the resolution of the pressure sensor is 1 psi respectively 6895 Pa. Translated into a pressure head (hydrostatic pressure column) assuming a mud density of 1,200 kg/m^3 and a gravity constant of 9.81 m/s^2 the pressure every 0.6 meter is measureable. This is true for the vertical well for the tangential well the height stays the same but as the well path follows an inclination of 45° a pressure difference of 1 psi is given every 0.83 meter.

Table 33: MWD Pressure Gauge Resolution and Accuracy (Schlumberger, 2010)

Resolution	1 psi
Accuracy	0 to 0.1% of full scale
Available ranges	0 to 5,000 psi 0 to 10,000 psi 0 to 20,000 psi

As the hydrostatic pressure stays the same in the horizontal section just the dynamic losses play a role. The model before yields a minimum annular pressure loss of 0.44 psi along one drillpipe in the OH and a maximum annular pressure loss of 0.88 psi along one drill collar in the OH. Concerning the DP a difference in pressure due to dynamic losses of more than 1 psi could therefore be seen every third pipe.

4.2.2.7 Temperature Sensor

As the pressure sensor the temperature sensor can be based on the principle of a mechanical transducer (deformation of a sensor due to temperature change is converted into an electrical signal). Another type of temperature sensor is the resistance temperature detector measuring the electrical resistance increase of a metal as temperature increases.

Temperature: Quality, Resolution and Meaningfulness of the Measurement

The resolution and accuracy of the temperature sensor is given below in Table 34 with a resolution of 1 °C and accuracy of 1 °C.

Table 34: MWD Temperature Resolution and Accuracy (Schlumberger, 2010)

Annular temperature resolution	1 degC
Annular temperature accuracy	1 degC

Taking a temperature increase with a standard geothermal gradient of 3°C/100m or 1°C/33m with increasing depth into account sets certain boundary conditions as the annular temperature resolution of the sensor equals 1 °C as well as the accuracy. This indicates for a vertical section that a sensor would be meaningful every 33 m or after every fourth pipe.

Being in a tangential section with a hold angel of 45° the path length equals about 47 m to overcome the height difference of 33 m. Indicating a meaningful placement of a temperature sensor after every fifth pipe.

In the horizontal section the surrounding temperature should stay the same, as does the hydrostatic pressure. Different temperature readings might occur due to a heated drilling fluid or the inaccuracy.

Temperature Accuracy

Taking the accuracy into consideration the readings of two temperature sensors might overlap if the sensors are positioned within 100 meter. With a sensor every 100 meter or 10 pipes a different reading can be expected in a vertical section.

4.2.3 Recap: Resolution of Single Sensors

The strain gauge sensors indicates ignoring possible errors that in a vertical section a theoretical difference in the measurement due to the deadweight of a single joint every second pipe can be seen. For the horizontal section a difference in the reading can be expected every fourth pipe due to the friction again resulting the deadweight of a single joint.

The temperature sensor on the other hand ideally could be placed every fourth pipe in a vertical section and after every fifth pipe in the tangential section concerning a geothermal gradient of 3 °C/33m. A change in the temperature in the horizontal section due to a heated fluid was not taken into consideration so far. Due to a constant depth it should stay the same along the horizontal section implying that if the fluid has an equalized temperature orientated on the environmental temperature all the sensors should measure the same temperature.

Concerning the pressure sensor the resolution of 1 psi indicates that in a vertical and tangential section a change in pressure could be measured after every single joint. Horizontally this changes as just dynamic pressure losses as the fluid is pumped occur. Based on the models a pressure difference due to dynamic losses greater than 1 psi can be seen every third pipe.

The other sensors are not a restricting factor concerning their axial placement and can be places everywhere along the string at one go with the other sensors.

4.3 Where to Measure

Based on the different resolutions of the sensors and assumptions where and due to which extend interactions between the string and the wellbore exists that are responsible for the different processes, the drillstring for each well plan introduced in the simple models is theoretically equipped with downhole measurement subs. These well plans represents ironically the maximum extend of the wells and the end of the drilling processes. Therefore the proposed amount of measurement subs for each well plan represents the maximum number of subs deployed for each plan. Further it has to be stated, that here in the previous chapter, the measurements was discussed as single measurements whereas in the field it is standard to accommodate all sensors in one downhole measurement sub. Some circumstances require the placement of multi sensors, with a narrower spacing as like especially along the BHA drilling dynamics play a significant role.

4.3.1 General Placement

Independent of the well path it is proposed after a consolidation with the industry to set a near bit measurement sub two feet behind the bit and due to at least a second measurement sub along the BHA. This second sub is normally set behind the directional control equipment at a distance of about 115 ft or 35 m. The near bit sub is normally relatively short (± 2 feet) to avoid a severe distribution of the drilling path dictated by followed directional equipment. Due to its shortness this sensor normally just contains accelerometers whereas the sub coming after the directional equipment will contain the full range of sensors.

The placement of the sensors along the rest of the drillstring is based on the sensor that has the worst resolution to avoid an overlapping of a single reading. The errors of the single sensors are for the time being not respected for the sensor placement.

4.3.1.1 Vertical Section

In a vertical section the temperature sensor seems to be the sensor with the lowest resolution constituted by the temperature increase with depth. Temperature changes due to a passing heated fluid are not taken into consideration. Therefore

ideally a sensor could be positioned after every fourth pipe thinking just of a vertical section.

4.3.1.2 Build Section

It is not accounted for the gradual changes of the measurable parameters along the build section. It is assumed to follow the resolutions set for a tangential section as soon as the inclination angle becomes greater than zero.

4.3.1.3 Tangential Section

The axial resolution of the strain gauge is the worst indicating a meaningful placement of an additional measurement sub after every sixth single joint along the tangential section.

4.3.1.4 Horizontal Section

Convenient is that the axial strain gauge has about the same resolution in the horizontal section as the temperature sensor in the vertical part. It seems that a sensor position in an ideal case could be every fourth single joint also for the horizontal part.

4.3.2 Vertical Well: Sensor Positioning along the Drillstring

A possible sensor position after every fourth pipe with a pipe length of 10 m in a vertical well of 1000 m depth results in 25 sensors that could be placed along the string based on the temperature sensor with the lowest resolution. These 25 options to place a sensor include also the two sensors deployed in any case near the bit and along the BHA.

4.3.3 Tangential Well: Sensor Positioning along the Drillstring

The tangential well with a total measured depth of 1200 m is set together out of a 300 m vertical section, a 450 m tangential section and section of 450 m building angle. Assuming that the axial resolution evaluated for the tangential section is also true for the building section a 900 m tangential section has to be measured with the help of 15 subs one placed after every sixth pipe. Additionally for the 300 m of

vertical section another 8 subs would be ideally resulting in a total of 23 measurement subs for the tangential well plan.

4.3.4 Horizontal Well: Sensor Positioning along the Drillstring

A horizontal section of 990 m, a build section of 900 m and a vertical section of 450 m length are the main elements of the planned horizontal well. Most ideally 25 subs could be placed along the horizontal section, assuming the build section to follow approximately the rules of a tangential section 15 subs could be placed along that one and another 11 subs along the vertical part. This gives a total of 51 subs for the horizontal well plan.

4.3.5 Interim Discussion: Quantity and Usefulness of the Measurements

For all three scenarios the highest amount of measurement subs was proposed based on closest spacing given by the sensor with the worst resolution in the discussed section of the well. To be realistic, deploying neither 50 measurement subs along the horizontal well plan or 25 along the vertical and tangential well plan will not be possible to complete. As far as I can assess it the upper limit of measurement subs that may be deployed is way lower probably in the range of 5 to 10 subs depending on the costs. For the moment a budget for the upcoming project was not yet defined resulting in no restriction of the amount of measurement subs proposed. Nevertheless every additional measurement point is a big advantage and helps to approach slowly a better understanding of the system.

4.3.5.1 Reducing the Error Reading

So far the errors of the different sensors either due to electronics or dependent on other readings were not taken into consideration for the placement of the subs along the string. Thinking of the errors discussed associated with the sensors several are influenced by the surrounding temperature. A solution could be either additional temperature sensors at each point of measurement providing a more accurate averaged temperature reading or a closer spacing in-between multiple sensors also leading if averaged to a more accurate value of the measured parameter.

5 Summary

In a first step, the governing differential equations, to describe the drilling system, were identified and several processes that contribute to the different models. In a second step, the positioning of several downhole measurement subs is proposed, based on the results of a minimalistic model and the resolution of the sensors. Therefore, the conclusion is subdivided into two sections treating each step separately.

5.1 The Governing Models

T&D, hydraulics and drilling dynamics are identified as the three superior models that describe the system. Each model represents a general theoretical principle that describes the process responsible for the energy consumption.

The change of the pipe force $\vec{F}$ and moment $\vec{M}$ at a point in the drillstring are given through the force balance and moment balance equation below in Table 35.

Table 35: Drillstring Mechanics Governing Equations

Force Balance Equation	$\frac{d\vec{F}}{ds} + \vec{w} = \vec{0}$
Moment Balance Equation	$\frac{d\vec{M}}{ds} + \vec{t} \times \vec{F} + \vec{m} = \vec{0}$

Therefore, to get a picture of the drilling mechanics the drillstring experiences at a certain point, the measure of the pipe force $\vec{F}$ and the moment $\vec{M}$ are of interest.

The hydraulic system is described with the help of the governing mass balance, momentum balance and energy balance equation, which are given below in Table 36

Table 36: Fluid Mechanics Governing Equations

Mass Balance Equation	$\frac{\partial \rho}{\partial t} + \frac{\partial \rho v_i}{\partial x_i} = 0$
Momentum Balance Equation	$\rho \frac{\partial v_i}{\partial t} + \rho v_j \frac{\partial v_i}{\partial x} - \mu \frac{\partial^2 v_i}{\partial x_j \partial x_j} = -\frac{\partial P}{\partial x_i} + \rho g_i$
Energy Balance Equation	$\int_{\Delta z} \rho C_p \frac{\partial T}{\partial t} A dz + \int_{\Delta z} \rho v C_p \frac{\partial T}{\partial z} A dz - \int_{\Delta z} v \beta T \frac{dp}{dz} A dz = \phi + Q + R$

The parameters that define the hydraulic system at every point are the density ρ, the velocity v, the pressure p and the temperature T.

The drilling dynamics are defined through the continuous vibration models for the different type of vibration given. The equations are listed below in Table 37.

Table 37: Drilling Dynamics Governing Equations

Classical Undamped Wave Equation	$\frac{\partial^2 \xi(x,t)}{\partial x^2} = \frac{1}{c^2}\frac{\partial^2 \xi(x,t)}{\partial t^2}$
Continuous Axial Vibration Model	$\rho\frac{\partial^2 \xi}{\partial t^2} - E\frac{\partial^2 \xi}{\partial x^2} + c_a\frac{\partial \xi}{\partial t} + \rho g_z = g_a\left(x,t,\xi,\frac{\partial \xi}{\partial x},\frac{\partial \xi}{\partial t}\right)$
Continuous Torsional Vibration Model	$\rho J\frac{\partial^2 \phi}{\partial t^2} - JG\frac{\partial^2 \phi}{\partial x^2} + c_\theta\frac{\partial \phi}{\partial t} = g_T(x,\phi,t)$
Continuous Lateral Vibration Model	$\rho\frac{\partial^2 u}{\partial t^2} + \frac{\partial^2}{\partial x^2}\left(EI_z\frac{\partial^2 u}{\partial x^2}\right) - P\frac{\partial^2 u}{\partial x^2} = g(x,t)$

The main results of interest are the axial displacement ξ for the axial vibrations, the angular displacement ϕ for the torsional vibrations and the lateral motion u concerning the lateral vibrations.

5.1.1 Contributing Processes

A distinction must be made between two types of energy losses, the intentionally- and the parasitic- energy losses whereas the parasitic energy loss can be broken down into unavoidable- and unintentional- parasitic energy loss. A classification of the processes discussed in this thesis is provided based on my personal opinion:

Table 38: Classification of the Processes

Type of Energy Loss:	***Superior Energy Group:***	***Process:***
Intended Energy Losses:	Rock Penetration	Cutting
Parasitic Unavoidable Energy Loss	T&D	Bit Torque
		T&D due to Deadweight
		Directional Control T&D
	Hydraulics	Dynamic Pressure Losses
		Skin Friction

		Pump-off Effect
	Low Magnitude Drilling Dynamics	Shocks
		Vibrations
Parasitic Unintentional Energy Losses	T&D	Bending
		Wellbore Geometry Irregularities
	Hydraulics	Insufficient Cleaning
	Severe Drilling Dynamics	Bit Bounce
		Whirl
		Stick Slip

5.2 Measurement of the Energy Consuming Processes

The finding that there are no models describing the behavior of the system sufficiently, lead to the suggestion to analyze the system with additional measurements along the whole drillstring.

5.2.1 The Single Sensors

In a first step, the different sensors, to measure the physical parameters of interest, defined by the governing equilibrium equations, are identified. An overview which sensors are used to measure the different physical parameters is given below in Table 39.

Table 39: Overview which Sensor Measures which Physical Property

Model	***Sensor Type***	***Measured Parameter***	
Drilling Mechanics	Strain Gauge	Pipe Force	$\vec{F}$
		Pipe Moment	$\vec{M}$
Hydraulics	Pressure Sensor	Hydraulic Pressure	p
	Temp. Sensor	Hydraulic Temp.	T
Drilling Dynamics	3 – Axis Accelerometer	Axial Displacement	ξ
		Lateral Displacement	u
	Torsional Strain Gauge	Angular Displacement	ϕ

Concerning the additional two physical parameters, the density ρ and the velocity v also describing the hydraulic system, no examples for common downhole measurements could be found. To counteract this problem it is assumed that along a wellbore interval with a constant cross sectional area and steady state flow the velocity stays the same. Further due to the assumption of an incompressible drilling fluid density is also assumed to be constant in the entire system.

Besides the sensors to measure the main parameters of interest introduced above in Table 39 a measurement sub normally brings along additional sensors. A classification, based on my own opinion, which one of the deployed sensors helps to quantify different processes is provided below in Table 40.

Table 40: Assigning the Sensors to the Different Processes

Sensor:	***Type of Energy Loss:***	***Process:***
Strain Gauge	Intended T&D	WOB
		Cutting
	Unavoidable T&D	Pipe Deadweight
		Directional Control
		Torsional Vibration
		Skin Friction
		Pump off Effect
	Unintentional T&D	Bending or Buckling
		Wellbore Geometry Irregularities
		Insufficient Cleaning
Shock Accelerometer	Drilling Dynamics	Shocks
3 – Axis	Drilling Dynamics	Axial Oscillation

Accelerometer		Lateral Oscillation
Magnetometer	Rotation	RPM
		Stick/Slip
Pressure Sensor	Hydraulic Pressure Loss	Inner Pressure
		Outer Pressure
Temperature Sensor	Work Done	Inner Temperature
		Outer Temperature

5.2.2 Sensor Positioning

A transparent workflow, useful to identify the number and positions subs deployed was set up in this thesis:

I. Prepare a T&D and hydraulic model for the previously defined well plan. Additional models like a temperature profile could help to point out bottlenecks influencing the sensor positioning.
II. Split the well plan into basic elements (vertical-, tangential-, horizontal- and building section) to filter out the minimum loads and pressure drops along a single joint for the given system to be expected.
III. Identify the sensor with lowest resolution for each section. The larger the spacing between two sensors needs to be to get a different measurement value the lower the resolution.
IV. Define how much spacing needs to be between two identical sensors in a certain section to measure different values. The Spacing can then be described in a number of single joints.
V. Through the spacing and the length of each section of a single well plan the total number of subs providing a maximum resolution is given.

Comparing the sensors with the results of the minimalistic T&D and hydraulic model gives the sensor with the worst resolution in the respective section:

- Vertical Section → Temperature Sensor
- Tangential Section → Strain Gauge Sensor
- Horizontal Section → Strain Gauge Sensor

- Building Section → Strain Gauge Sensor

This leads to a suggested placement of measurement sub in a vertical section after every fourth, in the tangential section after every sixth and in the horizontal section after every fourth single joint to avoid overlapping measurements. For the building section no separate classification was introduced therefore the spacing in this section is based on the same argumentations as present in the tangential section. Based on these findings it is proposed to deploy a total of 25 subs in the vertical-, 23 subs in the tangential- and 51 subs in the horizontal- well plan.

6 Discussion and Future Outlook

The discussion is used to justify additional measurements and point out possible accompanied difficulties. Some presented impulses will provide ideas how the additional data could be used to broaden the knowledge and improve the understanding of the processes going on downhole.

Optimize Simulations

The missing key point in almost every simulation is the implementation of a description of the drillstring based entirely on physical parameters doing without any assumptions. Some simulations use highly complex numerical solutions trying to represent the drilling process as realistic as possible. However, due to many unknowns their description of the behavior of the drillstring at some point differs from reality. A real time measurement along the entire string could help to improve them and provide new insights.

Predicting the Wellbore Geometry and Tortuosity

The idea is that by calculating backwards the borehole geometries could be approximated from the loads experienced at the different stain gauges. This idea would require several sensors narrowly spaced along a single measurement sub. Provided that the resolution is sufficient real time measurements would allow for a real time prediction of the tortuosity of the borehole. This may provide sufficient resolution and accuracy to quantify the severity and location of macro- and micro-tortuosity. The idea behind this approach is examined more in detail in the paper “Strain-Gauge Bending-Moment Measurements Used to Identify Wellbore Tortuosity” (Marland & Greenwood, 2015).

Assessing the Energy Loss

Translating the idea behind the MSE model of the bit to the total system could be a first approach to introduce an energy balance over the total system. In this case MSE would be a single mathematical term of an energy balance as would be the other energy consuming superior groups like T&D, hydraulics and drilling dynamics. A visualization of the idea behind an energy balance of an ideally working system is presented in Figure 34.

Figure 34: Proposed Energy Balance for an Ideal Working System

Every single term has its foundation in the basic differential equations used to describe the term.

A reference value for the energy input may be modeled closer to reality with advanced simulation than done in this thesis. Provided that, it is drilled without any complications the energy consumed by each of this different superior group should added up equal the predicted energy input. If the energy used is higher than the expected energy input this is an indication for inefficiencies or drilling problems.

These drilling problems contribute to every single term introduced before in Figure 34 as indicated below in Figure 35.

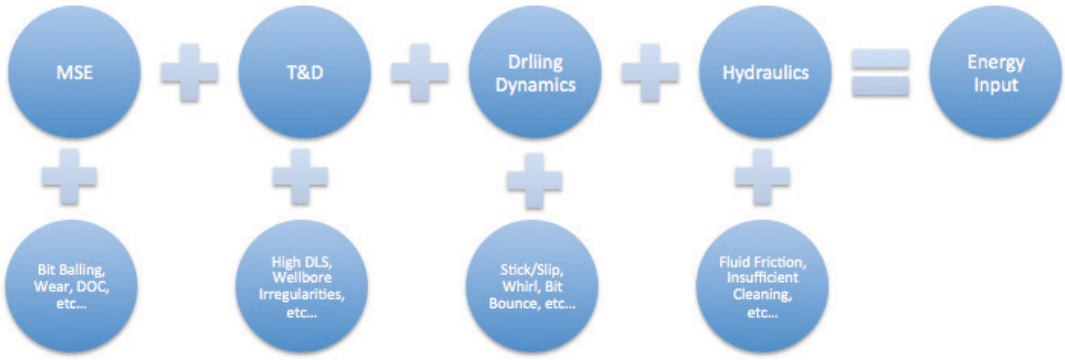

Figure 35: Break Down of the Drilling Problems within the Energy Balance

The branching could be extended to a maximum resulting in a mind map becoming more and more complex. This process is not followed up for for the time being but for a better understanding what these drilling problems might be was introduced. An energy balance used as a control framework of continuous real time measurements therefore could help to indicate if the system is operated efficiently or due to which reason an excessive amount of energy is wasted. It could help to increase the efficiency of the drilling process itself and simultaneously add an additional safety tool by identifying drilling problems in an early stage.

7 Conclusion

The governing differential equations of a drillstring's energy balance were identified: The force- and moment- balance equation describe the mechanical behavior of the drillstring; the mass-, momentum- and energy balance describe the hydraulic system; and the common wave equation describes the dynamical behavior of the drillstring to a certain extend.

The common simplifications taken into account by drilling engineers to solve the governing differential equations were highlighted. These simplifications indicate on the one hand that the models do not reflect the reality and on the other hand the actual unknowingness of what is actually happening downhole.

To better the understanding of the physical process going on downhole and to verify and improve complex models, downhole measurements are proposed along the entire drillstring becoming feasible with new telemetry techniques. In the case of real-time measurements, the efficiency of drilling operations could be evaluated on site to either confirm a well working system, or identify malfunctions and justify changes of the setup if necessary. An early identification of drilling problems through real-time measurements can not just help to save costs but also can act as an early warning system and reduce the occurrence of serious incidents.

It has been determined, which sensors are needed to measure the essential parameters and which additional measurements would be helpful whereas the essential parameters are defined through the changing parameters within the governing partial differential equations.

Based on the idea of another project to be carried out at the Montanuniversität Leoben, including several wells to be drilled for scientific reasons, the drillstring along three possible trajectories is theoretically equipped with multiple downhole measurement subs. For all three well plans it is assumed that the target is located at a depth of 1,000 meter and the well will be completed with a 5-inch casing. The three well profiles analyzed are a vertical-, a tangential- and a horizontal- well. For both the tangential- and horizontal- well a maximum buildup rate of 3°/100ft is suggested. The horizontal well has a horizontal section of 1,000 meter and the

tangential well a tangential section of 450 meter holding at a maximum inclination angel of 45 degree.

Based on the technical specifications of the sensors and a minimalistic T&D and hydraulic model of three pre-defined trajectories, a minimum number of downhole measurement subs and their distribution along the string were defined.

Some measurements are used to calibrate other sensors leading to mutual dependencies. Taking that into account, the distribution of the subs is based on the sensor with the lowest resolution in the vertical-, tangential- and horizontal section of the trajectories. It is proposed to deploy a total of 25 subs in the vertical-, 23 subs in the tangential- and 51 subs in the horizontal- well plan presented in the Methodology.

References

Aadnøy, B. S., Cooper, Iain, Miska, Stefan Z., Mitchel, Robert F. and Payne, Michael L. (eds.) (2009) *Advanced Drilling and Well Technology*, Richardson, TX, Society of Petroleum Engineers.

Adams, N. and Charrier, T. (1985) *Drilling engineering: a complete well planning approach*, Tulsa, Okla, PennWell Pub. Co.

Amoco EPTG Drilling Technology Teams (1996) *Training to Reduce Unscheduled Events*, Third Edition. Amoco Production Comapany.

Anon (1998) 'Technology gains momentum', *Oil&Gas Journal*, [online] Available from: http://www.ogj.com/articles/print/volume-96/issue-51/in-this-issue/drilling/technology-gains-momentum.html (Accessed 9 July 2015).

Bourgoyne, A. T. (ed.) (1986) *Applied drilling engineering*, SPE textbook series, Richardson, TX, Society of Petroleum Engineers.

Choudhary, D. (2011a) 'DIRECTIONAL DRILLING TECHNOLOGY: 6. Types of Directional Well Profile', *DIRECTIONAL DRILLING TECHNOLOGY*, [online] Available from: http://directionaldrilling.blogspot.co.at/2011/07/types-of-directional-well-profile.html (Accessed 31 July 2015).

Choudhary, D. (2011b) 'DIRECTIONAL DRILLING TECHNOLOGY: 9. Dog Leg Severity (DLS)', *DIRECTIONAL DRILLING TECHNOLOGY*, [online] Available from: http://directionaldrilling.blogspot.co.at/2011/07/dog-leg-severity-dls.html (Accessed 9 November 2015).

Choudhary, D. (2011c) 'DIRECTIONAL DRILLING TECHNOLOGY: 18. STABILIZERS', *DIRECTIONAL DRILLING TECHNOLOGY*, [online] Available from: http://directionaldrilling.blogspot.co.at/2011/07/stabilizers.html (Accessed 6 July 2015).

Duncan James Junor (2007) 'Challenges and developments in direct measurement of down hole forces affecting drilling efficiency', Aberdeen, The Robert Gordon University.

Dupriest, F. E. and Koederitz, W. L. (2005) 'Maximizing Drill Rates with Real-Time Surveillance of Mechanical Specific Energy', In *SPE-92194-MS*, SPE, Society of Petroleum Engineers.

Dykstra, M. W., Neubert, M., Hanson, J. M. and Meiners, M. J. (2001) 'Improving Drilling Performance by Applying Advanced Dynamics Models', In *SPE-67697-MS*, SPE, Society of Petroleum Engineers.

Fjar, E., Holt, R. M., Raaen, A., Risnes, R. and Horsrud, P. (2008) *Petroleum Related Rock Mechanics*, 2nd ed. Developments in petroleum science, Amsterdam ; Boston, Elsevier.

Gabolde, G. and Nguyen, J.-P. (2006) *Drilling data handbook*, 8th ed., completely rev. and expanded. IFP publications, Paris, Editions Technip.

Gabriel Gomes Müller (2015) 'Development of an Energy Consumption Model Based on Standard Drilling Parameters', Master Thesis, Leoben, Montanuniversität Leoben.

Hishida, H., Ueno, M., Higuchi, K. and Hatakeyama, T. (1996) 'Prediction of Helical / Sinusoidal Buckling', In *SPE-36384-MS*, SPE, Society of Petroleum Engineers.

Hsieh, L. (2010) 'Abrasive formations, shale wells drive new bit designs for hard-rock, high-temperature drilling', *Drilling Contractor*, [online] Available from: http://www.drillingcontractor.org/abrasive-formations-shale-wells-drive-new-bit-designs-for-hard-rock-high-temperature-drilling-5418 (Accessed 2 July 2015).

INTEQ, B. H. (1995) *Drilling Engineering Workbook–A Distributed Learning Course*, 80270H Rev, Houston.

Jack (2015) 'Tool Joint', *Oil & Gas Drilling Engineering*, [online] Available from: http://www.oilngasdrilling.com/tag/tool-joint (Accessed 23 July 2015).

Johnson, M. and Hernandez, M. (2009) 'Along String Pressure and Temperature Measurements in Real-Time: Early Field Use and Resultant Value', In *SPE-119540-MS*, SPE, Society of Petroleum Engineers.

Marland, C. and Greenwood, J. (2015) 'Strain-Gauge Bending-Moment Measurements Used to Identify Wellbore Tortuosity', In *SPE-173039-MS*, SPE, Society of Petroleum Engineers.

Mason, C. and Chen, D. C.-K. (2007) 'Step Changes needed to Modernise T&D Software', In *SPE-104609-MS*, SPE, Society of Petroleum Engineers.

Menand, S., Sellami, H., Tijani, M., Stab, O., Dupuis, D. C. and Simon, C. (2006) 'Advancements in 3D Drillstring mechanics: From the Bit to the Topdrive', In *SPE-98965-MS*, SPE, Society of Petroleum Engineers.

Mitchell, R. F., Miska, S., Aadnøy, B. S. and Society of Petroleum Engineers (U.S.) (eds.) (2011) *Fundamentals of drilling engineering*, SPE textbook series, Richardson, TX, Society of Petroleum Engineers.

M.Sc. Eng. Andreas Nascimento (2012) 'Drilling Fluid: A Stochastic ROP Optimization Approach for the Brazilian Pre - Salt Carbonates', Master Thesis, Leoben, Montanuniversität Leoben.

Philipp Doppringer (2014) 'Drillstring Mechanical Modeling and Real-time Monitoring', Master Thesis, Leoben, Montanuniversität Leoben.

Samuel, G. R. and Liu, X. (2009) *Advanced drilling engineering: principles and designs*, Houston, TX, Gulf Pub.

Schlumberger (2010) ‘Drilling Dynamics Sensors and Optimization’, Schlumberger, [online] Available from: http://www.slb.com/~/media/Files/drilling/brochures/mwd/drilling_dynamics_sensors_opt_br.pdf.

Society of Petroleum Engineers (U.S.) (2015) ‘Directional Deviation Tools’, *PetroWiki*, Wikipedia.

Stephane Menand (2012) ‘Latest Advancements in Drillstring Mechanics: BHA & Buckling Modeling’,.

Sugiura, J., Samuel, R., Oppelt, J., Ostermeyer, G. P., Hedengren, J. and Pastusek, P. (2015) ‘Drilling Modeling and Simulation: Current State and Future Goals’, In *SPE-173045-MS*, SPE, Society of Petroleum Engineers.

Teale, R. (1965) ‘The concept of specific energy in rock drilling’, In Elsevier, pp. 57–73.

The University of Aberdeen (n.d.) ‘The School of Engineering’, *Modelling and Analysis of BHA and Drill-String Vibrations*, [online] Available from: http://www.abdn.ac.uk/engineering/research/modeling-and-analysis-of-bha-and-drillstring-vibrations-149.php.

Appendix

A The Processes Behind the Minimalistic Model

Some of energy consuming processes identified in the main body due to a breakdown of the system into its single components is shortly described below.

A.1 Positive Displacement Mud Motor Power Consumption

Talking about the energy consumption of a PDM first the specific displacement, s in in^3/rev, per revolution of the rotor needs to be determined. Whereas the specific displacement equals the cross – sectional area of the fluid time the distance the fluid advances.

$$s = n_r * n_{st} * P_r * A \quad (38)$$

Where P is the rotor pitch, which is equivalent to the rotor wavelength, A in in^3, is the approximated cross sectional area of the fluid, d_0 the stator OD, n_r the number of rotor lobes and n_{st} stator lobes.

$$A = \frac{\pi d_0^2}{4} \frac{2n_{st} - 1}{(n_{st} + 1)^2} \quad (39)$$

Having the specific displacement s bit speed, N_b, is the flow rate, q in gal/min, divided by the specific displacement.

$$N_b = \frac{231q}{s} \quad (40)$$

The torque of the motor is given by Equation (41) where T is the torque in ft-lb, Δp the hydraulic pressure loss across the motor in psi and η the efficiency in the range of 80% for a PDM with a 1:2 lobe ration and 70% for a PDM with higher lobe ratios.

$$T = \frac{3.064 * q * \Delta p * \eta}{RPM} \quad (41)$$

A.2 Torque and Drag (T&D)

During drilling the drillstring is lowered and rotated at the same time resulting in corresponding drag and torque forces acting on the string resulting in change in axial load as well as rotational load on the string. For a better understanding the general idea of friction govern T&D are introduced below.

A.2.1 Friction

Friction is defined as the force acting against the relative motion of two surfaces against each other. Three empirical laws define the elementary properties of mechanical friction between two surfaces:

- Amontons' First Law: The force of friction is directly proportional to the applied load.
- Amontons' Second Law: The force of friction is independent of the apparent area of contact.
- Coulomb's Law of Friction: Kinetic friction is independent of the sliding velocity.

Mathematically the friction force, F_f, is defined by the product of the force exerted by each surface on the other whereas this force is always normal/perpendicular to the surface and therefore called the normal force F_N times the empirical friction factor, μ, that represents the roughness between the surfaces. The friction coefficient is dimensionless whereas the forces are expressed in newton.

$$F_f = \mu F_N \tag{42}$$

There are two regimes concerning friction the static friction between non-moving surfaces and the dynamic friction between moving surfaces. The direction of the friction force acts in the opposite direction of the movement or potential movement caused by external force acting on an object. The static friction hinders objects to move relative to each other and shows normally a linear relationship between the applied force, F_a, and the friction force, F_f, up to a certain limit that has to be overcome before an object starts to move. The resulting friction force in the dynamic mode is almost constant and therefore velocity independent as defined in Coulomb's Law of friction above. The concept of static- and dynamic- friction is graphically visualized in Figure 36.

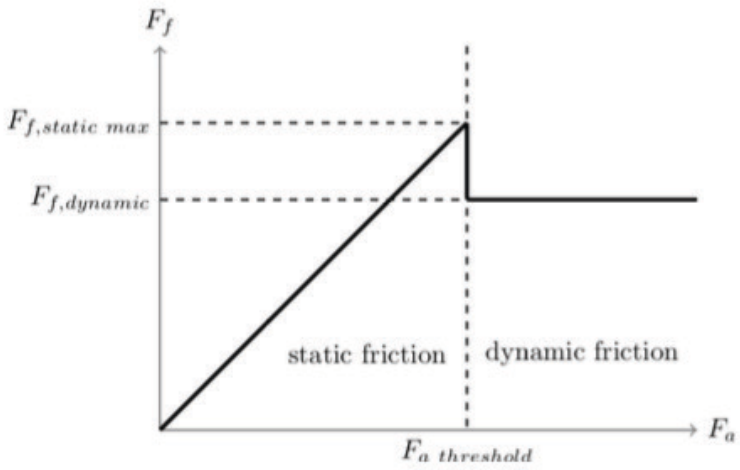

Figure 36: Change of the Friction Regime (Philipp Doppringer, 2014)

A.2.1.1 Friction Factor

The regimes are differentiated with the help of the friction coefficient, μ, which is a material parameter. It is differentiated between a static, μ_s, and dynamic or kinetic friction coefficient, μ_d. The maximum static friction is given by the static friction coefficient and therefore the dynamic friction force is given by the normally lower dynamic friction coefficient.

According to (Mason & Chen, 2007) the dynamic friction factor is more relevant for T&D modeling and normally in the range of 0.1 and 0.3 for rotary drilling operations. Extreme values can be as low as 0.05 and as high as 0.5. For the simple model above friction factors as high as 0.3 for the OH section and 0.15 for the CH section are assumed.

In its purest form the friction factor will only represent the true mechanical friction but in reality friction is following unwanted contributors influences the factor:

- Pipe stiffness effect (soft string models don't account for that)
- Wellbore obstructions (cutting beds, breakouts, micro-tortuosity, spiraling, etc.)
- Lubricity variations (formation types, circulation losses, etc.)

A.2.1.2 Normal Force

The compressional force between two objects is the normal force perpendicular to the surface. Normally the gravitational weight force is a part of this normal force spatially depending on the dip of the surfaces in space described by the angle Θ.

$$F_N = mg \quad (43)$$

A.2.2 Torque

Torque with the symbol T is the tendency of a force to rotate an object about an axis. In other words the torque is the force that gives an object a twist and is expressed in newton meter (Nm). Mathematically torque is defined as the product of an eccentric force, F, acting on the object multiplied by the lever arm, r, that is perpendicular to the acting force and has its origin in the rotating axis of the object.

$$T = F * r \quad (44)$$

Therefore the product of the frictional force and the radius, r, in case of a circular drilling tool gives the torque. A torque increment is calculated for several drillstring increments selected by the different tool lengths and in the end summed up to give the cumulative torque.

$$\Delta T = F_f * r = F_N * \mu * r \quad (45)$$

Theoretically there is no neither friction nor torque in a vertical borehole, as the drillstring isn't in contact with the borehole wall. In an inclined borehole it is assumed in a simplified case that the whole string is in contact with the wall at it's lowest point. In reality the pipe tries to climb the wall due to it's rotation and the friction force between the borehole and the pipe (Figure 37). This leads to a reduced contact force as not the total deadweight of the pipe contributes to it.

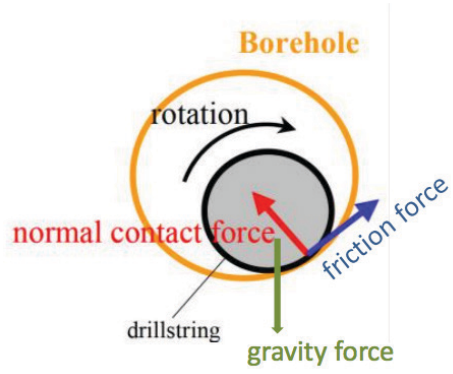

Figure 37: Equilibrium Position of a Rotating Pipe in an Inclined Wellbore Section (Menand et al., 2006)

With the help of the borehole friction coefficient, μ, the offset angel, ϕ, at which equilibrium is assumed can be found as presented with the following equation.

$$\varphi = \arctan(\mu) \quad (46)$$

With the offset angle a more accurate torque may be estimated.

$$\Delta T = F_N * r * \sin(\varphi) \quad (47)$$

A.2.2.1 Bit Torque

With the previous assumptions equation (11) is rearranged to equation (48) to express torque as a function of MSE, WOB, ROP and RPM. Whereas for an ideal case it is assumed that MSE equals UCS.

$$T = \frac{ROP}{2\pi * RPM} * \left(UCS * A - WOB\right) \quad (48)$$

A.2.3 Drag

As the drillstring is lowered or lifted in drilling operations the string experiences a change in axial load. This change in axial load that the drillstring experience comes from the friction forces acting on the string as it is pulled along the borehole wall. This resistance in axial movement due to friction is called “Drag” in the O&G industry. Mathematically it is expressed by the same equation as above (equation (42)) where the normal force results from the weight of the pipe depending of the borehole inclination. The friction force now influences the axial load in means of running the pipe in hole (RIH) or pulling the pipe out of the hole (POOH). Dependent on direction of movement the friction force is either added (POOH) or subtracted (RIH) from the axial load in means of tension. In the case of drilling we assume RIH plus the load needed at the bit (WOB) to achieve penetration.

A.3 Hydraulics

It is accounted for the pressure losses through the string, the bit nozzles and the losses in the annulus up to the surface. The pressure loss is modeled for a Bingham fluid. The relevant calculations for the model can be found below in the in the Table 41. The theoretical background can be looked up in the book “Applied Drilling Engineering; Chapter 4: Drilling Hydraulics”. (Bourgoyne, 1986, p. 113 ff.)

Table 41: Hydraulics – Frictional Pressure Loss Equations (Bourgoyne, 1986, p. 155)

	Newtonian Model	Bingham Plastic Model	Power-Law Model
Mean Velocity, $\bar{v}$	Pipe		
	$\bar{v} = \frac{q}{2.448 d^2}$	$\bar{v} = \frac{q}{2.448 d^2}$	$\bar{v} = \frac{q}{2.448 d^2}$
	Annulus		
	$\bar{v} = \frac{q}{2.448(d_2^{\,2} - d_1^{\,2})}$	$\bar{v} = \frac{q}{2.448(d_2^{\,2} - d_1^{\,2})}$	$\bar{v} = \frac{q}{2.448(d_2^{\,2} - d_1^{\,2})}$
Flow Behavior Parameters	$\mu = \theta_{300}$	$\mu_p = \theta_{600} - \theta_{300}$	$n = 3.32 \log \frac{\theta_{600}}{\theta_{300}}$
		$\tau_y = \theta_{300} - \mu_p$	$K = \frac{510\,\theta_{300}}{511^n}$
Turbulence Criteria	Pipe		
	$N_{Rec} = 2{,}100$	$N_{He} = \frac{37{,}100\,\rho\,\tau_y\,d^2}{\mu_p^{\,2}}$	N_{Rec} from Fig. 4.34
	$N_{Re} = \frac{928\,\rho\,\bar{v}\,d}{\mu}$	N_{Rec} from Fig. 4.33	$N_{Re} = \frac{89{,}100\,\rho\bar{v}^{\,2-n}}{K}\left(\frac{0.0416d}{3+1/n}\right)^n$
		$N_{Re} = \frac{928\,\rho\,\bar{v}\,d}{\mu_p}$	
	Annulus		
	$N_{Rec} = 2{,}100$	$N_{He} = \frac{24{,}700\,\rho\,\tau_y\,(d_2-d_1)^2}{\mu_p^{\,2}}$	N_{Rec} from Fig. 4.34
	$N_{Re} = \frac{757\,\rho\bar{v}(d_2-d_1)}{\mu}$	$N_{Re} = \frac{757\,\rho\bar{v}(d_2-d_1)}{\mu_p}$	$N_{Re} = \frac{109{,}000\,\rho(\bar{v})^{2-n}}{K}\left[\frac{0.0208(d_2-d_1)}{2+1/n}\right]^n$
Laminar Flow Frictional Pressure Loss	Pipe		
	$\frac{dp_f}{dL} = \frac{\mu\bar{v}}{1{,}500\,d^2}$	$\frac{dp_f}{dL} = \frac{\mu_p\bar{v}}{1{,}500\,d^2} + \frac{\tau_y}{225\,d}$	$\frac{dp_f}{dL} = \frac{K\bar{v}^{\,n}\left(\frac{3+1/n}{0.0416}\right)^n}{144{,}000\,d^{1+n}}$
	Annulus		
	$\frac{dp_f}{dL} = \frac{\mu\bar{v}}{1{,}000\,(d_2-d_1)^2}$	$\frac{dp_f}{dL} = \frac{\mu_p\bar{v}}{1{,}000\,(d_2-d_1)^2} + \frac{\tau_y}{200\,(d_2-d_1)}$	$\frac{dp_f}{dL} = \frac{K\bar{v}^{\,n}\left(\frac{2+1/n}{0.0208}\right)^n}{144{,}000\,(d_2-d_1)^{1+n}}$
Turbulent Flow Frictional Pressure Loss	Pipe		
	$\frac{dp_f}{dL} = \frac{f\,\rho\,\bar{v}^{\,2}}{25.8\,d}$	$\frac{dp_f}{dL} = \frac{f\,\rho\,\bar{v}^{\,2}}{25.8\,d}$	$\frac{dp_f}{dL} = \frac{f\,\rho\,\bar{v}^{\,2}}{25.8\,d}$
	or	or	
	$\frac{dp_f}{dL} = \frac{\rho^{0.75}\bar{v}^{\,1.75}\mu^{0.25}}{1{,}800\,d^{1.25}}$	$\frac{dp_f}{dL} = \frac{\rho^{0.75}\bar{v}^{\,1.75}\mu_p^{\,0.25}}{1{,}800\,d^{1.25}}$	
	Annulus		
	$\frac{dp_f}{dL} = \frac{f\,\rho\,\bar{v}^{\,2}}{21.1\,(d_2-d_1)}$	$\frac{dp_f}{dL} = \frac{f\,\rho\,\bar{v}^{\,2}}{21.1\,(d_2-d_1)}$	$\frac{dp_f}{dL} = \frac{f\,\rho\,\bar{v}^{\,2}}{21.1\,(d_2-d_1)}$
	or	or	
	$\frac{dp_f}{dL} = \frac{\rho^{0.75}\bar{v}^{\,1.75}\mu^{0.25}}{1{,}396\,(d_2-d_1)^{1.25}}$	$\frac{dp_f}{dL} = \frac{\rho^{0.75}\bar{v}^{\,1.75}\mu^{0.25}}{1{,}396\,(d_2-d_1)^{1.25}}$	

A.3.1 Pressure Drop Depending on the Annulus Size

Knowing that the fluid velocity allows a conclusion about the pressure loss it can be said that high fluid velocities result in a larger pressure drop along a pipe of same diameter due to higher shear forces. These can be described by the losses due to

friction in straight pipes, which are mathematically described with the so-called Darcy – Weisbach equation.

$$\Delta p = \lambda * \frac{\Delta L}{D_H} * \frac{v_m^2}{2 * g} \quad (49)$$

Here ΔL is the length of pipe with the same diameter, D_H the hydraulic diameter, v_m the average velocity of the fluid along this section, g gravitational acceleration and λ the dimensionless Darcy friction factor. The friction factor can either be found from a Moody diagram or calculated with the help of the Reynolds Number (Re) for laminar flow by Equation (50) and for turbulent flow by Equation (51).

$$\lambda = \frac{64}{Re} \quad (50)$$

$$\frac{1}{\sqrt{\lambda}} = 2 * \log\left(Re * \sqrt{\lambda}\right) - 0.8 \quad for\ Re > 3000 \quad (51)$$

The Reynolds Number helps as a dimensionless value to predict the flow pattern of the fluid is either laminar or turbulent and can be calculated with the help of the equation below where ρ is the fluid density, v_m as above the average velocity of the fluid, D_H the hydraulic diameter and μ the dynamic viscosity of the fluid.

$$Re = \frac{\rho * v_m * D_H}{\mu} \quad (52)$$

Additionally the hydraulic diameter (D_H) introduced in Equation (49) & (52) needs to be defined. It is commonly used when a flow has to be described in noncircular tubes and channels like the annulus. In the general form A is the cross sectional area and P the wetted perimeter (the boundary in contact with the fluid).

$$D_H(Annulus) = \frac{4A}{P} = \frac{4 * \frac{\pi * (D^2 - d^2)}{4}}{4 * (D + d)} = D - d \quad (53)$$

Finally having defined all the parameters needed for the Darcy – Weisbach Equation it can be analyzed the influence of the reduced annulus on the pressure drop. Despite a reduced friction factor λ as the Reynolds Number increases with higher velocities along the pipe the pressure drop is higher due to a reduced hydraulic

diameter and average fluid velocity both influencing the absolute value of the pressure drop in Equation (49).

A.4 Buckling

The critical force indicating buckling in this thesis if given by equation (54) where the first term is the standard term for buckling in inclined wells and becomes zero as long as the wells stays vertical. The second term describes the buckling tendency in a vertical well and on the other hand becomes zero in a horizontal section. In the equation E is the Young's Modulus of the material, I the geometric moment of Inertia, ω the effective weight per unit length, Θ the angle of inclination and r the radial clearance between the borehole and the drillstring. (Hishida et al., 1996)

$$F_{crit} = 2\sqrt{\frac{EI\omega \sin\theta}{r}} + 2.705\sqrt[3]{EI\omega^2 \cos^2\theta} \qquad (54)$$

B Graphical Results of the Minimalistic Models

B.1 Vertical Well

Starting with the vertical well the planned well trajectory is presented in Figure 38.

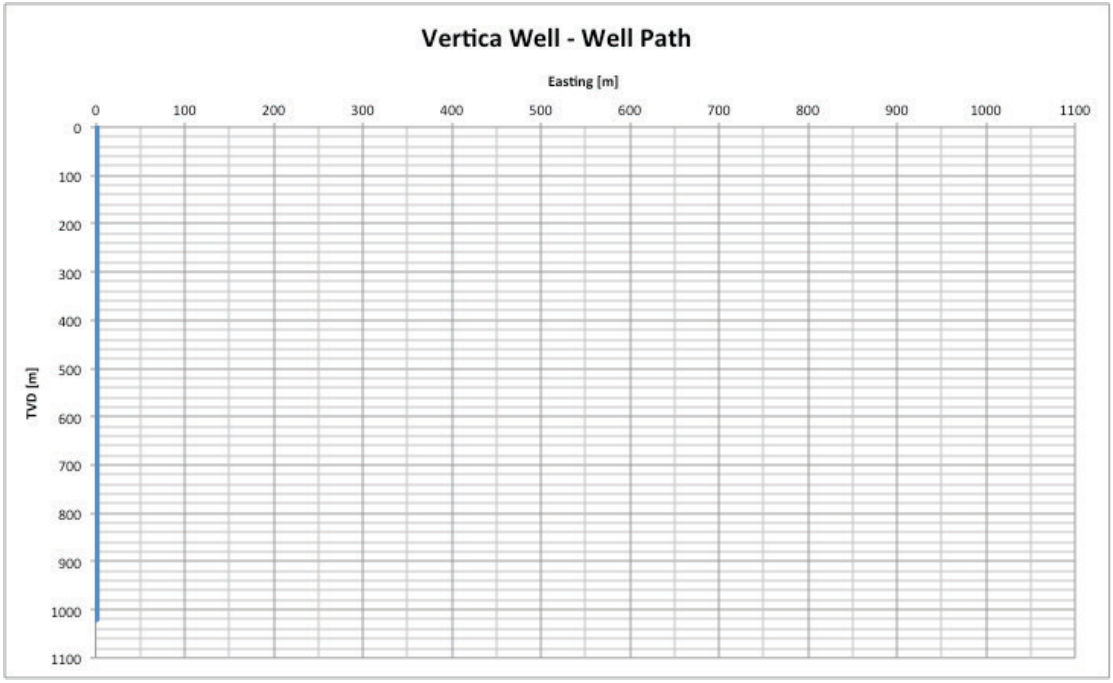

Figure 38: Vertical Well - Well Profile

The vertical well is indicated as a straight vertical blue line with its origin in the zero point. It is planned to drill vertically to final depth of 1,000 m.

Figure 39 represents the results from the minimalistic T&D model. The axial loads the drillstring experiences when it is “Run Into the Hole” (RIH), “Rotated Of Bottom” (ROB) and “Pulled Out Of Hole” (POOH), are visualized. In the case of the vertical well it is assumed that the string is perfectly centralized, not touching the borehole wall, resulting in zero friction. Therefore the results for ROB and POOH are equal and overlap each other. The RHI model also represents the drilling operations as we count for WOB. A certain part is under compression as indicated below. The orange line is the critical force calculated based on the geometrical properties of the borehole and string. Experiences the string a higher compressional force as the critical force it is assumed that it would buckle.

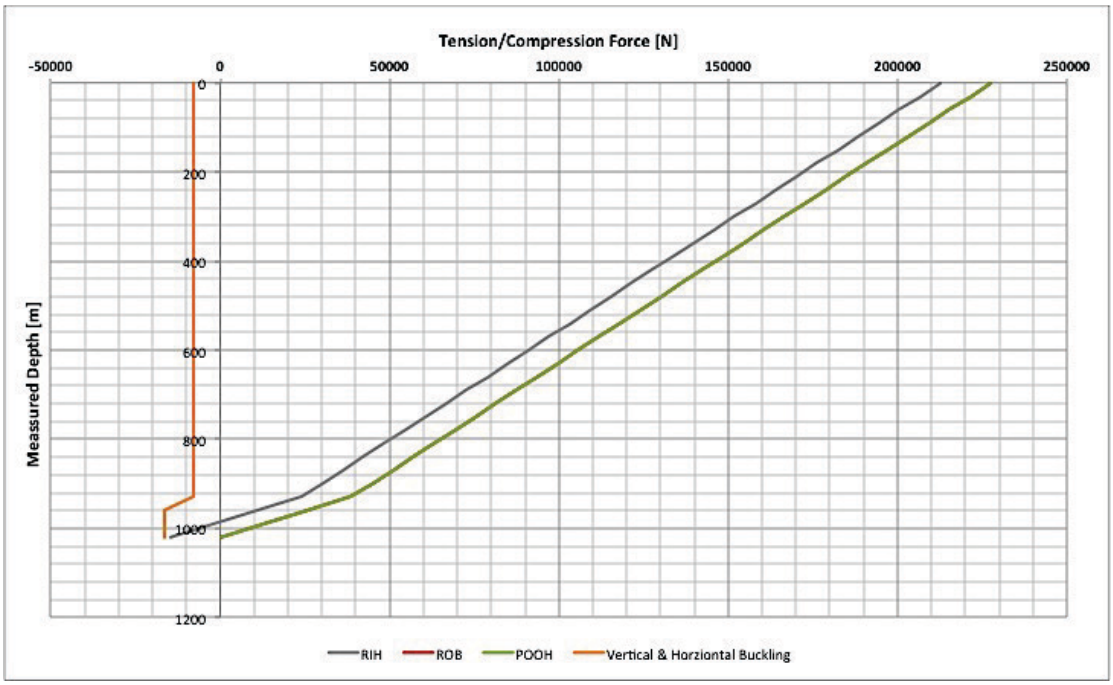

Figure 39: Vertical Well - Tension/Compression Profile

Figure 40 represents the torque expected for the vertical well. As it is just governed by the torque at the bit it stays constant up to the surface. The critical value for the torque is normally given through the maximum make-up torque of the tool joints. The tool joints therefore represent the weak points of the drillstring concerning torque. For all three models the maximum make-up torque of the weakest tool joint is taken into consideration along the entire string.

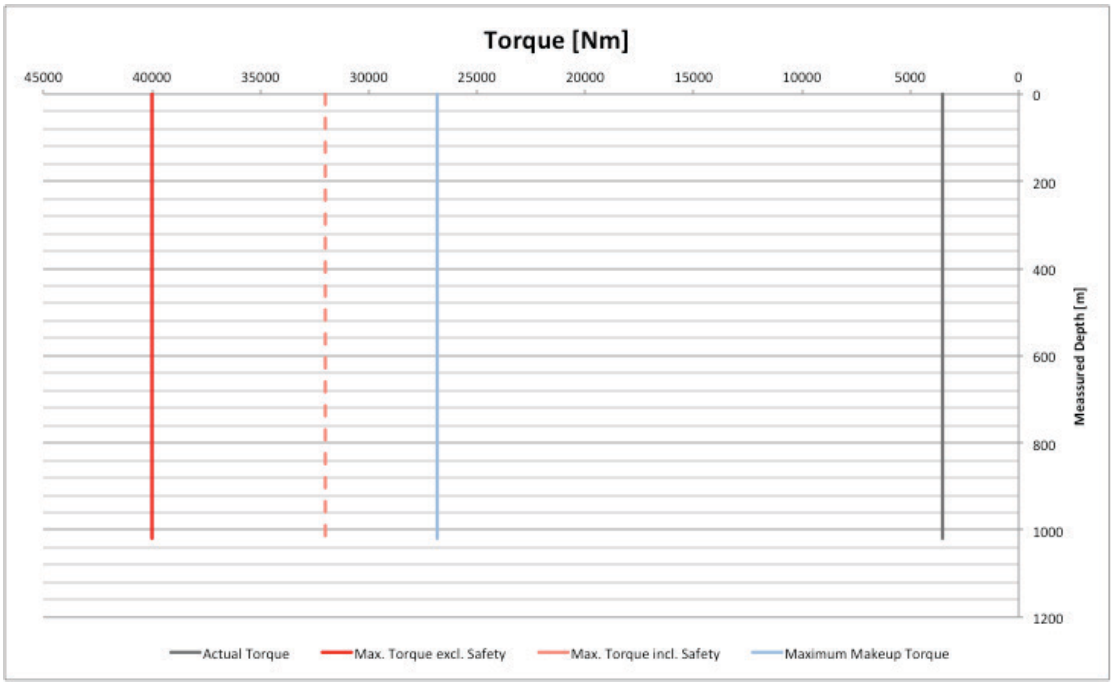

Figure 40: Vertical Well - Torque Profile

The last graph (Figure 41) for the vertical well is giving a feeling for the overall pressure loss in its hydraulic system.

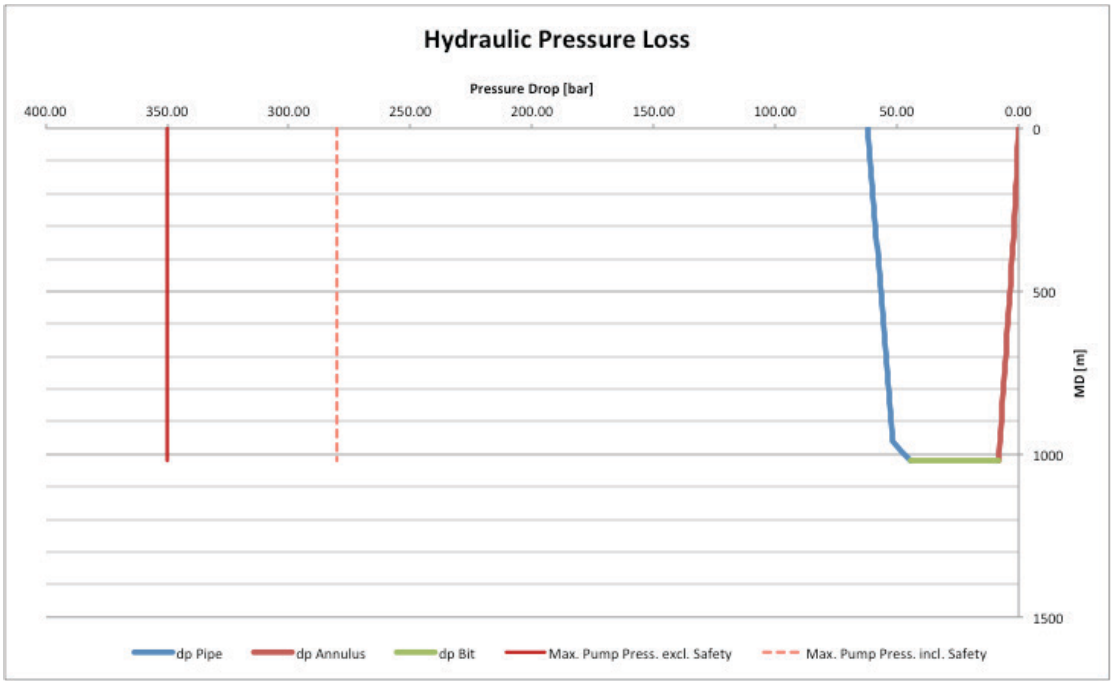

Figure 41: Vertical Well - Hydraulic Pressure Loss Profile

The surface pumps give the upper limit for the pressure drop. The actual pressure loss in the system is indicated through the pressure loss through the pipe (blue line), across the nozzles (green line) and along the annulus (red line).

B.2 Tangential Well

Following the graphical results for the minimalistic T&D and hydraulic model are presented for the predefined tangential well path shown in Figure 42.

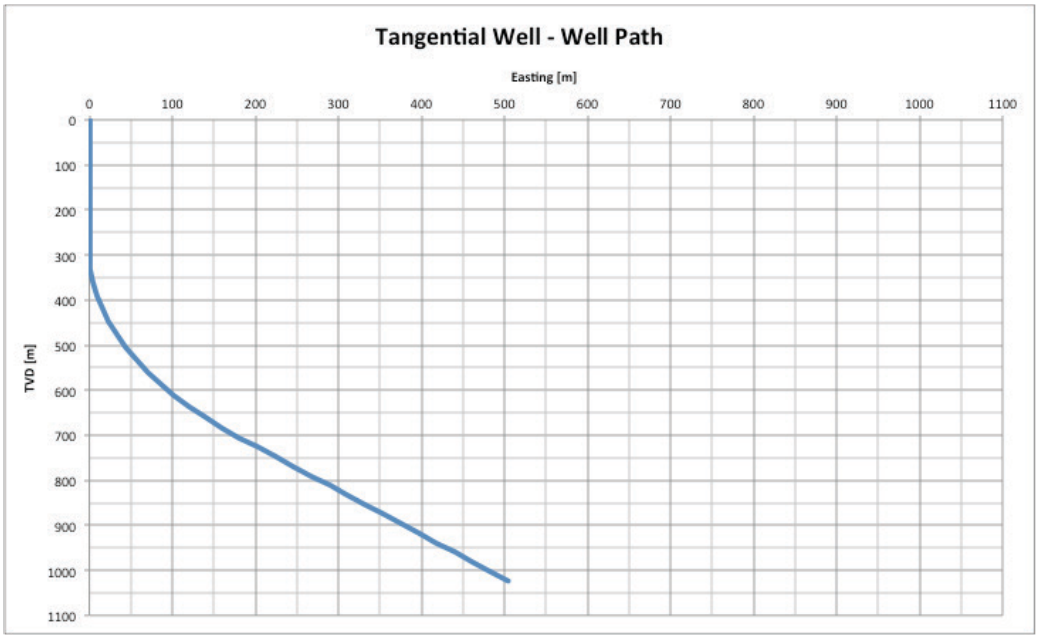

Figure 42: Tangential Well - Well Profile

The results from the T&D model for the tangential well are presented in Figure 43.

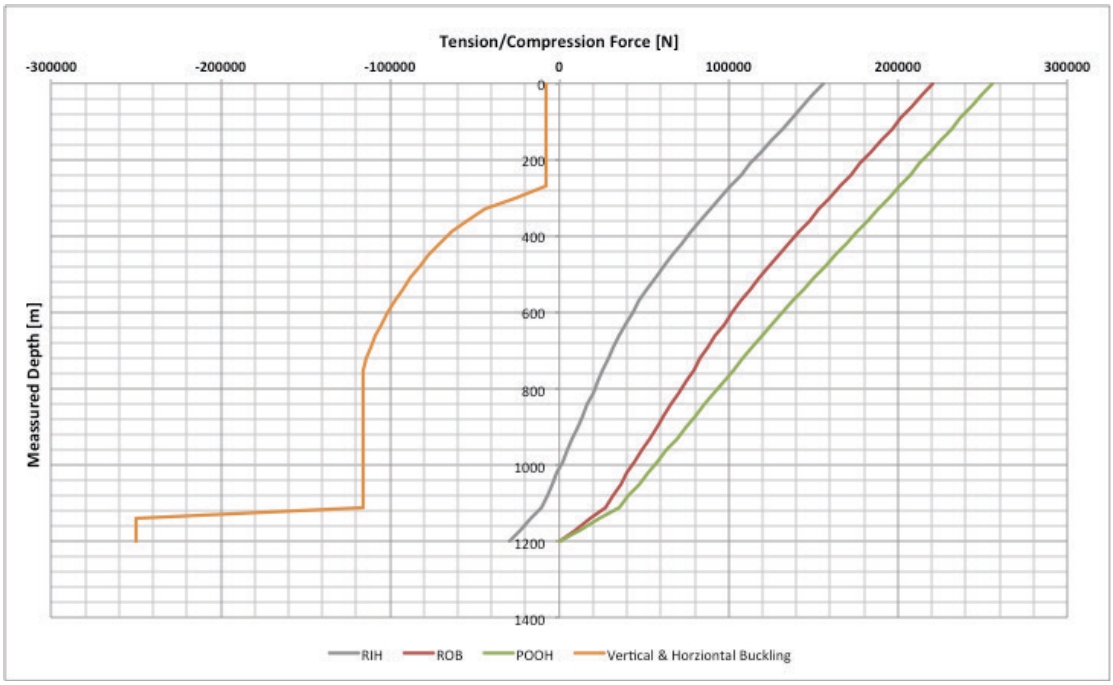

Figure 43: Tangential Well - Tension/Compression Profile

Compared to the vertical well the difference between the two operations ROB and POOH is obvious. It shows clearly that the tensional force as the string is POOH is the

highest as the frictional forces have to be taken into account that act against the direction of movement. The change in inclination also leads to a change of the torque that the drillstring experiences along the wellbore as visualized in Figure 44.

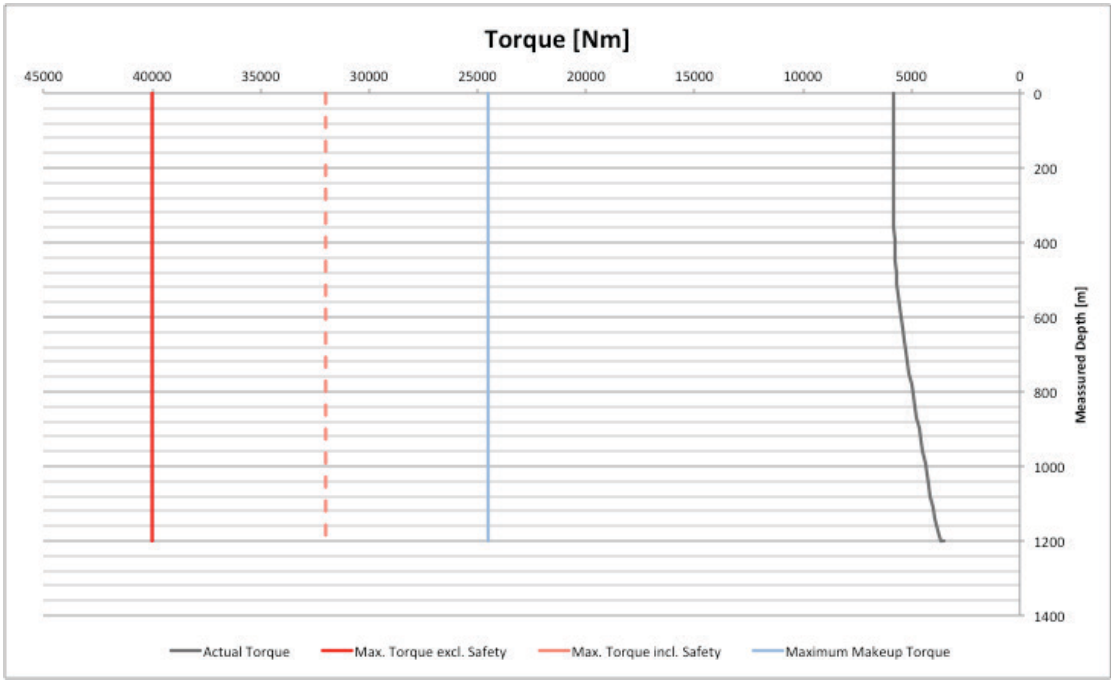

Figure 44: Tangential Well – Torque Profile

The graphical result of the hydraulic model is presented in Figure 45.

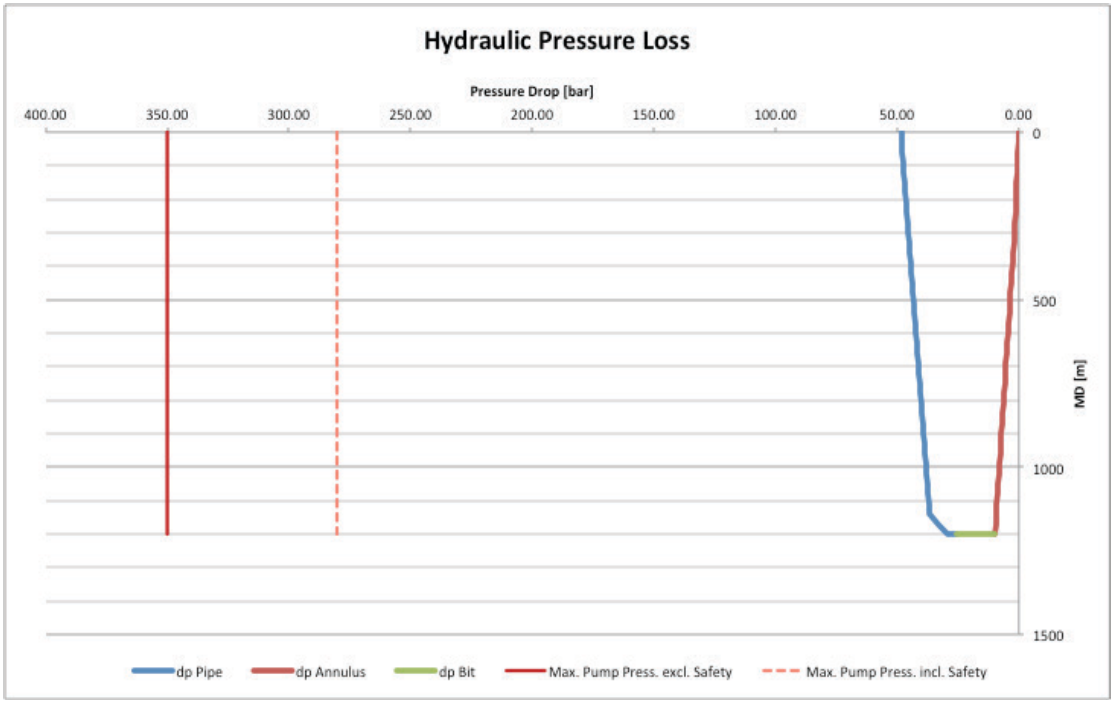

Figure 45: Tangential Well - Hydraulic Pressure Losses

B.3 Horizontal Well

As for the vertical- and tangential- well the graphical results of the T&D and hydraulic model for the horizontal well profile shown in Figure 46 are represented in this chapter.

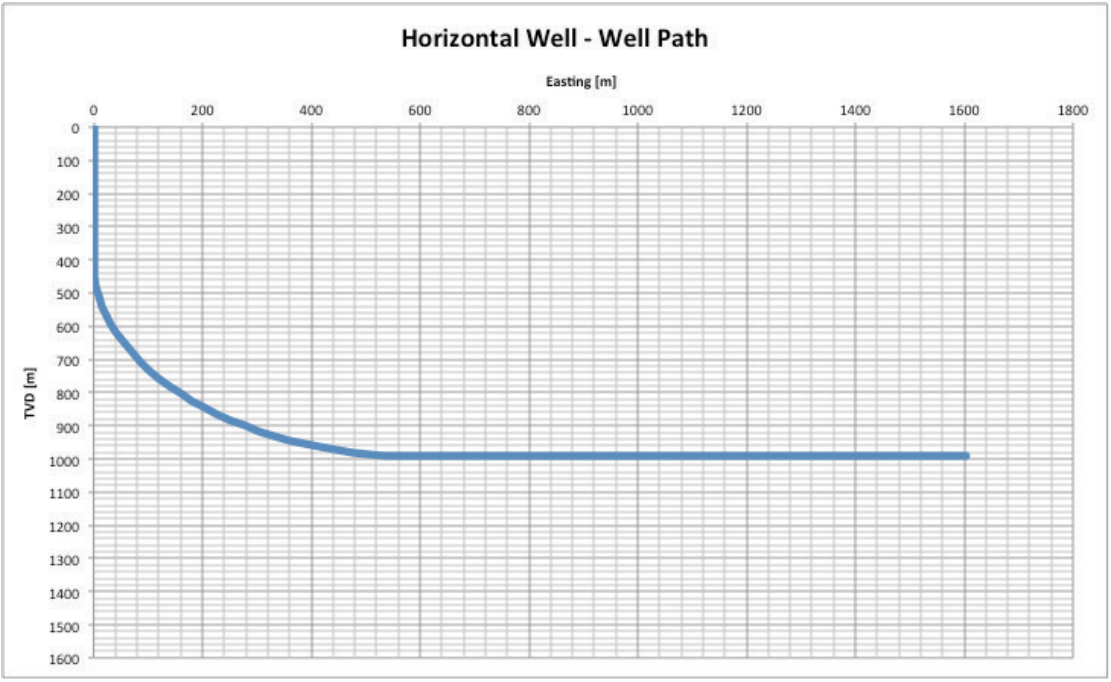

Figure 46: Horizontal Well – Well Profile

The well profile in this case indicates a 1,000 m long OH horizontal section leading to the fact that during drilling most of the string is under compression as shown in Figure 47. Due to this high compressional forces the string comes very close the margin indicating the critical compressional force.

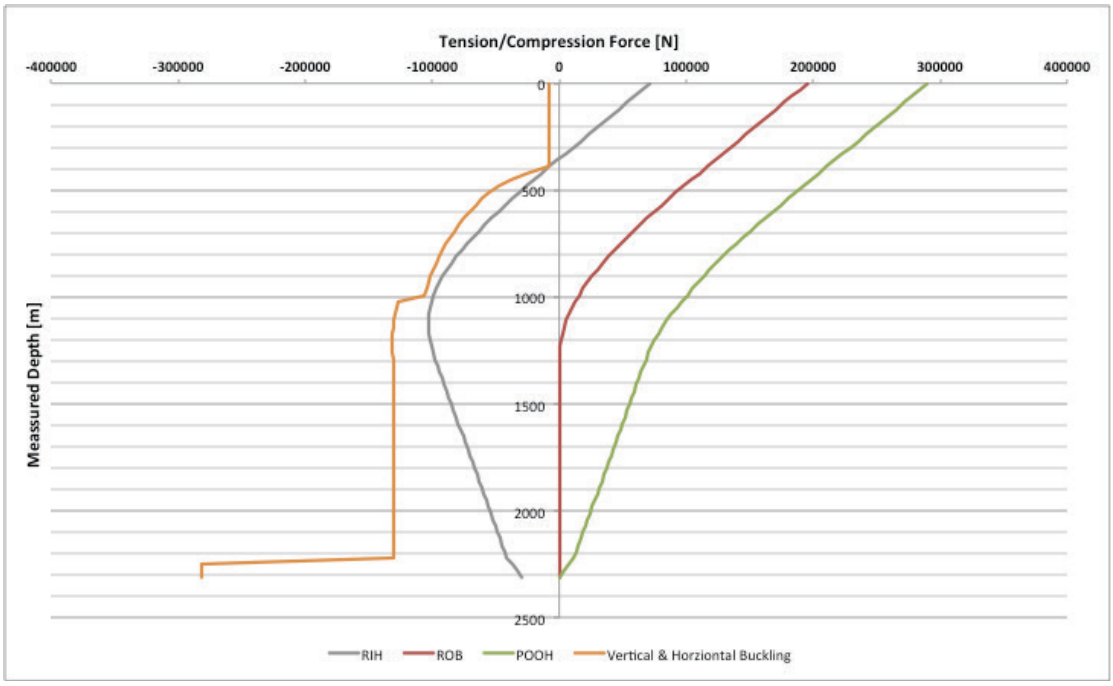

Figure 47: Horizontal Well – Tension/Compression Profile

The torque is the highest in the horizontal well as shown in Figure 48 compared to the vertical and tangential well. Nevertheless the expected torque readings aren't close to any upper limit for neither of the different well plans.

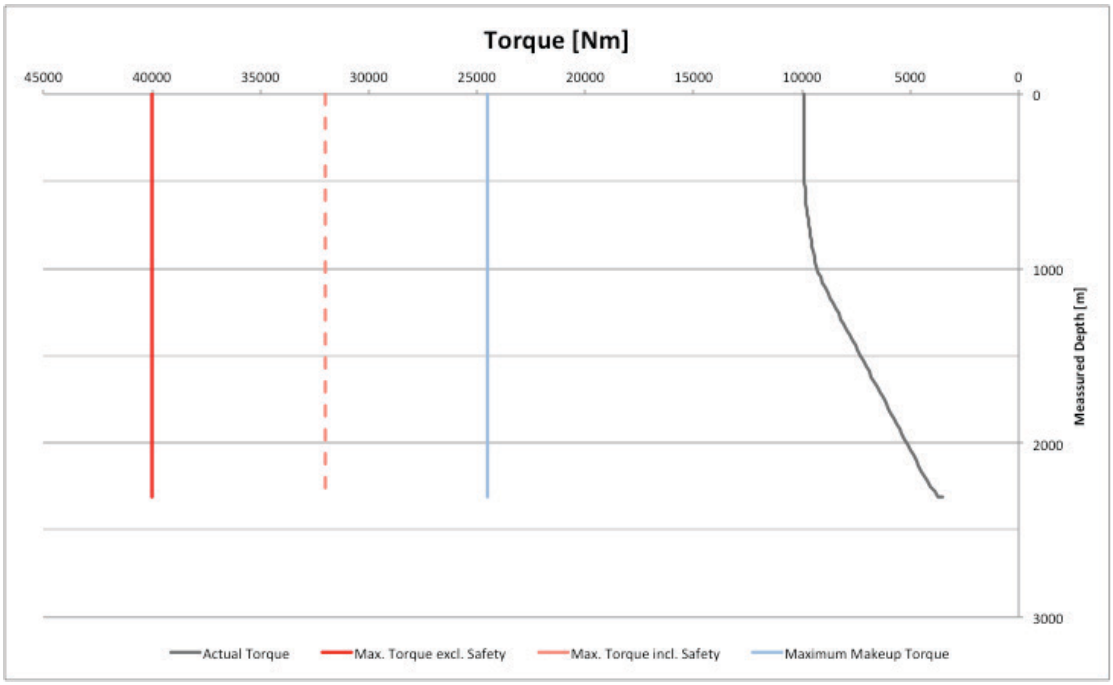

Figure 48: Horizontal Well – Torque Profile

The hydraulic pressure loss for the horizontal well is graphically visualized in Figure 49. The modeled loss doesn't point out any restrictions for the planned well.

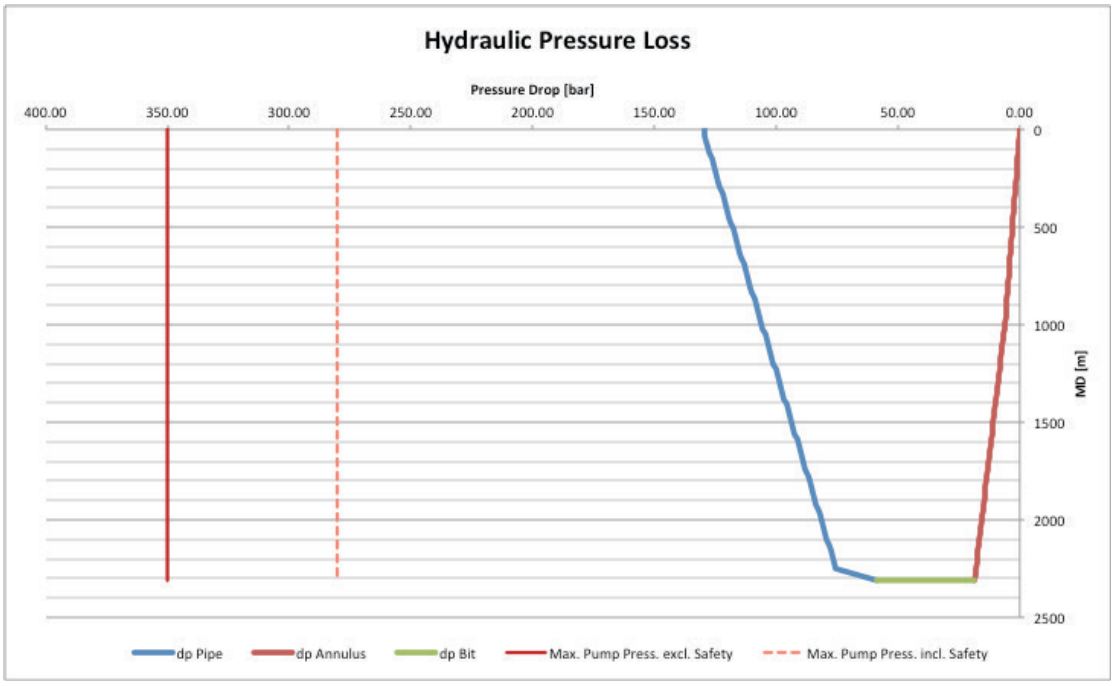

Figure 49: Horizontal Well - Hydraulic Pressure Losses

C Extending the Model

C.1 Drilling Dynamics

As stated before the dynamical behavior of the drillstring can be split into two dominant processes first into so-called “Shocks” and secondly into “Vibrations”. A shock is given through the unexpected input of energy due to the impact of downhole components with the borehole. The vibrations are the periodic response as a result of the shock. Both are measured in Gs where one G equals the gravity that is defined by the acceleration (9.81 m/s^2, or 32.3 ft/s^2). The occurrence of vibrations is linked to the drillstring design like its dimensioning, weight and stiffness and also to the interrelation of the string and borehole.

C.1.1 Vibrations

Vibrations are always present of different magnitude during drilling due to dynamic loads. Different types of vibrations occur during drilling detracting some of the energy brought into the system through WOB, drillstring rotation and hydraulics. All have in common that they in general reduce the drilling performance as well as advanced minor or catastrophic failure of a BHA component. It is differentiated between three main categories presented in Figure 50, which are axial (green), lateral (blue) and torsional (red) vibrations. Axial and torsional vibrations may be

seen up to the surface in severe cases whereas lateral vibrations are usually trapped below the neutral point.

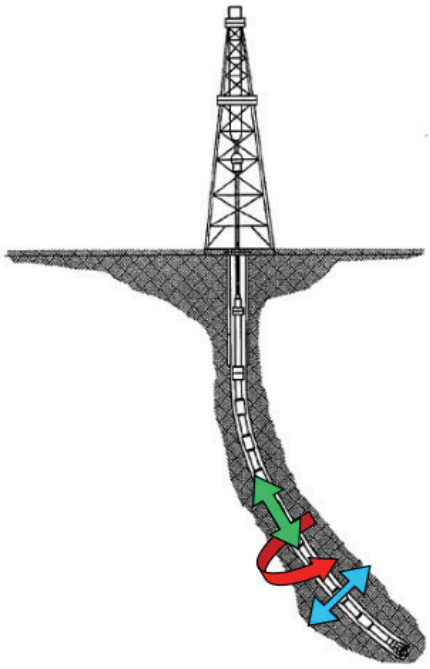

Figure 50: The Three Categories of Downhole Vibrations; green arrow indicates axial direction of action for axial vibrations the blue ones for lateral vibrations and the red one for torsional vibrations along the drillstring. (Stephane Menand, 2012)

All three types may occur during drilling and are also coupled. Therefore axial vibrations at the bit may result in lateral vibrations at the BHA as well as axial and torsional vibrations seen at the surface can be an indicator for severe lateral vibrations downhole. All three types are introduced shortly below. For a more detailed description of the different type see the book: “Advanced Drilling and Well Technology; Chapter 3: Drillstring Vibrations” (Aadnøy et al., 2009, p. 117).

C.1.1.1 Axial Vibration

Axial vibrations are vibrations involving motions of the drillstring components along its longitudinal axis. Axial vibrations may have a positive or negative effect on drilling as they affect the WOB and therefore the ROP. The most severe type of axial vibrations results in the so-called “Bit Bounce”. Whereas bit bounce can be seen as the intermitted lift of the bit and therefore the BHA off the formation followed by an impact on the formation.

C.1.1.2 Lateral Vibration

Lateral vibrations arise as the BHA goes into a mechanical resonance. These are the most destructive type of vibrations. The intensity of the lateral vibrations is dependent on the amount of energy transferred from rotational to lateral movement. If this energy is greater compared to the energy absorbed by the rock during the impact the severity of the lateral vibrations increases. Thinking about the formation downhole that means that limestone and sandstone (normally hard formations with a higher friction and restitution coefficient) absorb less energy and result in high shocks compared to soft shales. Severe lateral vibrations may result in so-called “Whirl”. Whirl is the eccentric defined as the eccentric rotation of the BHA or Bit around the wellbore. It can be distinguished between three types of whirl: forward, backward and chaotic.

C.1.1.3 Torsional Vibrations

Torsional Vibrations are vibrations associated with the twisting motion of the drillstring and are generally seen together with PDC bits, as those are associated with high downhole friction coefficients. Torsional vibration means that although the string is rotated with a certain RPM on the surface the bit at the bottom doesn’t rotate necessarily with the same RPM. Rather large fluctuation in amplitude over time concerning the downhole RPM can be seen and translate into fluctuations in downhole torsion. Torsional vibration does not just occur due to bit rock interaction, it also can be seen along the BHA and the rest of the drillstring. As the freely rotating BHA or Drillpipe contacts the borehole wall can result into an impulse impeding rotation. Therefore torsional vibrations may damage pipe connections, the bit and slows down drilling. The most severe type of torsional vibration ends in the so-called “Stick/Slip” behavior of the bit. Stick/slip behavior is a cyclic phenomenon of torsional oscillation meaning that the drill bit will come to a sudden standstill till the string torques up to a certain limit until it comes loose again.

C.1.2 Wellbore Geometry Irregularities

C.1.2.1 Keyseat

(a) (b) (c)

Figure 51: Schematic Sequence of a Keyseat; (a) abrupt change in angle or direction in a medium soft to a medium hard formation (orange layer = clay stone or shale; yellow layer = sandstone); (b) high string tension and pipe rotation wears a slot into the formation; (c) the formed slot geometry is smaller that the original wellbore and doesn't fit the bigger downhole equipment. (Amoco EPTG Drilling Technology Teams, 1996, p. 48)

A typical change in the geometry of the wellbore is represented by Figure 51 showing the change of the geometry due to the mechanism forming a keyseat during drilling operations. The new slot worn into the formation and represented by the slotted line as seen above (Figure 51 (b)) has less curvature and is smaller in diameter. Although free sting movement below the keyseat is possible it is obviously changing the forces acting on the string and as the string is pulled out of hole it even can get stuck as the bigger pipes in the BHA won't fit through the smaller slot (Figure 51 (c)).

C.1.2.2 Micro Doglegs

Figure 52 (a) shows a pipe getting stuck in a series of micro doglegs establishing due to a sequence of Hard/Soft formations (orange layer = clay stone or shale; yellow layer = sandstone) or frequent correction in the wellbore angle. Sections of stiffer pipe like DC's and tools with larger diameter like stabilizers are prone to drag along the wellbore in parts with frequent direction/angle changes. The micro doglegs lead to additional side forces and bending of the string that need to be counted for. If theses forces are becoming to big the string a stuck pipe situation as represented here cannot be ruled out.

C.1.2.3 Ledges

Ledges like in Figure 52 (b) in general occur in an alternation of soft and hard formations (soft = orange = clay stone or siltstone; hard = black = Limestone or Dolostone) as the soft formation is washed out and the hard one is in gauge and forms the ledge. These ledges are often associated with micro doglegs and like them they lead to additional drag and bending forces acting on the string while drilling due to a frequent change in direction and angle changes. During tripping operations like implied here stabilizer blades and tool upsets are prone to become stuck under ledges.

C.1.2.4 Mobile Formations

An example of the reduction of the wellbore diameter leading to a jammed BHA as a formation squeezes in is shown Figure 52 (c). This normally happens, as the overburden of the formations above (orange layers) is high enough to squeeze the underlying plastic formation (green = salt or shale) into the wellbore. Leading to additional side forces as the wellbore geometry changes and sometimes to a stuck pipe like illustrated here. If the formation moves fast enough the drillstring could even get stuck during drilling operations.

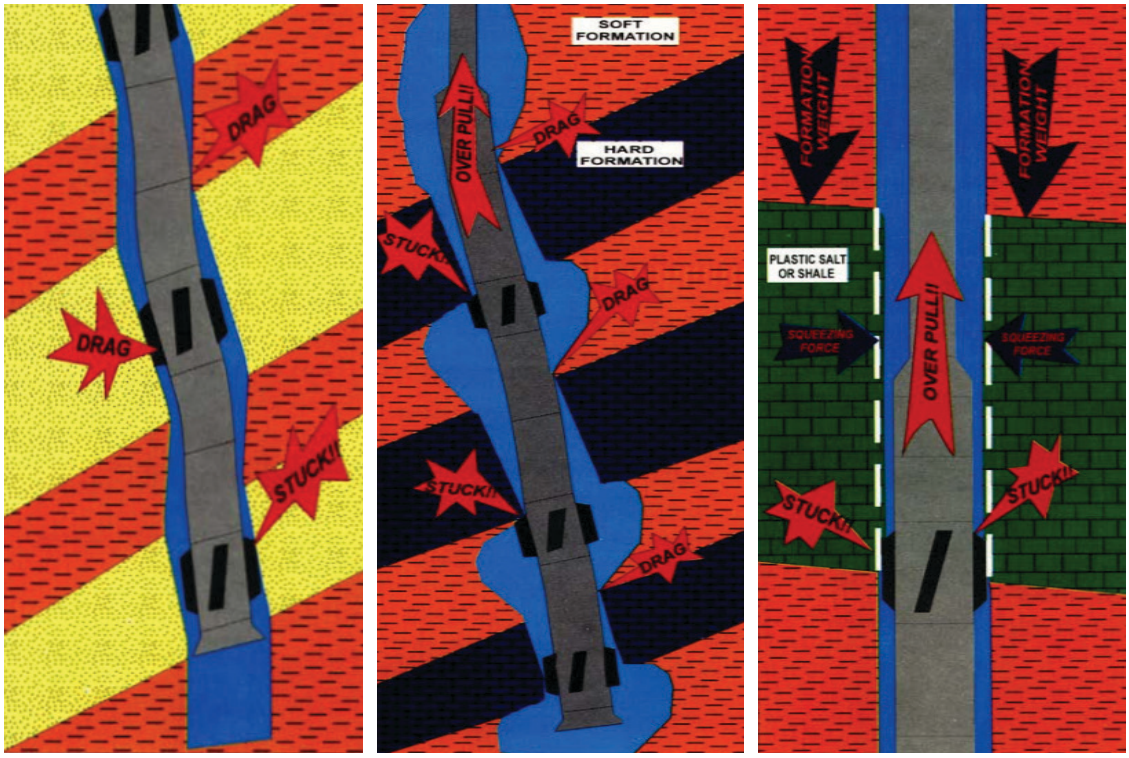

(a) (b) (c)

Figure 52: Sketch of a Stuck Pipe due to Various Wellbore Geometry Irregularities; (a) due to Micro Doglegs, (b) due to Ledges, (c) due to a Mobile Formation. (Amoco EPTG Drilling Technology Teams, 1996)

D Introduction to Surface and Downhole Measurements

The reliability of surface measurements is questionable especially when it is thought of deviated or extended reach wells where friction losses along the borehole have a major impact on the transmission of the surface forces to the bit and the formation being drilled. Therefore the O&G industry began to conduct downhole measurements that give some indication what is going on downhole in “real time”. The restricting factor to get these measurements in real time are not the measurements themselves, it’s rather the telemetry system.

D.1 Surface Measurements

WOB is commonly measured on the surface by comparing of bottom and the drilling hook load. As the bit is on bottom and drilling precedes the hook load becomes less and therefore the difference of weight is assumed to act axial at the bit.

The torque acting at the bit is normally observed on the surface by measuring the current that is needed at the top drive- or rotary table- motor to rotate the

drillstring. In case of a hydraulic motor the pressure difference is measured that yields the torque.

Counting the rotations of the string on the surface is meant to be equal to the rotations at the bit.

Coming to the ROP it has to be stated that there is no actual real time measurement of ROP it more or less is the try to represents a near real time measurement of penetration rate. Therefore the crown blocks position is recorded how it changes over time that yields an approach how fast we drilled the previous interval depending on the time segment.

D.2 Problems with Traditional Telemetry System

With current traditional MWD telemetry like the common mud – pulsing there is a significant bottleneck in bandwidth regarding to the data transfers from the downhole measurements to the surface and the other way.

D.2.1 Limitation of Mud – Pulse Telemetry

Even with just two points of measurement downhole, one next to the bit and another one in the BHA, the amount of data gathered due to the measurements is too much to be transmitted in real time with traditional MWD mud – pulse telemetry to the surface. The constraints coming along with mud – pulse telemetry can be summarized:

- Maximum bandwidth is up to 40 bit/sec and becomes less with further distance to overcome.
- Not really real time due to a high latency.
- Extended by interval setting
- Without circulation flow no data transmissions.
- Noise in the circulation system may affect mud – pulses and makes them hard to read.

D.3 Wired – Pipe Telemetry Network

The relatively new high speed and high bandwidth wired – pipe telemetry network technique discussed is based on the wired drillpipe technology used by NOV as it is

the best reference material to be found although other industry competitors are also working on wired – pipe telemetry systems.

In field-test done in 2009 by NOV with the main objective to achieve the first well on record drilled with multiple distributed sensors transmitting annular pressure and temperature data in real time the theoretical setup of the drilling and telemetry equipment is explained. Whereas Figure 53 shows ongoing drilling operations including the necessary equipment as a drilling rig, a drill string from the bottom of the hole up to the surface and bit at the lower end of the string. Furthermore the BHA also includes besides the bit, a bit-sensor package and a directional drilling equipment. Coming to the wired – pipe network this consists out of:

- Interface subs that provide a mechanical and electrical crossover connecting the downhole measurement tools (MWD) to the telemetry network.
- Network link nodes that give the data signal a boost and maybe also take measurements at their location along their drillstring. Link nodes are connected to link pipes together (as the link pipe is shorter than a standard drillpipe) that match the dimensions and specifications of a standard – length drill pipe.
- Drilling pipes that contain a network cable (designated as communication link in Figure 53) and have the same tubular dimensions and specifications as those of non-wired tubular. The pipes are connected in the case of the equipment deployed by NOV by inductive coils at the pin and box ends of the pipe joints.
- A computer on the surface is connected to the downhole network through an intelligent swivel.

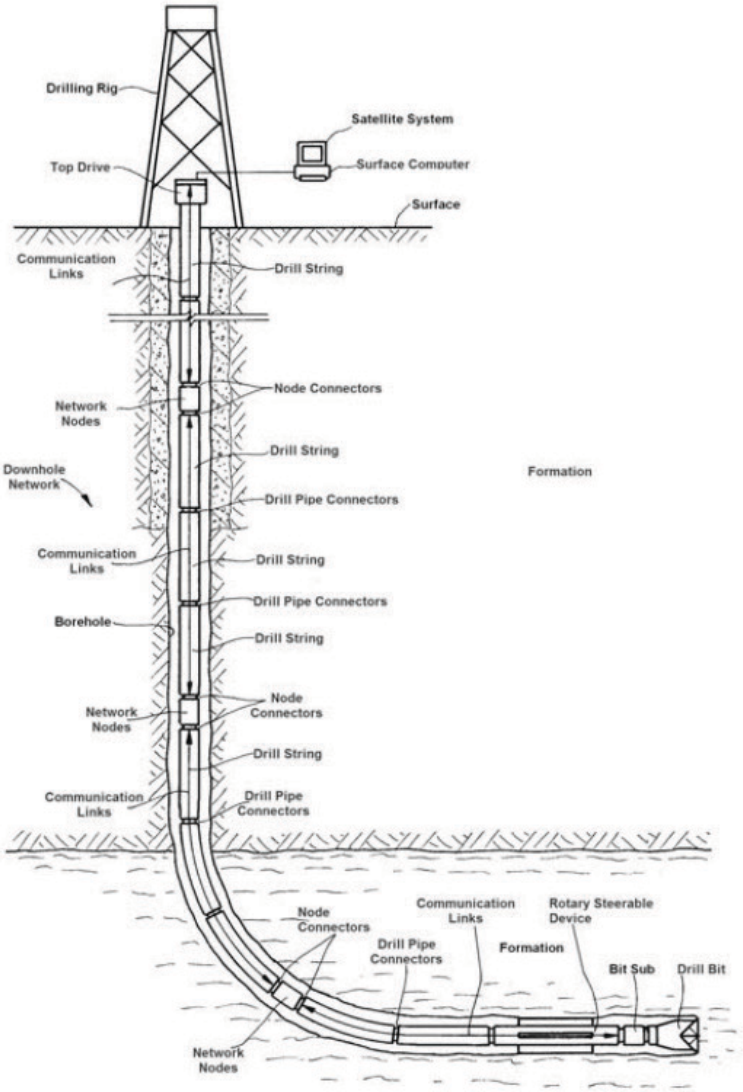

Figure 53: Wired-Pipe Telemetry Network Implementation in Drilling Operations (Johnson & Hernandez, 2009)

A prime feature of the wired pipe system with multiple sensors deployed along the drillstring is that information from a sensor at a specific depth can be compared to the measurement of a subsequent sensors measurement from the same specific depth with a time gap in-between. Further information on wired – drillpipe and how field – test done by NOV can be found in the paper “Along String Pressure and Temperature Measurements in Real Time: Early Field Use and Resultant Value” (Johnson & Hernandez, 2009)